

***Identifying mechanisms that regulate Human Sodium  
Iodide Symporter (NIS) gene expression in breast cancer***

**By**

**Maitreyi Rathod**

LIFE09201404007

**TATA MEMORIAL CENTRE**

**MUMBAI**

*A thesis submitted to the Board of Studies in Life Sciences  
in partial fulfilment of the requirements for the Degree of*

**DOCTOR OF PHILOSOPHY**

*of*

**HOMI BHABHA NATIONAL INSTITUTE**



**March 2020**

**Homi Bhabha National Institute**  
**Recommendations of the Viva Voce Committee**

As members of the Viva Voce Committee, we certify that we have read the dissertation prepared by Ms Maitreyi Rathod entitled "Identifying mechanisms that regulate human sodium iodide symporter gene (hNIS) in breast cancer" and recommend that it may be accepted as fulfilling the thesis requirement for the award of Degree of Doctor of Philosophy.

*S. V. Dalal*

Chairperson - Dr. Sorab Dalal

Date:

*Abhijit De*

Guide Convener - Dr. Abhijit De

Date:

*06-08-2020*

*Samit Chattopadhyay*

External Examiner - Dr. Samit Chattopadhyay

Date:

*6/8/20*

*Dibyendu Bhattacharya*

Member - Dr. Dibyendu Bhattacharya

Date:

*06-8-2020*

*Tanuja Leni*

Member - Dr. Tanuja Leni

Date:

*13-08-2020*

Final approval and acceptance of this thesis is contingent upon the candidate's submission of the final copies of the thesis to IIBNL.

I hereby certify that I have read this thesis prepared under my direction and recommend that it may be accepted as fulfilling the thesis requirement.

Date:

Place: Navi Mumbai

Dr. ....

Co-Guide

Dr. ....

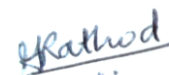
Guide

*Abhijit De* *06-08-2020*

## STATEMENT BY AUTHOR

This dissertation has been submitted in partial fulfilment of requirements for an advanced degree at Homi Bhabha National Institute (HBNI) and is deposited in the Library to be made available to borrowers under rules of the HBNI.

Brief quotations from this dissertation are allowable without special permission, provided that accurate acknowledgement of source is made. Requests for permission for extended quotation from or reproduction of this manuscript in whole or in part may be granted by the Competent Authority of HBNI when in his or her judgment the proposed use of the material is in the interests of scholarship. In all other instances, however, permission must be obtained from the author.



Date: 03/03/2020

**Maitreyi Rathod**

Place: Kharghar, Navi Mumbai.

## DECLARATION

I, hereby declare that the investigation presented in the thesis has been carried out by me. The work is original and has not been submitted earlier as a whole or in part for a degree / diploma at this or any other Institution / University.

Date: 03/03/2020

Place: Kharghar, Navi Mumbai.



**Maitreyi Rathod**

## LIST OF PUBLICATIONS:

### Research article published from PhD thesis:

1. **Maitreyi Rathod**, Sushmita Chatterjee, Shruti Dutta, Rajiv Kalraiya, Dibyendu Bhattacharya and Abhijit De, Mannose glycosylation is an integral step for human NIS localization and function in breast cancer cells , **Journal of Cell Science**, 2019, 10.1242/jcs.232058.
2. **Maitreyi Rathod**, Madhura Kelkar, Girish Salve and Abhijit De, “FOXA1 regulation turns benzamide HDACi treatment effect specific in breast cancer promoting NIS gene mediated targeted radioiodine therapy”- **Accepted in Molecular Therapy Oncolytics**.
3. **Maitreyi Rathod**, Madhura Kelkar and Abhijit De, “CREB activation by PKA positively regulates NIS expression in breast cancer” (Manuscript under preparation)

### Review and book chapter published:

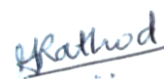
1. Pranay Dey, **Maitreyi Rathod** and Abhijit De, “Targeting stem cells in the realm of drug resistant breast cancer”, *Breast Cancer - Targets and Therapy* 2019;11 115–135
2. **Maitreyi Rathod**, Arijit Mal and Abhijit De, “Reporter based BRET sensors for measuring biological functions in vivo. *Methods in molecular biology*, 2018 p 51-74

### Manuscript Communicated (from collaboration work):

1. Rutika D. Godse, **Maitreyi Rathod**, Rahul Thorat, **Abhijit De**, Ujwala A. Shinde, “Intravitreal Galactose Conjugated Polymeric Nanoparticles of Etoposide for Retinoblastoma”.

**Abstracts presented at conferences:**

- 1. Maitreyi Rathod, Madhura kelkar, Girish salvi and Abhijit De.** Benzamide class of HDACi differentially enhance sodium iodide symporter expression in breast cancer. 25<sup>th</sup> Biennial **EACR** (European association for cancer research), held in Amsterdam, Netherlands from **30<sup>st</sup> June to 3<sup>rd</sup> July 2018**.
- 2. Maitreyi Rathod, Sushmita Chatterjee, Dibyendu Bhattacharyya and Abhijit De.** Functional sodium iodide symporter in breast cancer is regulated by N-linked mannose modifications. International congress of cell biology (**ICCB**), held in Hyderabad from **27<sup>th</sup> January to 31<sup>st</sup> January, 2018**.
- 3. Maitreyi Rathod, Shruti Dutta, Sushmita Chatterjee and Abhijit De.** Prying the intracellular path controlling iodine pump protein localization and function in breast cancer cells. XL All India cell biology conference (**AICBC**), held in Gwalior from **17<sup>th</sup> to 19<sup>th</sup> November, 2016**.
- 4. Madhura Kelkar, Maitreyi Rathod, Abhijit De.** Translational Success of Endogenous Iodine Pump Protein (NIS) Based Targeted Therapy in Breast Cancer may rely on its Maneuverability by Transcriptional Modulations. A conference on new ideas in cancer-challenging dogmas, **TMC platinum jubilee**, held in Mumbai from **26<sup>th</sup> to 28<sup>th</sup> February 2016**.



**Maitreyi Rathod**

## **ACKNOWLEDGEMENT:**

*The entire journey of PhD would not have been possible without the contributions of various people. Thus I would like to acknowledge the contributions from every member who has been an integrated part of my PhD life.*

*Firstly and most importantly, I would like to express sincere thanks to my mentor Dr. Abhijit De for guidance and constant motivation throughout these years. I would like to express deep gratitude to him for helping me grow as a researcher and teaching me the importance of thoroughness and perseverance in science. He has taught me to get rid of the fear of unknown and helped me develop writing and verbal communication skills. I take this opportunity to thank him for believing in me to grow through my scientific journey.*

*I thank Director and Deputy Director of ACTREC for providing an excellent infrastructure facility at ACTREC. I would also like to thank my doctoral committee members Dr. Sorab Dalal, Dr. Dibyendu Bhattacharyya and Dr Tanuja Teni for their invaluable suggestions throughout all doctoral committee meetings. I would like to specially thank Dr. Pritha Ray for her suggestions and time for the development of the project with time.*

*I am grateful to the staff of microscopy, animal house, Flow cytometry facility and Molecular Imaging facility for their support. I specially thank Mrs. Vaishali and Ms. Snehal Valvi for their innumerable help. I also thank the staff of scope cell, steno pool, library, administration, accounts and IT department. Mr. Dandekar for his prompt assistance during any problems with the instruments.*

*I am thankful to ACTREC for fellowship. HBNI and Sam Mistry funding agencies for assistance to present my work at the 25<sup>th</sup> European association for cancer research (EACR) at Amsterdam, Netherlands 2019.*

*I thank my seniors Madhura, Amir, Shalini and Sushmita for helping me through my learning curve. I would like to thank Sir and Amir for teaching me Adobe Photoshop software. My batchmate Arijit, juniors Sumit, Pranay, Aaiyas, Mansi and Chetna for maintaining a joyful environment in the lab and participating in scientific discussions. Special thanks to my friends Arijit, Aniketh, Snehal and Pranay for all the wonderful memories and times spent together in good and bad times. Thanks for bearing with me through my tough times and standing by me. This PhD journey would be difficult without your support. I would like to thank Renu for helping me with purchase and getting reagents on time. I specially thank prassana, pravin and ram who assisted in buffer making, autoclaving and technical help throughout. I also thank my trainees Shourya and Girish for their contribution to the project. I also thank Ray lab members specially Bhushan, Ram, Ajit, Aniketh, Abhilash and Shouvik for their support and sharing chemicals and reagents. Last but not the least I am thankful to my parents and in laws for their endless support, understanding and patience throughout my Ph.D. I am highly obliged to them for bearing my absence from many important occasions and never complaining for the same. This journey would not have been completed without the enormous love, support, care, patience and encouragement of my husband, Mr. Waseem Naik. Thank you*

**Maitreyi Rathod**

## Table of contents

<b>Synopsis</b>	12-26
<b>List of figures</b>	27-28
<b>List of tables</b>	29
<b>Abbreviations</b>	30-34
<b>Chapter 1</b>	
<b>1. Introduction and Review of literature</b>	35
<b>1.1</b> Chronicles of breast cancer	36-38
<b>1.2</b> Breast cancer epidemiology	38-39
<b>1.3</b> Anatomy of normal breast	40-41
<b>1.4</b> Histological classes of breast cancer	41-44
<b>1.5</b> Molecular subtypes of breast cancer	44-45
<b>1.6</b> Disease management regimes for breast cancer	46-47
<b>1.7</b> Sodium Iodide Symporter (NIS)	47-51
<b>1.8</b> Discovery of NIS	51-52
<b>1.9</b> NIS as a diagnostic target for cancer	52
<b>1.10</b> Therapeutic application of NIS in thyroid cancer	53-54
<b>1.11</b> NIS mediated gene therapy for non-thyroidal malignancies	54-55
<b>1.12</b> Regulation of NIS in thyroid	55-56
<b>1.13</b> Expression of NIS in breast cancer	56-58
<b>1.14</b> Modulators of NIS in breast cancer	59-60
<b>1.15</b> Molecular imaging	60-63
<b>1.16</b> Cerenkov luminescence imaging	63-64
<b>1.17</b> Rationale of study	65-66
<b>1.18</b> Aims and objectives	66
<b>Chapter 2</b>	
<b>2. To elucidate the role of HDACi (benzamide class) in regulating NIS expression and function in breast cancer as compared to thyroid cancer</b>	67
<b>2.1 Introduction</b>	68-69
<b>2.2 Materials and Methods</b>	
<b>2.2.1</b> Chemicals and cell lines	69-70
<b>2.2.2</b> Luciferase assay	70-71
<b>2.2.3</b> Quantitative real time PCR	71
<b>2.2.4</b> Western blotting and Immunofluorescence	71
<b>2.2.5</b> Intracellular staining and flow cytometry	72
<b>2.2.6</b> MTT cell cytotoxicity assay	72
<b>2.2.7</b> Non-radioactive iodine uptake assay	72-73
<b>2.2.8</b> In vitro long term survival assay using <sup>131</sup> I	73
<b>2.2.9</b> In vivo orthotopic breast cancer model development and drug treatment	73
<b>2.2.10</b> Immunohistochemistry	74
<b>2.2.11</b> In vivo non-invasive bioluminescence imaging	74
<b>2.2.12</b> TF profiling and promoter binding array	74
<b>2.2.13</b> Cloning of shRNA and lenti-viral mediated generation of FOXA1 knockdown stable cell model	75

2.2.14 Cerenkov luminescence imaging	75
2.2.15 Statistical analysis	75
<b>2.3 Results</b>	
2.3.1 Non-toxic dose profiling of benzamide class HDAC inhibitors (bHDACi) on breast and thyroid cancer cells	76
2.3.2 Benzamide class HDACi show anti-proliferative effect on BC cells and are able to induce acetylation of its substrate	77
2.3.3 Benzamide class HDACi differentially modulate NIS promoter activity in breast cancer cells	78-79
2.3.4 bHDACi enhance endogenous NIS expression preferentially in BC cells	79-81
2.3.5 Benzamide class HDACi significantly enhance NIS function in breast cancer cells	82
2.3.6 Depletion of HDAC1 from MCF-7 cells leads to an increase in NIS expression	82-83
2.3.7 Transcription factor (TF) profiler array reveals differential TF activated by CI-994 in MCF-7 and ARO	84-85
2.3.8 FOXA1 expression is higher in breast cancer in contrast to thyroid cancer	86-87
2.3.9 FOXA1 is a positive transcriptional modulator of NIS expression in breast cancer	88-89
2.3.10 Enhanced function of NIS in BC, leads to significant induction of DNA damage in response to <sup>131</sup> I	89-90
2.3.11 bHDACi reinforces the <sup>131</sup> I mediated radio ablation effect differentially in breast cancer cells	90-91
2.3.12 Low dose AR-42 and MS-275 boost NIS expression <i>in vivo</i>	92
2.3.13 AR-42 elevates NIS promoter activity in breast tumour <i>in vivo</i>	93-94
2.3.14 NIS expression is differentially regulated in non-breast organs and cells	95-96
2.3.15 bHDACi mediated elevation of NIS, leads to a potential radio ablation effect on orthotopic breast tumour <i>in vivo</i>	96-98
2.3.16 <sup>131</sup> I accumulation in tumour is higher in MS-275+ <sup>131</sup> I group	98-99
2.4 Discussion	99-102
<b>Chapter 3</b>	
<b>3. Understanding the role of cAMP-PKA-CREB axis on regulating NIS expression</b>	103
<b>3.1 Introduction</b>	104-105
<b>3.2 Materials and Methods</b>	
3.2.1 Reagents and antibodies	105
3.2.2 Luciferase assay	106
3.2.3 Immunoblotting	106
3.2.4 Immunofluorescence	106
3.2.5 Real Time PCR	106
3.2.6 Chromatin Immunoprecipitation	107
<b>3.3 Results</b>	
3.3.1 NIS promoter activity is positively regulated by CREB in breast cancer cells	108
3.3.2 Activation of CREB can induce NIS expression in breast cancer cells	109-110

3.3.3 Inhibition of PKA attenuates NIS expression	111-112
3.3.4 CREB is directly recruited to NIS promoter, in order to regulate NIS gene expression	113-114
<b>3.4 Discussion</b>	115-117
<b>Chapter 4</b>	
<b>4. Investigating the role of glycosylation as a regulatory mechanism to control NIS cellular localization</b>	118
<b>4.1 Introduction</b>	119-120
<b>4.2 Material and Methods</b>	
4.2.1 Reagents and antibodies	121
4.2.2 Generation of NIS overexpressing stable cell line	121
4.2.3 Luciferase assay	121
4.2.4 Immunoblotting	122
4.2.5 Immunofluorescence	122
4.2.6 Real Time PCR	122
4.2.7 Iodine uptake assay	122
4.2.8 Immunoprecipitation and lectin western blot	123
4.2.9 Statistics	123
<b>4.3 Results</b>	
4.3.1 Standardization of Golgi deformation and reformation time kinetics, post BFA treatment	124
4.3.2 MCF-7 cells show defective NIS trafficking through secretory pathway	125-126
4.3.3 Overexpression of NIS gene in MCF-7 cells, reveals two distinct type of clones with karyotype heterogeneity	127-129
4.3.4 NIS follows classical intracellular trafficking path in membrane clones	129-130
4.3.5 EGFR can cross ERES and reach Golgi in MCF-7 parent and clonal cells	131-132
4.3.6 NIS shows a higher association with calnexin in cells with trafficking defect	133-134
4.3.7 N linked Glycosylation is an important PTM that regulates the sub cellular localization of NIS	134-137
4.3.8 Glycosylation gene expression profile of cells expressing NIS on membrane versus NIS in cytoplasm	137-138
4.3.9 The role of mannosidase in modulating the localization of NIS in breast cancer cell clones	139-141
4.3.10 The role of mannosidase in modulating the localization of HER3 in breast cancer cell clone	141-142
4.3.11 NIS is directly associated with mannose modification in breast cancer cell models	142-143
<b>4.4 Discussion</b>	143-148
<b>Summary</b>	149-151
<b>Bibliography</b>	152-168
<b>Appendix</b>	169-209
<b>Publications</b>	209-222

## *Synopsis*



## Homi Bhabha National Institute

### SYNOPSIS OF Ph. D. THESIS

- 1. Name of the Student:** Maitreyi Rathod
- 2. Name of the Constituent Institution:** Tata Memorial Centre-ACTREC
- 3. Enrolment No. :** LIFE09201404007
- 4. Title of the Thesis:** Identifying mechanisms that regulate human sodium iodide symporter gene (NIS) in breast cancer

### SYNOPSIS

#### Introduction:

Human Sodium Iodide Symporter (hNIS), a transmembrane pump protein that actively symport one I<sup>-</sup> and two Na<sup>+</sup> ions is mostly found in thyroid follicular cells. NIS (SLC5A5) belongs to solute carrier family, in which all members use electrochemical sodium gradient as the driving force for solute transport within the cell as classified by Online Mendelian Inheritance in Man (OMIM) [1]. It is primarily located in thyroid, where it is used for synthesis of thyroid T3, T4 hormones. NIS expression is also recorded in various extra thyroidal tissues such as bladder,

colon, kidney, endometrium, salivary gland and lactating mammary gland. NIS consists of 13 transmembrane domains with amino terminus facing extracellular and carboxy terminus facing cytoplasmic side [2]

The protein comprises 643 amino acids leading to a molecular weight of 50-100kD. NIS is a glycoprotein, with three putative N-linked glycosylation sites i.e. Asn497, 225, 485.

The ability of thyroid to concentrate iodine 20-40 times higher than plasma was first measured by Bauman 1896. A breakthrough study took place in 1942, where Grave's disease patients were treated with radioactive iodine and it led to a significant management of the disease. This iodine trapping ability in thyroid tissue has become a standard radio-ablation treatment practice using radioiodine ( $^{131}\text{I}$ ) for thyroid malignancies. The hope of extending this treatment regime for breast cancer started from the first report, showing presence of NIS in breast cancer, where more than 80% of invasive ductal carcinomas expressed NIS [3].

Further in subsequent reports various groups showed abrupt NIS expression in breast cancer (BC), where 4/25 patients represented positive technetium 99m ( $^{99\text{m}}\text{Tc}$ ) uptake [4]. 65% of TNBC cases also showed positive NIS expression [5]. NIS expression was also seen in brain metastasis of BC cases [6]. Published work from our own group showed BC subtype specific NIS expression where a positive correlation between NIS expression with ER receptor was shown [7].

Although there is presence of NIS in BC patients, only very few patients show spontaneous uptake of radioiodine. Thereby limiting its scope as an effective therapeutic candidate for breast cancer.

## **Rationale:**

Although NIS expression is recorded in breast cancer tissues, the defective sub cellular localization and insufficient expression of NIS remains the bottleneck for successful translation of NIS gene therapy in breast cancer. Only 30% cases show 2+/3+ score for NIS staining, while majority of the positive cases are actually NIS low (1+). Hence studying the regulation of inherent NIS expression and subcellular localization may eventually help in finding a way to elevate NIS mediated uptake of iodine in cells.

Many studies in the past have attempted to identify regulators of hNIS in BC, where one of the major well-studied regulators is all trans-retinoic acid (ATRA). ATRA binds to two nuclear receptors RAR/RXR to induce NIS expression. Glucocorticoid agonists like dexamethasone and hydrocortisone have been reported to augment NIS expression in MCF-7 cells [8]. Molecules like insulin, IGF-1, 2, ATRA and prolactin have also been proved as enhancers of NIS expression and function in MCF-7 cells [9] [10]. Carbamazepine, a PXR agonist, showed 1.8 fold increase in iodine uptake mediated through tRA in breast cancer cells [11]. A transcription factor Nkx2.5 was identified as a positive modulator of NIS in MCF-7 cells [12]. Recently, we also reported that p53 acts as a suppressor of NIS expression in breast cancer [13]. Cyclic AMP (C-AMP) pathway is very well characterized for positively regulating TSH mediated induction of NIS gene in thyroid cancer, however the modulatory role of cAMP response element binding protein (CREB) on NIS gene, in BC scenario remains elusive.

Inhibition of Histone deacetylase (HDAC) has also been a strategy used for stimulating NIS in several thyroid cancer cell lines. One HDACi candidate, LBH589, was used for inducing NIS expression and function in several BC lines [14]. Past work from our group has verified various chemical classes of HDACi for enhancing NIS expression, iodine uptake, and thus increased

therapeutic efficacy in BC cells [15]. However, modulators which can induce the function of endogenous NIS specifically in BC, with minimal off target effects remains unknown. Another long-standing and important aspect appeared frequently in research literature is sub-cellular localization of NIS. This aberrantly overexpressed protein mostly found to be accumulated in the cytoplasm instead of plasma membrane [16]. Only a few reports so far have investigated on regulation aspects of NIS protein localization inside the BC cells. It has been shown that EGF mediates membrane targeting of NIS via MAPK pathway [17, 18]. Thus, identification of regulatory mechanisms involved in defective localization of NIS in BC cell is considered also here thinking that it may open new avenues for effective NIS function.

### **Aims and Objectives:**

Based on the current limitations pertaining to NIS mediated therapy in breast cancer, we have set the following objectives in an attempt to address the lacunae in our current understanding pertaining to the modulation of endogenous NIS in breast cancer:

**Objective 1:** To elucidate the role of HDACi (benzamide class) in regulating NIS expression and function in breast cancer as compared to thyroid cancer

**Objective 2:** Understanding the role of cAMP-PKA-CREB axis on regulating NIS expression

**Objective 3:** Investigating the role of glycosylation as a regulatory mechanism to control NIS cellular localization

### **Results:**

The results have been divided into 3 sections as per the respective objectives

**1. To elucidate the role of HDACi (benzamide class) in regulating NIS expression and function in breast cancer as compared to thyroid cancer**

Four drugs belonging to benzamide class of HDAC inhibitors (bHDACi) were selected for the study. The non-toxic doses for all these drugs (i.e. < IC-30), across MCF-7, ZR-75-1 and ARO were selected, to rule out the anti-tumor effect of HDACi itself on BC. To study the effect of HDACi on NIS promoter activity, we developed a stable NIS promoter driven firefly luciferase (pNIS-FL2.Turbo overexpressing) reporter model in MCF-7, ZR-75-1 and ARO cells. Treatment of breast cancer (BC) cells i.e. MCF-7 and ZR-75-1 with benzamide class HDACi, leads to a significant ( $p \leq 0.0005$ ) increase in NIS promoter activity (*in vitro* and *in vivo*), while these same drugs have no significant effect on NIS promoter activity in thyroid cancer (TC) cell ARO. The effect of differential modulation of NIS in breast cancer cells by benzamide class HDACi (bHDACi), were validated by measuring the NIS transcript levels, protein expression and function. bHDACi were able to induce NIS expression and function in BC cells but not in thyroid cancer cells or normal thyroid of mice. bHDACi (MS-275) did not elevate the NIS expression in other organs like liver, ovary, lung, brain. Further, we also tested the role of HDAC1 on regulating NIS. Viral mediated stable knockdown of HDAC1 in MCF-7 cells could significantly enhance NIS expression. Thus HDAC1 was proved to act as a negative regulator of NIS in BC cells. bHDACi mediated increase in NIS function in BC cells, also augmented the NIS mediated  $^{131}\text{I}$  therapy *in vitro* and *in vivo* (orthotopic breast cancer ZR-75-1 cell tumor model). Cerenkov Luminescence imaging also showed higher accumulation of  $^{131}\text{I}$  in tumors treated with MS-275 as compared to untreated tumors. Further, to gain mechanistic insights into the differential modulation of NIS by bHDACi, we performed a high throughput assay for profiling 96 different transcription factors in response to CI-994 in MCF-7 and ARO cells. FOXA1 was identified as a novel TF from the array, which was induced by CI-994 in BC cell and not in TC cell. Further, by viral shRNA mediated stable knockdown of FOXA1 in MCF-7, we show that FOXA1 is a positive modulator of NIS in BC cell.

## 2. Understanding the role of cAMP-PKA-CREB axis on regulating NIS expression

In an attempt to elucidate the role of CREB in modulating NIS expression in BC, we used two activators of CREB, i.e. Forskolin and 8-Bromo-cAMP. Forskolin elevates the levels of a secondary messenger i.e. cAMP, which can directly activate PKA, which can activate CREB downstream, by phosphorylation at serine 133 residue. 8-Bromo-cAMP is an analog of cAMP, which can directly bind to PKA, leading to its activation. The effective concentrations of these drugs were determined by measuring pCREB levels. Inhibitor against PKA activation i.e. KT-5720 was also used to validate the specific effect of PKA mediated CREB phosphorylation on NIS expression.

By using NIS promoter (pNIS-FL2.Turbo overexpressing) driven stable reporter cells (ZR-75-1 NF and MCF-7 NF), we measured the effect of CREB activators and inhibitors on NIS promoter modulation. 24 hours treatment of Forskolin and 8-Br-cAMP to MCF-7 NF and ZR-75-1 NF cells, showed a significant ( $p < 0.0001$ ) increase in NIS promoter activity. On the other side, inhibition of CREB activation, lead to a significant ( $p < 0.005$ ) decrease in NIS promoter activity. NIS transcript levels also increased significantly with the treatment of 8-bromoCAMP, Forskolin in MCF-7 and ZR-75-1 cells. NIS transcript levels decreased up to 40% in response to PKA inhibitor KT-5720, as quantified by real time qPCR.

The effect of PKA mediated CREB activation/inhibition on NIS protein expression was also judged by immunofluorescence and FACS analysis, validating the findings further. As a transcription factor, activated CREB modulates NIS gene expression by directly binding to NIS promoter. Chromatin Immunoprecipitation (ChIP) assay revealed enhanced binding of pCREB as compared to CREB on NIS promoter in response to Forskolin treatment, on two of the CRE binding sites present on NIS promoter.

### **3. Investigating the role of glycosylation as a regulatory mechanism to control NIS cellular localization**

In order to understand the intracellular trafficking of NIS in BC cells, across the classical secretory pathway, NIS co-localization with organelle i.e. endoplasmic reticulum (ER), ER exit site (ERES) and Golgi specific markers was quantified by measuring the overlap co-efficient. It was observed that the basal MCF-7 cells and the cytoplasmic clone (cl6) showed a significant decrease in the overlap co-efficient with Golgi marker GalNac-T2, indicating that NIS trafficking to Golgi in these cells was disrupted. The ER and ER exit sites showed increased co-localization with NIS. In membrane clone (cl31), there was a significant increase in the co-localization co-efficient with the Golgi marker, indicating that in these cells, the trafficking of NIS from ER to Golgi bodies was un-disturbed. Since the ER to Golgi transit in MCF-7 and cl6 cells was significantly lower as compared to cl31 cells, we assessed the association of nascent NIS with an ER resident folding chaperone calnexin. NIS co-localization with NIS in cl31 was significantly less as compared to MCF-7 and cl6 cells, indicating that NIS was present in a folding incompetent state in MCF-7 and cl6 cells. A high throughput q-RT PCR profiler array for 84 key genes which regulate the process of N- glycosylation, revealed that cytoplasmic NIS expressing clones and basal MCF-7 cells clustered separately from the membranous NIS expressing clones. The array data revealed a dramatic difference in the expression profile of 32 different genes in cytoplasmic versus membrane NIS clones, which were up regulated in the membranous NIS expressing lineages. Thus the array indicated the importance of N-linked glycosylation process for subcellular localization of NIS. Further, by using N-linked glycosylation specific inhibitors, it was observed that NIS localization to plasma membrane was perturbed. By lectin western blotting of purified NIS from cl31 and basal MCF-7 cells, we confirmed that NIS is a mannose type glycoprotein, where the completely glycosylated mature form of NIS (100kDa) is concavalin A positive. Thus we picked top 3 candidate mannosidase genes from the array results, i.e. MAN1A1, MAN1B1 and

MAN2A1 and by using siRNA mediated knockdown, we confirmed that the loss of these mannosidase from the cells, abrogates the membrane localization of NIS and also reduces the 100kDa fraction of NIS in cl31 cells. Since these mannosidase have global effect, we also validated the knockdown effect on another control protein i.e. HER3. Triple combination of all 3 siRNA causes a drastic decrease in the expression and membrane localization of HER3.

### **Conclusion:**

In this study, we have attempted to study a few major clinical concerns associated with the application of NIS as a gene target for radio-ablation therapy in breast cancer. In the first approach, using epigenetic modulators, we have attempted to enhance NIS gene expression that is specific for breast cancer cells. Strikingly, here we have shown that a few of the benzamide class of HDAC inhibitors are able to exert very high NIS gene expression in breast cancer cells such as MCF7 and ZR-75-1 cell lines, but not in thyroid cancer cell (ARO and NPA). Further, these HDACis do not effectively enhance NIS expression in transformed normal breast cell line, MCF-10A. This finding is very interesting and important to develop the clinical application of NIS gene targeted radio-iodine therapy for breast cancer. Thereafter, to verify their effect *in vivo*, orthotopic BC tumor bearing mice were treated with MS-275, and found that the drug can enhance the NIS protein expression in tumor, while not affecting the NIS protein contents in cells of thyroid gland, liver, lung, and ovary tissues. Thus benzamide class HDACi provides a unique platform for achieving breast cancer specific radio- ablation therapy, and can potentially avoid the risks associated with off-target effects on other critical organs while performing this systemic treatment in patients. Our study also demonstrated the pre-clinical use of AR-42 and MS-275 as mediators of NIS mediated  $^{131}\text{I}$  therapy, where a systemic injection of single dose of  $1\text{mCi }^{131}\text{I}$  in mice can reduce the breast cancer tumor burden by 40%. The point to be noted here is that we have verified the use of a low dose AR-42 and

MS-275 to boost NIS based radio-iodine therapy. This leaves the scope of long term use of the drug along with multiple doses of  $^{131}\text{I}$  at intervals, which could possibly be checked in future to achieve better tumor ablation.

In the second approach, we have attempted to develop a deeper understanding of mechanistic insights where internal cellular factors plays regulatory role on NIS gene expression in BC versus TC. In the context of benzamide drug mediated gene regulation studied above, we have shown that FOXA1 is a breast cancer specific TF that gets induced by CI-994 in MCF-7 (BC) cells, but not in ARO (TC) cell. Additionally, FOXA1 is found to be a novel modulator that positively regulate NIS gene expression and function. Further, in chapter three, we have studied transcriptional modulation of NIS gene by another important TF, i.e. CREB, which positively regulates NIS in BC. CREB is having 5 binding sites on human NIS promoter sequence. We have found activation of CREB (at serine 133) by PKA, can increase direct binding of CREB on the NIS promoter, resulting enhanced NIS gene expression in BC cell lines. Therefore, inhibition of the PKA mediated activation of CREB can significantly reduce NIS promoter activity, thus verifying the importance of CREB phosphorylation for controlling NIS transcript expression.

The third aspect that we have also addressed here is an important clinical limitation for NIS therapy application which is due to defective subcellular localization of the protein in BC. We have identified that the defective localization of NIS in breast cancer cells is due to impeded trafficking of NIS from ER to Golgi in BC cells. The impaired trafficking of NIS from ER to Golgi apparatus was also verified by studying the association of nascent NIS with ER resident protein folding chaperone i.e. calnexin. Higher association of NIS with calnexin in basal MCF-7 and cytoplasmic clonal cells implied the presence of NIS in folding incompetent state in these cell types. Further, N-linked glycosylation was identified as a key to proper trafficking of NIS to plasma membrane. N-linked glycosylation array for 84 genes involved in glycosylation

process in the cells, revealed that the cell clones having NIS at plasma membrane clustered separately from the ones having cytosolic NIS. Thus from our study we identified three potential mannosidase i.e. MAN1A1, MAN1B1 and MAN2A1, which regulate the localization of NIS to cell surface.

### **References:**

1. Dohan, O., et al., *The sodium/iodide Symporter (NIS): characterization, regulation, and medical significance*. Endocr Rev, 2003. **24**(1): p. 48-77.
2. Kogai, T. and G.A. Brent, *The sodium iodide symporter (NIS): regulation and approaches to targeting for cancer therapeutics*. Pharmacol Ther, 2012. **135**(3): p. 355-70.
3. Tazebay, U.H., et al., *The mammary gland iodide transporter is expressed during lactation and in breast cancer*. Nat Med, 2000. **6**(8): p. 871-8.
4. Moon, D.H., et al., *Correlation between <sup>99m</sup>Tc-pertechnetate uptakes and expressions of human sodium iodide symporter gene in breast tumor tissues*. Nucl Med Biol, 2001. **28**(7): p. 829-34.
5. Renier, C., et al., *Endogenous NIS expression in triple-negative breast cancers*. Ann Surg Oncol, 2009. **16**(4): p. 962-8.
6. Wapnir, I.L., et al., *The Na<sup>+</sup>/I<sup>-</sup> symporter mediates iodide uptake in breast cancer metastases and can be selectively down-regulated in the thyroid*. Clin Cancer Res, 2004. **10**(13): p. 4294-302.
7. Chatterjee, S., et al., *Quantitative immunohistochemical analysis reveals association between sodium iodide symporter and estrogen receptor expression in breast cancer*. PLoS One, 2013. **8**(1): p. e54055.

8. Unterholzner, S., et al., *Dexamethasone stimulation of retinoic Acid-induced sodium iodide symporter expression and cytotoxicity of <sup>131</sup>I in breast cancer cells*. J Clin Endocrinol Metab, 2006. **91**(1): p. 69-78.
9. Ryan, J., et al., *The sodium iodide symporter (NIS) and potential regulators in normal, benign and malignant human breast tissue*. PLoS One, 2011. **6**(1): p. e16023.
10. Arturi, F., et al., *Regulation of iodide uptake and sodium/iodide symporter expression in the mcf-7 human breast cancer cell line*. J Clin Endocrinol Metab, 2005. **90**(4): p. 2321-6.
11. Willhauck, M.J., et al., *Stimulation of retinoic acid-induced functional sodium iodide symporter (NIS) expression and cytotoxicity of <sup>131</sup>I by carbamazepine in breast cancer cells*. Breast Cancer Res Treat, 2011. **125**(2): p. 377-86.
12. Dentice, M., et al., *Transcription factor Nkx-2.5 induces sodium/iodide symporter gene expression and participates in retinoic acid- and lactation-induced transcription in mammary cells*. Mol Cell Biol, 2004. **24**(18): p. 7863-77.
13. Kelkar, M.G., et al., *Tumor suppressor protein p53 exerts negative transcriptional regulation on human sodium iodide symporter gene expression in breast cancer*. Breast Cancer Res Treat, 2017. **164**(3): p. 603-615.
14. Fortunati, N., et al., *The pan-DAC inhibitor LBH589 is a multi-functional agent in breast cancer cells: cytotoxic drug and inducer of sodium-iodide symporter (NIS)*. Breast Cancer Res Treat, 2010. **124**(3): p. 667-75.
15. Kelkar, M.G., et al., *Enhancement of human sodium iodide symporter gene therapy for breast cancer by HDAC inhibitor mediated transcriptional modulation*. Sci Rep, 2016. **6**: p. 19341.
16. Rathod, M., et al., *Mannose glycosylation is an integral step for human NIS localization and function in breast cancer cells*. J Cell Sci, 2019.

17. Jung, K.H., et al., *Mitogen-activated protein kinase signaling enhances sodium iodide symporter function and efficacy of radioiodide therapy in nonthyroidal cancer cells*. J Nucl Med, 2008. **49**(12): p. 1966-72.
18. Chung, T., et al., *Glycosylation of Sodium/Iodide Symporter (NIS) Regulates Its Membrane Translocation and Radioiodine Uptake*. PLoS One, 2015. **10**(11): p. e0142984.

### **Publications in Refereed Journal:**

a. Research article published (from thesis)

1. **Maitreyi Rathod**, Sushmita Chatterjee, Shruti Dutta, Rajiv Kalraiya, Dibyendu Bhattacharyya and Abhijit De, Mannose glycosylation is an integral step for human NIS localization and function in breast cancer cells , **Journal of Cell Science**, 2019, 132 (20): jcs232058. *Published 23 October 2019*.

b. Accepted: None

c. Communicated:

1. **Maitreyi Rathod**, Madhura Kelkar, Snehal Valvi, Girish Salvi and Abhijit De, “FOX A1 Regulation Deliberates a Specific and Enhanced hNIS Gene Based Therapy in Benzamide HDACi Treated Breast Cancer Cells”
2. Rutika D. Godse, **Maitreyi Rathod**, Rahul Thorat, Abhijit De, Ujwala A. Shinde, “Intravitreal Galactose Conjugated Polymeric Nanoparticles of Etoposide for Retinoblastoma”

## **Other Publications:**

### a. Book Chapter and Review article:

1. **Maitreyi Rathod**, Arijit Mal and Abhijit De, “Reporter based BRET sensors for measuring biological functions in vivo. *Methods in molecular biology*, 2018, p 51-74
2. Pranay Dey, **Maitreyi Rathod** and Abhijit De, “Targeting stem cells in the realm of drug resistant breast cancer”, *Breast Cancer - Targets and Therapy* 2019:11, 115–135

### b. Conference/Symposium

1. **Maitreyi Rathod**, Madhura kelkar, Girish salvi and Abhijit De. Benzamide class of HDACi differentially enhance sodium iodide symporter expression in breast cancer. 25<sup>th</sup> Biennial **EACR**

Synopsis – PhD thesis of Maitreyi Rathod

(European association for cancer research), held in Amsterdam, Netherlands from 30<sup>th</sup> June to 3<sup>rd</sup> July 2018.

2. **Maitreyi Rathod, Sushmita Chatterjee, Dibyendu Bhattacharyya and Abhijit De.** Functional sodium iodide symporter in breast cancer is regulated by N-linked mannose modifications. International congress of cell biology (ICCB), held in Hyderabad from 27<sup>th</sup> January to 31<sup>st</sup> January, 2018.
3. **Maitreyi Rathod, Shruti Dutta, Sushmita Chatterjee and Abhijit De.** Prying the intracellular path controlling iodine pump protein localization and function in breast cancer cells. XL All India cell biology conference (AICBC), held in Gwalior from 17<sup>th</sup> to 19<sup>th</sup> November, 2016.
4. **Madhura Kelkar, Maitreyi Rathod, Abhijit De.** Translational success of endogenous iodine pump protein (NIS) based targeted therapy in breast cancer may rely on its manoeuvrability by transcriptional modulations. A conference on new ideas in cancer- challenging dogmas, TMC platinum jubilee, held in Mumbai from 26<sup>th</sup> to 28<sup>th</sup> February 2016.

*M Rathod*

Signature of Student

Date: 10.12.19

Doctoral Committee:

S. No.	Name	Designation	Signature	Date
1.	Dr. Sorab N. Dalal	Chairman	<i>S. N. Dalal</i>	19/12/19
2.	Dr. Abhijit De	Guide/ Convener	<i>Abhijit De</i>	10-12-19
3.	Dr. Dibyendu Bhattacharyya	Member	<i>D. B. Bhattacharyya</i>	19-12-19
4.	Dr. Tanuja Teni	Member	<i>T. Teni</i>	19.12.19

Forwarded Through:

*S. V. Chiplunkar*  
26/12/19  
Chairperson, Academic &  
Training Programme, ACTREC  
**Prof. Dr. S. V. Chiplunkar**  
Chairperson, Academic &  
Training Programme, ACTREC

*S. D. Banavali*  
27/12/19  
Prof. S. D. Banavali,  
Dean (Academics)  
T.M.C.

PROF. S. D. BANAVALI, MD  
DEAN (ACADEMICS) 12  
TATA MEMORIAL CENTRE  
MUMBAI - 400 012.



## List of Figures

<b>Figure 1.1</b>	Illustration of Halsted surgery	37
<b>Figure 1.2</b>	Incidence of breast cancer subtypes based on race and age	39
<b>Figure 1.3</b>	Anatomy of mammary gland	41
<b>Figure 1.4</b>	Histological classification of breast cancer	44
<b>Figure 1.5</b>	Molecular subtypes of breast cancer	45
<b>Figure 1.6</b>	The secondary structure model of NIS	49
<b>Figure 1.7</b>	Physiological action of NIS in thyroid	50
<b>Figure 1.8</b>	Characterization of NIS promoter	51
<b>Figure 1.9</b>	Diagnostic application of NIS	52
<b>Figure 1.10</b>	Therapeutic application of NIS	54
<b>Figure 1.11</b>	Modulators of NIS expression in thyroid	56
<b>Figure 1.12</b>	NIS expression in lactating mammary gland of mice and breast cancer tissues	57
<b>Figure 1.13</b>	Functional NIS expression in primary and metastatic BC	57
<b>Figure 1.14</b>	Differential NIS expression across ER+ and ER- BC subtypes	58
<b>Figure 1.15</b>	Cerenkov luminescence principle	63
<b>Figure 1.16</b>	Non-invasive imaging of NIS gene function and expression in vivo	64
<b>Figure 2.3.1</b>	Cytotoxicity measurement of bHDACi on breast and thyroid cancer cells	76
<b>Figure 2.3.2</b>	Effect of bHDACi on cell proliferation and histone acetylation	77
<b>Figure 2.3.3</b>	NIS promoter activity is specifically enhanced in breast cancer cells	79
<b>Figure 2.3.4</b>	bHDACi positively regulate NIS expression in breast and thyroid cancer cells, in a differential manner	81
<b>Figure 2.3.5</b>	bHDACi differentially enhance the function of NIS in BC cells	82
<b>Figure 2.3.6</b>	HDAC1 is a negative regulator of NIS expression in BC cells	83
<b>Figure 2.3.7</b>	TF profiler and promoter binding array unfolds differential TF activation and binding in MCF-7 cells	85
<b>Figure 2.3.8</b>	FOXA1 shows differential expression in breast versus thyroid cancer	87
<b>Figure 2.3.9</b>	FOXA1 positively modulates NIS expression in MCF-7 cells	88
<b>Figure 2.3.10</b>	Enhanced NIS function leads to an increase in <sup>131</sup> I mediated DSB in breast cancer cells	90
<b>Figure 2.3.11</b>	<sup>131</sup> I mediated radio ablation effect is differentially enhanced in breast cancer cells	91
<b>Figure 2.3.12</b>	MS-275 and AR-42 induce NIS expression in in vivo breast tumour model	92
<b>Figure 2.3.13</b>	AR-42 induce NIS promoter activity at non tumorigenic sub optimal dose in breast tumour model in vivo	94
<b>Figure 2.3.14</b>	MS-275 differentially regulates NIS expression in non-breast organs and cells	96
<b>Figure 2.3.15</b>	bHDACi augments NIS mediated <sup>131</sup> I therapy in breast tumours	97
<b>Figure 2.3.16</b>	MS-275+ <sup>131</sup> I treated breast tumours have a higher accumulation of <sup>131</sup> I	98
<b>Figure 2.4.1</b>	Schematic illustrating the bHDACi mediated regulation of NIS across breast and thyroid cancer cells	102
<b>Figure 3.3.1</b>	CREB activation leads to elevation of NIS promoter activity	108

<b>Figure 3.3.2</b>	Activated CREB enhances endogenous NIS expression in breast cancer cells	110
<b>Figure 3.3.3</b>	Inhibition of PKA decreases NIS expression	112
<b>Figure 3.3.4</b>	pCREB physically interacts with NIS promoter	114
<b>Figure 3.4.1</b>	Diagrammatic representation of the modulatory role of cAMP-PKA-CREB pathway for NIS gene regulation in BC cells	117
<b>Figure 4.3.1</b>	The effect of BFA on Golgi morphology	124
<b>Figure 4.3.2</b>	Breast adenocarcinoma cell show impaired trafficking of NIS through cellular compartments	126
<b>Figure 4.3.3</b>	NIS overexpression in MCF-7 cells leads to clonal heterogeneity and differential sub cellular localization of NIS	128
<b>Figure 4.3.4</b>	NIS follows differential sub cellular trafficking path in MCF-7 and its clones	130
<b>Figure 4.3.5</b>	EGFR follows conventional trafficking pathway in MCF-7 cells	132
<b>Figure 4.3.6</b>	NIS association with calnexin is lower in cells with membranous NIS expression	134
<b>Figure 4.3.7</b>	N-linked glycosylation controls the localization of NIS to plasma membrane	136
<b>Figure 4.3.8</b>	Genes encoding enzymes for N-linked glycosylation, show a differential expression across membrane versus cytoplasmic cell clones	138
<b>Figure 4.3.9</b>	Lack of mannosidase enzymes in BC cells leads to mis-localization of NIS	140
<b>Figure 4.3.10</b>	MAN1A1, MAN1B1 and MAN2A1 together regulate the sub cellular localization of HER3 in MCF-7 cells	141
<b>Figure 4.3.11</b>	NIS represents the mannose rich subtype of glycoproteins	143
<b>Figure 4.4.1</b>	Diagrammatic representation of differential NIS protein trafficking across cytoplasmic and membrane over-expressing cell population	148

### List of Tables

<b>Table 1.1</b>	TNM (tumour, nodes, and metastases) classification for staging of invasive breast carcinoma	43
<b>Table 1.2</b>	Therapeutic approaches for different breast cancer subtypes	47
<b>Table 1.3</b>	Natural bioluminescence sources	61
<b>Table 2.1</b>	Benzamide class HDAC inhibitors selected for the study, showing their respective HDAC targets in the cell and the different clinical trials they belong as anti-tumour agents	70
<b>Table 3.1</b>	CREB binding sites on NIS promoter sequence	107
<b>Table 3.2</b>	PCR conditions for CHIP- PCR for CRE amplification on NIS promoter	107

## Abbreviations

1	Brefeldin A	BFA
2	Endoplasmic Reticulum	ER
3	Endoplasmic Reticulum exit site	ERES
4	Deoxymanojirimycin	DMM
5	Swainsonine	SW
6	Kilo dalton	kDa
7	3, 3'-diaminobenzidine tetra hydrochloride	DAB
8	4, 6'-diamidino-2-phenylindole	DAPI
9	Alpha fetoprotein	AFP
10	Aromatase inhibitors	AIs
11	All-trans retinoic acid	atRA
12	Basic-leucine zipper	b-ZIP
13	Bioluminescence imaging	BLI
14	Bovine serum albumin	BSA
15	Breast cancer	BC
16	Breast cancer gene 1	BRCA1
17	Carbamazepine	CBZ
18	Cerenkov luminescence imaging	CLI
19	Cerenkov radiation	CR
20	Charge-coupled device	CCD
21	Chicken beta-actin	CAG
22	Chromatin immunoprecipitation	ChIP
23	cAMP responsive element binding protein	CREB
24	Cutaneous T cell Lymphoma	CTCL

25	Cytokeratin	CK
26	Cytomegalovirus	CMV
27	Dexamethasone	Dex
28	Doxorubicin	Dox
29	Dual Oxidase 2	DUOX2
30	Ductal carcinoma in situ	DCIS
31	Epidermal growth factor receptor	EGFR
32	Estrogen Response Element	ERE
33	Estrogen receptor	ER
34	Estrogen receptor alpha	ER $\alpha$
35	Food and Drug Administration	FDA
36	Foetal bovine serum	FBS
37	Fine needle aspiration	FNA
38	Firefly luciferase	Fluc
39	Formalin fixed paraffin embedded	FFPE
40	<i>Gaussia</i> luciferase	Gluc
41	Glucose transporters	GLUTs
42	Glyceraldehyde- 3-phosphate dehydrogenase	GAPDH
43	Green fluorescent protein	GFP
44	Hank's Balanced Salt Solution	HBSS
45	Hepatocellular carcinoma	HCC
46	Histone acetyltransferases	HATs
47	Histone deacetylases	HDACs
48		HDACi

	Histone deacetylase inhibitors	
49	Horse radish peroxidase	HRP
50	Human epidermal growth factor receptor	HER2
51	Human sodium iodide symporter	NIS
52	Immunohistochemistry	IHC
53	Infiltrating ductal carcinoma	IDC
54	Inflammatory breast cancer	IBC
55	Insulin-like growth factor	IGF
56	Interleukin	IL
57	Interferon- $\gamma$	IFN- $\gamma$
58	Magnetic Resonance Imaging	MRI
59	Matrix metalloproteinases	MMPs
60	Mean fluorescence intensity	MFI
61	Molecular imaging	MI
62	Near-infrared	NIR
63	NIS upstream enhancer	NUE
64	Optical imaging	OI
65	Papillary thyroid carcinoma	PTC
66	Peroxisome proliferator-activated receptor- $\gamma$	PPAR $\gamma$
67	Phosphate buffered saline	PBS
68	Pituitary Tumour-transforming gene	PTTG
69	PTTG-binding factor	PBF
70	Positron emission tomography	PET
71	Pregnane X receptor	PXR

72	Progesterone receptor	PR
73	Prostate specific antigen	PSA
74	Protein kinase-A	PKA
75	Real time polymerase chain reaction	RT-PCR
76	Region of interest	ROI
77	Relative light units	RLUs
78	<i>Renilla</i> luciferase	Rluc
79	Response elements	RE
80	Retinoic acid	RA
81	Retinoic Acid Receptor	RAR
82	Single photon emission computed tomography	SPECT
83	Sodium butyrate	NaB
84	Sodium iodide symporter	NIS
85	Solute carrier	SLC
86	Suberoylanilide hydroxamic acid	SAHA
87	Terminal ductal lobular unit	TDLU
88	Thymidine kinase	TK
89	Thyroglobulin	Tg
90	Thyropoxidase	TPO
91	Thyroid transcription factor-1	TTF-1
92	Thyroid stimulating hormone	TSH
93	Thyroxine	T4
94	Triple negative breast cancer	TNBC
95	Transcription factor	TF

96	Transforming growth factor- $\beta$ 1	TGF- $\beta$ 1
97	Trichostatin A	TSA
98	Triiodothyronine	T3
99	Tris borate saline-tween20	TBST
100	TSH receptor	TSHR
101	Tubastatin A	TBA
102	Tumour necrosis factor $\alpha$	TNF- $\alpha$
103	Ultraviolet	UV
104	Valproic acid	VPA

**CHAPTER 1:**

*Introduction and Review of Literature*

## 1.1 Chronicles of breast cancer:

The first reports of breast cancer date back to 3500 years. Edwin Smith Surgical Papyrus and the Ebers Papyrus were the ancient Egyptian medical records which described the conditions of breast cancer which correlate with the modern descriptions. Ebers Papyrus reported “swollen vessels”, from 39 cases of breast cancer [19]. 460 BCE was the era of Hippocrates, who was regarded as the father of western medicine. Hippocrates put forward the “humoral theory” of cancer, where he postulated that the accumulation of black bile leads to breast cancer. Hippocrates for the first time coined the term “karkinos” which means crab, due to the crab like appearance of breast cancer [19]. Roman physicians started treating breast tumours with hot cautery and mastectomy. Galen introduced the concept of chemotherapy i.e. the use of castor oil, sulphur, licorice for breast cancer treatment, as surgery was prohibited by catholic churches in those days. The humoral theory for cancer faced a large number of criticisms in the beginning of 17<sup>th</sup> century, where a Dutch professor Francois de la Boe Sylvius, also called Franciscus Sylvius, Paris physician Claude-Deshais Gendron started opposing this theory. Following which John Hunter proposed lymphatic theory for breast cancer, which states that the coagulation of lymph leads to palpable breast tumours. John Hunter is considered as the father of surgery as he introduced lymph node resection as a part of breast cancer surgery. Virchow in early 1900 demonstrated that tumours were composed of cells. William Halsted, was a professor of surgery at John Hopkins, who introduced different methods of surgery. The most important was radical mastectomy, where along with breast tumour resection, Halsted surgery also included removal of axillary lymph nodes in 1882.

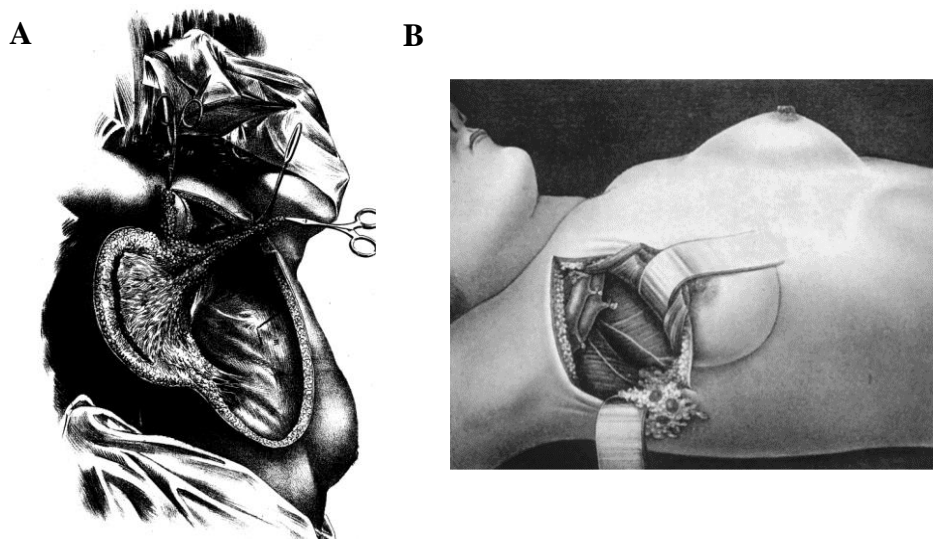


**Figure 1.1 : Illustration of Halsted surgery :** *A. Image depicting mastectomy of breast cancer [20] B. Axillary lymph node resection prior to mastectomy [21].*

The incidences of local recurrence also decreased dramatically with this surgical procedure. Radical mastectomy remained one of the gold standard surgery method from 19<sup>th</sup>-20<sup>th</sup> surgery [20]. The cure to breast cancer shifted its attention from surgery to hormonal therapy, after a landmark publication by Thomas Beatson in 1896, where he demonstrated regression of metastatic breast cancer after surgical oophorectomy. He put forward a theory based on his observations that certain factors from the ovary, favour the growth of breast Tumours [22]. Hence he was titled as the father of hormonal therapy.

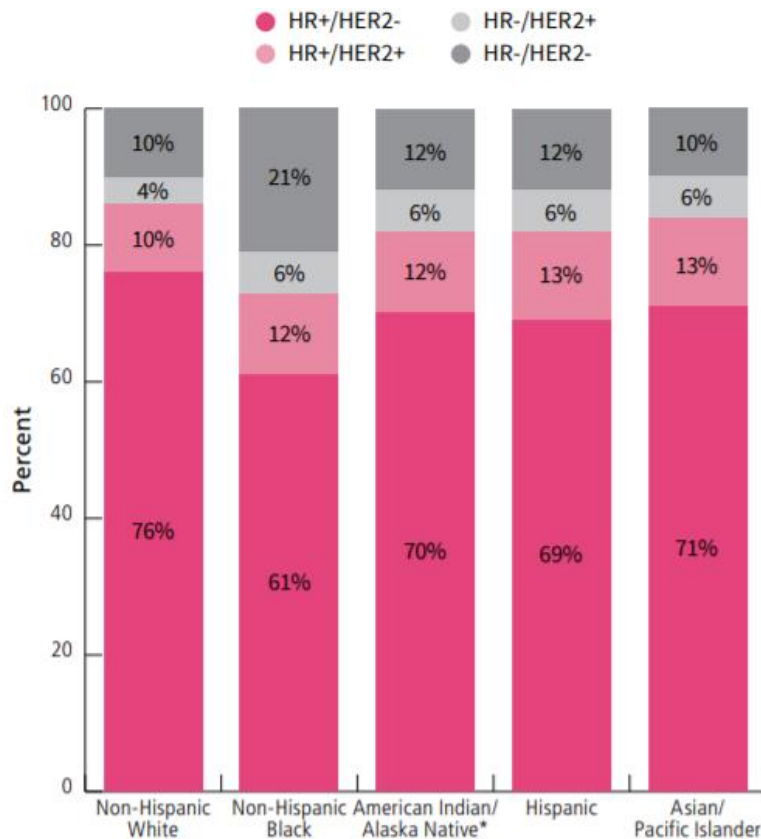
After the discovery of X-rays by Wilhelm Conrad Röntgen [23] from 1930, radiation therapy became an important addition to the treatment strategies alongside radical mastectomy. Many surgeons like Geoffrey Keynes and George Pfahler used radium implants and showed improved 5 year survival of 80% stage 1 patients [19]. The discovery of X-rays by Roentgen not only helped in radiation therapy, but also laid the base for mammography. Albert Salomon, a German surgeon, performed X-ray mammography of tumour samples and found micro calcifications along with major differences between normal and tumour tissues [24]. Robert

Egan used mammography to diagnose 53 patients in 1962, and is known as the father of modern mammography [19]. The entire field of breast cancer treatment changed after Dr. Bernard Fisher for the first time introduced clinical trials and the use of statistical analysis for treatment. He strongly opposed Galen theory and hypothesised that cancer begins from cells. Some cells disseminate from primary tumour and travel to distant sites through blood or lymph system, thus surgery alone cannot cure breast cancer [25]. He conducted many randomised clinical trials with the use of lumpectomy [26]. He quoted that “for the first time, the treatment of breast cancer was based on science rather than on anatomic and mechanistic principles” [25]. 1980s is considered as an important era of drug discovery, where in 1977 FDA approved tamoxifen for the treatment of metastatic ER receptor positive breast cancer. In 1986 FDA also approved tamoxifen for adjuvant therapy in post-menopausal women [27]. Following which important landmark discoveries took place that form modern medicine for breast cancer. Herceptin was approved by FDA in 1998, breast cancer subtypes were established in 2000, fulvestrant approved in 2002, lapatinib in 2010 [19].

## 1.2 Breast cancer epidemiology

Breast cancer is a challenging disease to deal with due to its heterogeneous nature. The incidences of breast cancer across the world is increasing at an alarming rate, with a record of 1,384,155 new cases recorded in 2008 and 459,000 deaths, which increased to 522,000 deaths by 2012. Breast cancer is the most common female cancers across the globe which accounts for 25% of the cancer burden [28]. As per GLOBOCON 2012 data, India, U.S and china account for one third of the BC burden worldwide. The breast cancer related deaths in India are high and similar to the death rate in UK i.e. 12.7 per 100000 women [29]. In 2017, 252,710 cases of IDC and 6,341 cases of DCIS were reported in U.S [30]. Breast cancer occurrence depends upon various factors like race, ethnicity, age, hormonal status, developed

or underdeveloped countries, lifestyle, hereditary for example the incidence rate is 27 per 100000 in Africa and east Asia whereas America has an incidence rate of 92 per 100000 [31]. The breast cancer incidences increase with age [32]. Individuals harbouring BRCA1 mutations are more prone to developing receptor negative breast cancer by the age of 70 [33].



HR = hormone receptor, HER2 = human epidermal growth factor receptor 2. Statistics based on data from PRCA counties.

Source: NAACCR, 2019.

©2019, American Cancer Society, Inc., Surveillance Research

**Figure 1.2: Incidence of breast cancer subtypes based on race and age (Adapted from American cancer society, breast cancer facts and figures 2019-2020**

<https://www.cancer.org/content/dam/cancer-org/research/cancer-facts-and-statistics/breast-cancer-facts-and-figures/breast-cancer-facts-and-figures-2019-2020.pdf>) : Chart showing the percentage of incidences of different breast cancer subtypes across different ethnicities and age

### 1.3 Anatomy of normal breast

The milk streak or the mammary ridge develops in the fifth week during gestation along the trunk from either side of axilla. The mammary gland is made up of lobules which drain into a system of ducts. The ducts end at the areola which surround the nipples. The lobules and ducts are connected by inelastic fibrous structures. Mammary gland is attached to the chest wall by pectoralis muscles. Each duct terminates into tubuloalveolar glands organized into lobes. The lobes have an outer myoepithelium layer which provides support to the lobules and assist in milk ejection during lactation [34]. The inner layer is the luminal epithelium, which secrete milk during lactation. The blood supply to the breast is majorly from the internal thoracic artery, which forms vessels that perforate the chest wall, and the axillary arteries. The axillary and internal thoracic also form the lymphatic drainage for breast. The internal mammary lymph nodes are generally small (2-3mm) and lie along the internal thoracic vessels. However 75% of the lymphatic drainage from the breast takes place through the axillary lymph nodes [35].

#### Breast anatomy and histology

Eric Wong

Clin Obstet Gynecol. 2011 Mar;54(1):91-5.

The breast is composed of glandular and stromal tissue. Glandular tissue includes the ducts and lobules. **Stroma** comprises area between lobes.

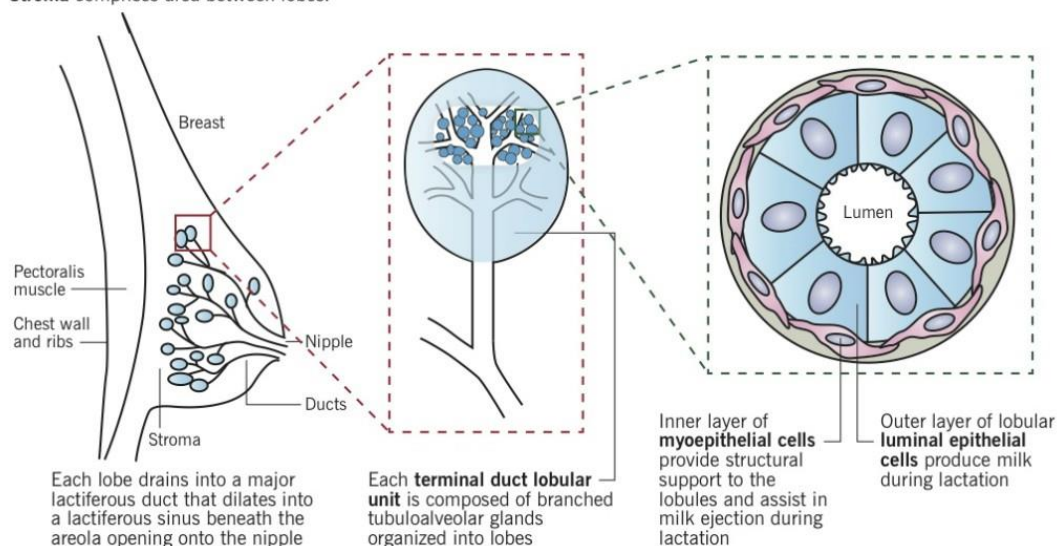


**Figure 1.3: Anatomy of mammary gland** (<http://www.pathophys.org/breast-cancer/>): Schematic diagram showing the anatomy of breast, which is divided into lobules and ducts within the stroma.

#### 1.4 Histological classes of breast cancer

The breast cancer is classified into two major types based on the tissue of origin i.e. lobular or ductal. The second criteria is whether the tumour is restricted to the epithelial boundaries (in situ) or has invaded the stroma of the breast (invasive). Thus broadly 3 major types fall under this classification system [36]

- **Ductal carcinoma in situ (DCIS)**

DCIS is the neoplastic transformation of epithelial cells associated with ducts. DCIS patients are at high risk of developing invasive carcinoma as compared to non DCIS cases. They have a comedo, solid, cribriform, papillary, and micropapillary type morphological architecture. Deaths due to DCIS is very rare. The tumours are palpable in nature, as they form a solid mass. DCIS is generally marked by positive E-cadherin and  $\beta$  catenin and low keratin (CK8-18) expression [37].

- **Lobular carcinoma in situ (LCIS)**

LCIS is the intralobular proliferation of small cells in the terminal ductal lobular unit (TDLU). Unlike DCIS, these tumours do not have a dense solid mass, but are generally loosely bound cluster of proliferating cells. Unlike DCIS, LCIS is marked by low E-cadherin and  $\beta$  catenin and high keratin (CK8-18) expression. Only 1% of the LCIS cases have the risk of developing invasive cancer [37].

- **Invasive ductal carcinoma (IDC)**

IDC is the proliferating ductal cells which invade to the stroma. IDC accounts for 80% of the cases and invasive lobular carcinoma accounts for 10-15% of the cases. Majority of the IDC (75-80%) lack a definitive distinct morphology thereby histological classification of IDC is not done for these tumour types. IDC and ILC are further classified based on their molecular subtypes, tumour stage, and grade. The TNM grading system is widely accepted for tumour grading i.e T- Tumour size, N- Lymph node status and M- Metastasis to other organs (except lymph nodes) [37].

**TNM (Tumour, nodes, metastases) staging classification of invasive breast carcinoma (American Joint Committee on Cancer 7th edition)**

Stage	Description
	<b>Primary Tumour</b>
Tis	Carcinoma in situ
T1	Tumour <2 cm diameter
T2	Tumour 2-5 cm diameter
T3	Tumour >5 cm diameter
T4	Tumour (any size) fixed to skin or chest wall
	<b>Regional lymph nodes</b>
N0	No nodal metastases
N1	Mobile ipsilateral node(s) involved
N2	Fixed ipsilateral node(s) involved
N3	Ipsilateral internal mammary or supraclavicular node(s) involved
	<b>Metastases</b>

M0	No evidence of distant metastases
M1	The presence of distant metastases (supraclavicular lymph nodes, lung, brain, liver, bone) would result in a clinical M1 stage if the metastasis has been identified on clinical/radiological assessment alone. Pathological confirmation of distant metastases (via liver biopsy) is required for a pathological staging of pM1

**Table 1.1: TNM (Tumour, nodes, and metastases) classification for staging of invasive breast carcinoma:** Table showing the staging system of breast cancer based on the tumour size, lymph node and metastasis to distant organs as per TNM classification

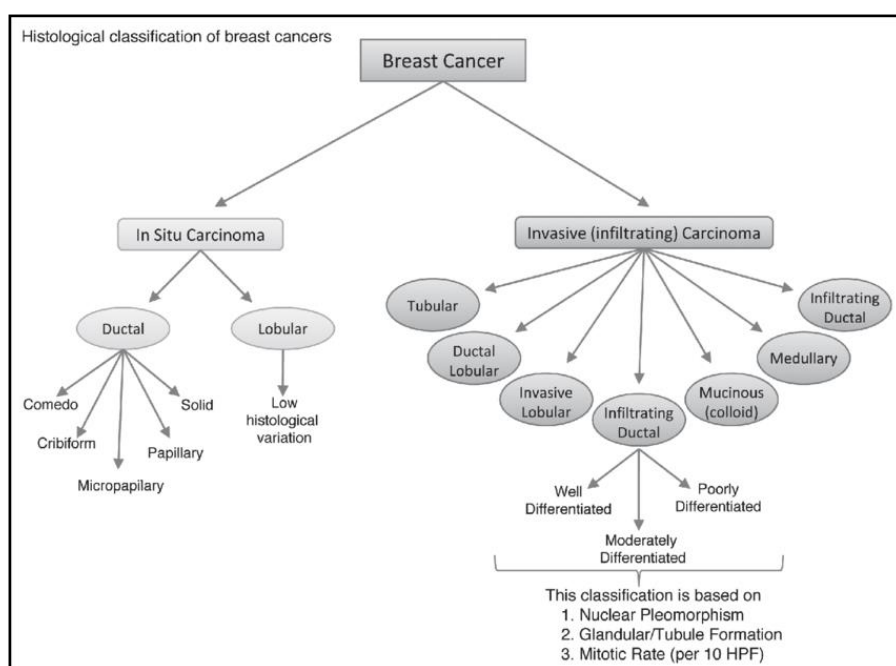


**Figure 1.4: Histological classification of breast cancer [36]:** Classification of breast cancer as per their site of origin and pathological behaviour i.e. invasive or non-invasive

## 1.5 Molecular subtypes of breast cancer

Breast cancer is classified into 4 major subtypes based on standard molecular markers present on these tumours. These molecular subtypes have different prognosis and vary in their pathogenicity. Hormone receptors ER and PR positive tumours are classified under luminal subtype, which is further divided into luminal A and luminal B. Luminal A are ER/PR+, HER2 low, ki67 low. These subtypes have the best prognosis compared to all other breast cancer subtypes and have the least tendency to metastasize. Luminal A comprises of 23% cases. Luminal B subtype on the other hand is ER/PR/HER2+ and Ki67 high, which accounts for 53% of the total breast cancer subtypes. These tumours are highly proliferative in nature and are more aggressive as compared to luminal A subtype. Patients harboring HER2 amplification are classified under HER2 subtype. These subtypes consists 23-30% cases. The last class is TNBC i.e. triple negative breast cancer, which as the name suggests is negative for all 3 markers ER/PR/HER2-. These are the most aggressive forms of breast cancer, since there is no receptor present for selective targeting. Also these tumours are associated with p53 and BRCA mutations, posing a great challenge for therapies. These tumours have a high propensity for distant metastasis to brain, lungs. These class accounts for only 10-12% of breast cancer cases [38, 39].

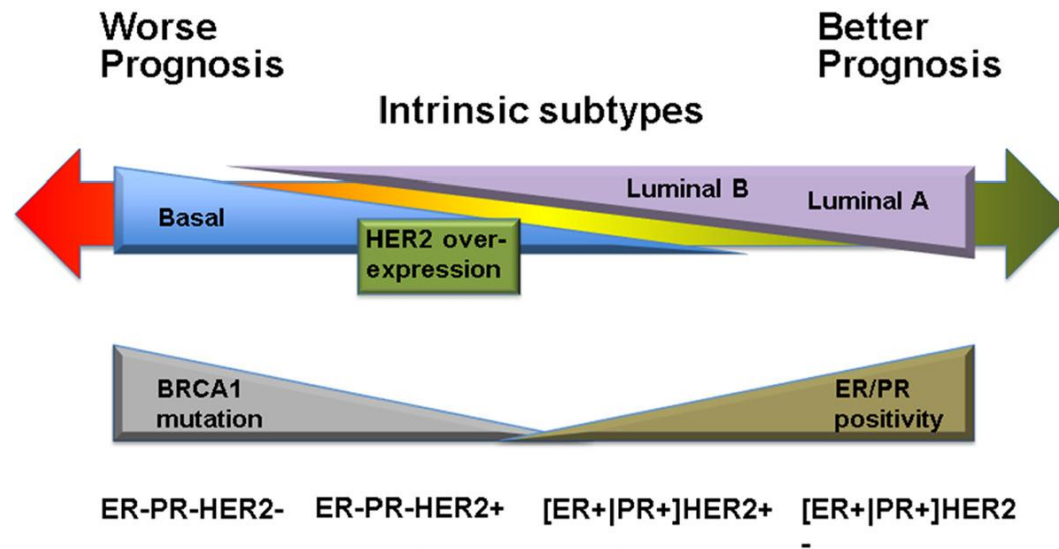


*Figure 1.5: Molecular subtypes of breast cancer [40]: Classification of breast tumours based on their molecular signatures i.e. hormone receptor positive, HER2 amplification and the association of these subtypes to their respective prognosis in clinics*

## 1.6 Disease management regimes for breast cancer

The major lines of therapy for breast cancer include surgery, radiation therapy, chemotherapy and targeted therapies. Chemotherapies are given either in adjuvant or neo-adjuvant settings depending on the tumour type and stage. Surgical removal of tumours include either mastectomy, lumpectomy or breast conservation surgery, which is decided by surgeons depending on the tumour location and size. Removal of axillary, sentinel lymph nodes along with primary tumour is a standard practice in clinics. The lymph node mapping during the surgical process is achieved with the help of methylene blue dye or indocyanin green dye [41]. Radiation therapy post-surgery is also an established therapeutic strategy for breast cancer, to prevent tumour recurrence after surgery. Radiation can be given as external beam radiation or internal (brachytherapy). External beam radiation can also be given intra-operative i.e. single beam radiation can be given during operation before closing the wound [42]. Classical

chemotherapy options for breast cancer include mainly taxols and anthracyclins based drugs. The commonly used chemotherapeutic agents are docetaxel, doxorubicin, cyclophosphamide, carboplatin, paclitaxel, gemcitabine and 5-FU [43]. Targeted therapies like Tamoxifen, which inhibits the estrogen receptor (ER) signalling, aromatase inhibitors like exemestane, anastrozole, and letrozole, which inhibits the conversion of androgens to estrogens thereby depleting estrogen in the body [44] and fulvestrant that is a specific ER inhibitor, are widely used for luminal subtype patients [44, 45]. Patients harbouring HER2 amplification i.e. the HER2 subtypes, are treated with targeted antibodies or small molecule inhibitors against HER2 [46]. Trastuzumab (specific anti-HER2 monoclonal antibody [mAb]) alone and in combination with chemotherapeutic agents [47], ado-trastuzumab emtansine which is trastuzumab conjugated with emtansine (microtubule inhibitor) [48], pertuzumab (specific anti-HER2 mAb with distinct binding site on HER2 extracellular region and lapatinib, which is a small molecule inhibitor of tyrosine kinase (TKI) that inhibits both HER2 and epidermal growth factor receptor (EGFR) signalling [49]. Patients falling under the TNBC subtype are generally treated with olaparib (PARP inhibitor) [50], anthracyclins, taxanes, bevacizumab (VEGF inhibitor) [51] [46].

	Hormone Receptor (HR) +/ERBB2-	ERBB2+ (HR+ or HR-)	Triple-Negative
Pathological definition	≥1% Of tumor cells stain positive for estrogen receptor or progesterone receptor proteins	Tumor cells stain strongly (3+) for ERBB2 protein or ERBB2 gene is amplified in tumor cells. Approximately half of ERBB2+ tumors are also HR+	Tumor does not meet any pathologic criteria for positivity of estrogen receptor, progesterone receptor, or ERBB2
Molecular pathogenesis	Estrogen receptor $\alpha$ (a steroid hormone receptor) activates oncogenic growth pathways	The oncogene ERBB2, encoding ERBB2 receptor tyrosine kinase from the epidermal growth factor receptor family, is overactive	Unknown (likely various)
Percentage of breast cancer cases, % <sup>12</sup>	70	15-20	15
Prognosis			
Stage I (5-y breast cancer-specific survival), % <sup>13,a</sup>	≥99	≥94	≥85
Metastatic (median overall survival) <sup>14-16,b</sup>	4-5 y	5 y	10-13 mo
Typical systemic therapies for nonmetastatic disease (agents, route, and duration)	<ul style="list-style-type: none"> <li>• Endocrine therapy (all patients): <ul style="list-style-type: none"> <li>• Tamoxifen, letrozole, anastrozole, or exemestane</li> <li>• Oral therapy</li> <li>• 5-10 y</li> </ul> </li> <li>• Chemotherapy (some patients): <ul style="list-style-type: none"> <li>• Adriamycin/cyclophosphamide (AC)</li> <li>• Adriamycin/cyclophosphamide/paclitaxel (AC-T)</li> <li>• Docetaxel/cyclophosphamide (TC)</li> <li>• Intravenous therapy</li> <li>• 12-20 wk</li> </ul> </li> </ul>	<ul style="list-style-type: none"> <li>• Chemotherapy plus ERBB2-targeted therapy (all patients): <ul style="list-style-type: none"> <li>• Paclitaxel/trastuzumab (TH)</li> <li>• Adriamycin/cyclophosphamide/paclitaxel/trastuzumab <math>\pm</math> pertuzumab (AC-TH<math>\pm</math>P)</li> <li>• Docetaxel/carboplatin/trastuzumab <math>\pm</math> pertuzumab (TCH<math>\pm</math>P)</li> <li>• Intravenous therapy</li> <li>• 12-20 wk of chemotherapy; 1 y of ERBB2-targeted therapy</li> </ul> </li> <li>• Endocrine therapy (if also hormone receptor positive) <ul style="list-style-type: none"> <li>• Tamoxifen, letrozole, anastrozole, or exemestane</li> <li>• Oral therapy</li> <li>• 5-10 y</li> </ul> </li> </ul>	<ul style="list-style-type: none"> <li>• Chemotherapy (all patients): <ul style="list-style-type: none"> <li>• AC</li> <li>• AC-T</li> <li>• TC</li> <li>• Intravenous therapy</li> <li>• 12-20 wk</li> </ul> </li> </ul>

**Table 1.2: Therapeutic approaches for different breast cancer subtypes** [42]: Table describing various chemotherapy/targeted therapy agents for different subtypes of BC patients with different pathological and molecular disease patterns..

## 1.7 Sodium Iodide Symporter (NIS)

Human sodium iodide symporter (NIS) is a member of solute carrier family of proteins (SLC) - SLC5A5. NIS is a membrane glycoprotein with 13 transmembrane domains. NIS has 3 putative N-linked glycosylation sites i.e. Asn 225, 485 and 497 on the extracellular NH<sub>2</sub>-terminus [52]. The intracellular COOH-terminus has a PDZ domain and dipeptide motifs that help in the intracellular localization of NIS. NIS contains many sorting signals on its COOH terminus, which are known in other proteins to regulate intracellular trafficking and sorting. NIS has a PDZ domain motif T/S-X-V/L, which is known for its involvement in protein-protein interactions. Additionally, NIS has a dileucine motif, L<sup>557</sup> L<sup>558</sup>, which is reported previously to

modulate trafficking of proteins within a cell [1]. Also, 3 acidic dipeptide motifs E<sup>573</sup>D<sup>574</sup>, E<sup>579</sup>E<sup>580</sup>, and E<sup>587</sup>D<sup>588</sup> are located on COOH terminus of NIS, which generally serve as retrieval signals for other proteins [53]. Some important amino acid positions have been identified which possibly modulate the function and trafficking of NIS as observed from studies on iodine transport defect (IDT) mutations. T354P mutant showed impaired function of NIS in thyroid, showing the importance of T354 position for the function of NIS. Additionally Q267E mutations showed impaired intracellular trafficking of NIS in thyroid [1,58, 59].

Earlier it was thought that NIS had 12 transmembrane domains with both NH<sub>2</sub> and COOH termini present at intracellular region, however later the secondary model stating 13 transmembrane domains was demonstrated and is the currently accepted model [53]. Electron microscopy experiments conducted showed 9nm intramembranous particles of NIS, which suggested the presence of NIS in oligomeric form. The molecular characterization of NIS was possible after its successful cloning in 1996 [54, 55]. The stoichiometry of NIS was determined to be 2:1 Na<sup>+</sup>/I<sup>-</sup>, by electrophysiological methods from *X. laevis* oocytes [56]. Additionally these authors also showed that the transport of both the ions was simultaneous in similar direction, thereby making NIS a symporter. Apart from iodine, NIS can also transport other ions like ClO<sub>3</sub><sup>-</sup>, SCN<sup>-</sup>, SeCN<sup>-</sup>, NO<sub>3</sub><sup>-</sup>, Br<sup>-</sup>, BF<sub>4</sub><sup>-</sup>, IO<sub>4</sub><sup>-</sup>, and BrO<sub>3</sub><sup>-</sup> [56]. NIS gene is located on chromosome 19 (19p13.2-p12). NIS gene is 1.3kb in size, composed of 15 exons interrupted by 14 introns, which encodes 643 amino acids [55]. Both human and rat NIS were characterized and found to be 84% identical and 93% similar to each other. Rat NIS encoded 618 amino acids, and was different from human NIS by a 20 amino insertion in the COOH terminus of human NIS. NIS, being a glycoprotein, has varying molecular weights as per the glycosylation status of NIS ranging from 55 kDa (non-glycosylated form of NIS) to 100 kDa (completely glycosylated mature form) [53, 57].

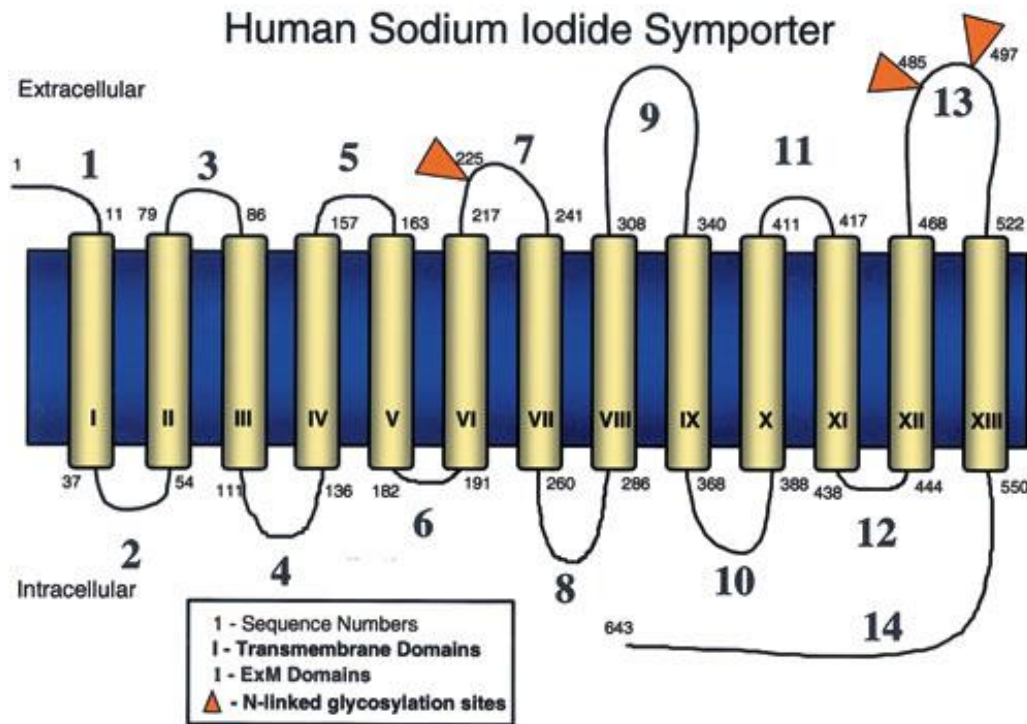


**Figure 1.6: The secondary structure model of NIS [60]:** Diagrammatic representation of the secondary structure of NIS showing 13 transmembrane domains of NIS indicated by roman numbers, orange flags depict the 3 putative N-linked glycosylation sites of NIS.

Physiologically, NIS is naturally expressed in the basolateral membrane of thyroid follicular cells, where it plays a role in transporting iodine into the follicular cells. NIS mediates active transport of iodine against its concentration gradient from the blood into the thyroid cells. This active transport is supported by the energy generated from  $\text{Na}^+/\text{K}^+$  ATPase pump which co- transports 2  $\text{Na}^+$  ions along the electrochemical gradient. Followed by which, iodide crosses the apical membrane and goes to lumen through pendrin transporter, where it is organified by thyroid peroxidase (TPO) and incorporated in the tyrosine residues of thyroglobulin (Tg). This is further converted to Triiodothyronine (T3) or Thyroxine (T4) thyroid hormones. The thyroid has 30-40 times higher iodine as compared to blood due to the functional NIS present [1]. NIS is also expressed in other organs like salivary gland, lactating mammary glands, stomach,

gastric mucosa, liver. The lactating mammary glands express NIS which helps in providing iodine in the colostrum for the newborn. However the physiological role of NIS in gastric mucosa and salivary gland is unknown.

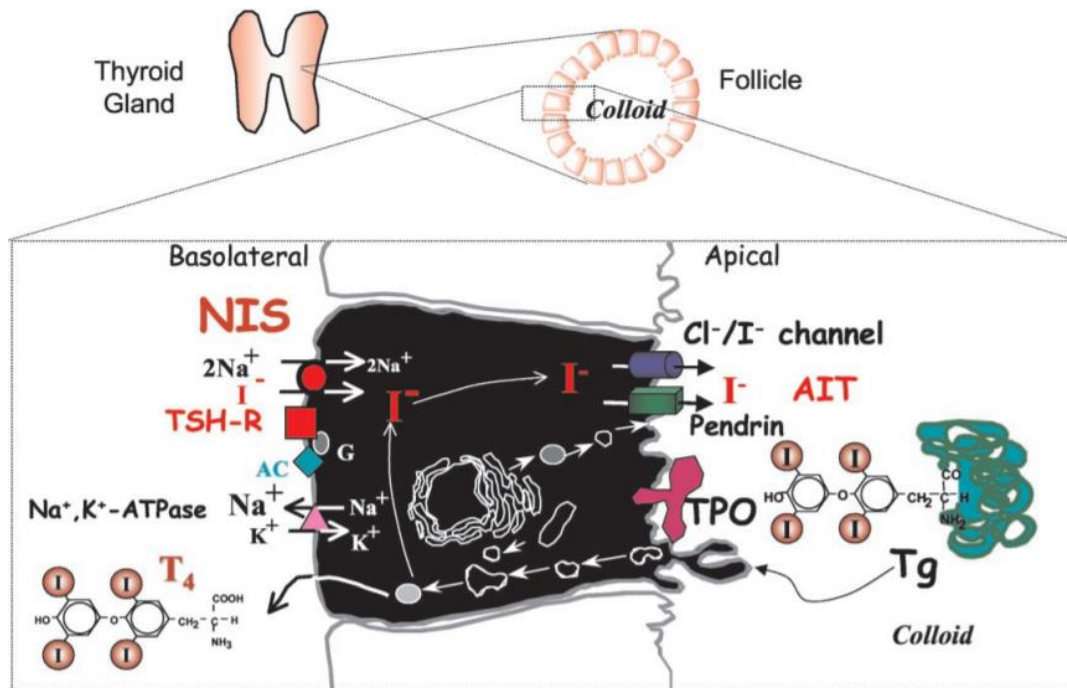


**Figure 1.7: Physiological action of NIS in thyroid [1]:** Schematic diagram explaining the physiological role of NIS mediated iodine transport across the basolateral membrane of thyroid, which is organized and used for T3, T4 synthesis.

The characterization of NIS promoter from rat and human NIS, revealed an upstream enhancer region (NUE) from -9847 to -8968bp positions in human NIS and -2495 to -2264 positions in rat NIS, with respect to the start codon of NIS. Rat NIS has 2 PAX8 transcription factor start sites in the enhancer region and a CRE element. Human NIS has Pax8, CRE element and TTF-1 (thyroid transcription factor-1) binding sites in the NUE [61]. Disruption of pax8 sites in rat NIS showed loss in NIS transcriptional activity, indicating the importance of Pax8 for NIS expression. Along with Pax8, b-ZIP family of TF especially CREB and AP-1 bind to CRE sites

and mediate NIS transcription in thyroid. NIS proximal promoter region contains TATA box elements [62-64].

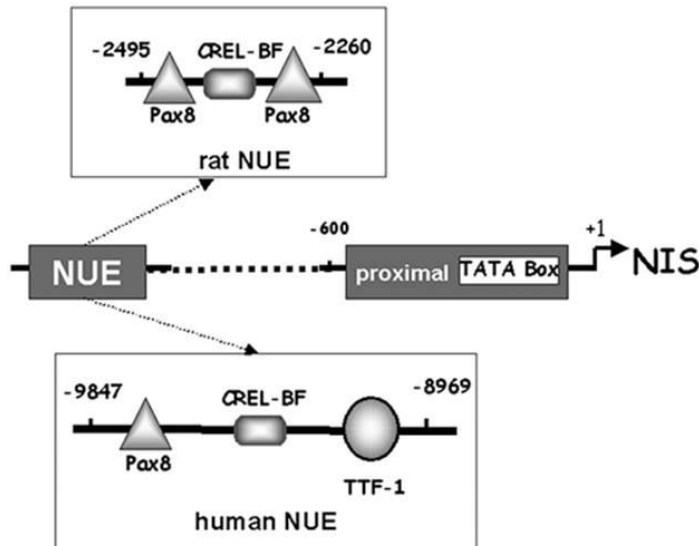


**Figure 1.8: Characterization of NIS promoter:** Structure of NIS proximal promoter and upstream enhancer region (NUE) from rat and human derived NIS gene. NUE from both species shows differential binding sites for transcription factors.

## 1.8 Discovery of NIS

The keen observations of the thyroid gland capable of accumulating iodine 20-40 times more as compared to bloodstream [65], raised a curiosity regarding the presence of a transport system in the cells. Iodine being a scarce element found in nature, lead to many diseases related to insufficient iodine in the body like endemic goitre and cretinism. The use of iodine to treat these diseases started, where a trial was conducted for goitre and cretinism in which patients received iodized oil and saline. The group treated with iodine showed an excellent response in reducing the disease load [66]. Thus the idea of administering external iodine came into picture. A breakthrough study took place when grave's disease patients were treated with radioactive iodine and showed a phenomenal response. Thus the advent of utilizing radio-active isotopes

for treatment started. Subsequently NIS was identified as the transporter responsible for the accumulation of iodine in thyroid [53]. Following which this radioactive iodine mediated therapy was applied successfully to thyroid cancer patients after thyroidectomy [67].

### 1.9 NIS as a diagnostic target for cancer

NIS became a promising theranostic molecule due to its ability to transport various radioactive isotopes of iodine like  $I^{123}$ ,  $I^{124}$ ,  $I^{125}$  that are used for diagnostic purpose through scintigraphy, PET and SPECT imaging respectively and  $I^{131}$  which serves for therapeutic application. The major advantage of using NIS as a reporter gene is that it allows non-invasive, quantitative imaging in real time [68-70]. The first demonstration of NIS mediated imaging was done by transfecting the rat NIS cDNA in FRTL cells [71]. NIS mediated imaging forms a strong platform not only for tumour imaging but also other applications like cardiac imaging. Stable expression of NIS in cardiac stem cells helps dynamic real time imaging of heart functions by  $I^{125}$  mediated SPECT [72]. Similarly NIS can be used to image trafficking of cells, recruitment of macrophages to the site of inflammation [73, 74]

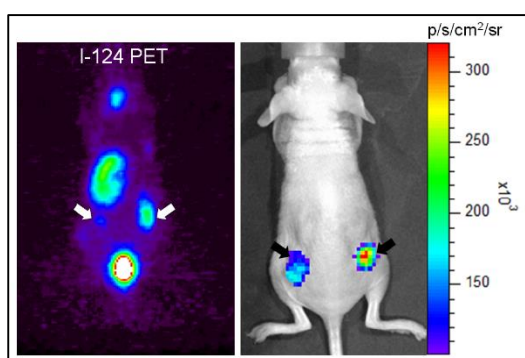


**Figure 1.9: Diagnostic application of NIS [75]:** PET scan showing  $I^{124}$  uptake in breast tumour xenografts (indicated by arrow), thyroid and stomach region of mice on the left side and corresponding bioluminescence image on the right side showing tumour.

### 1.10 Therapeutic application of NIS in thyroid cancer

Total thyroidectomy followed by radio iodine therapy for primary and metastatic thyroid cancer, is a successful clinical practice past seventy years. Well differentiated thyroid cancers have sufficient NIS expression for assisting in gamma camera imaging with  $I^{123}$  and  $I^{124}$  mediated PET imaging [76]. Following which, the residual lesions are treated with radioactive  $^{131}I$  which has DNA damaging abilities. Apart from treating the primary tumour, the metastatic lesions which retain functional NIS can also be ablated using  $^{131}I$ . This strategy helps in reducing the rate of recurring disease up to a great extent, thereby improving the overall survival of patients. In poorly differentiated thyroid cancer subtypes and metastatic cancers, NIS expression is compromised. Thus an inducer of endogenous NIS expression is required. Thyroid stimulating hormone (TSH) is the currently used inducer for NIS in thyroid cancer which can lead to an increase in NIS expression and cell surface localization. TSH treatment also enhances the stability of membranous NIS in thyroid cancer cases which can augment the function of NIS [77, 78]. Repeated cycles of TSH followed by  $^{131}I$ , is a fruitful means of curing the primary as well metastatic thyroid cancer. TSH levels can be induced in thyroid cancer by T4 withdrawal. Studies have also shown that various inhibitors of oncogenic signalling pathways like PI3K and MAPK can induce NIS expression in thyroid cancer cells [2]. Various other molecules like HDAC inhibitors [79], anti HIV drug nevirapine (reverse transcriptase inhibitor) [80] have also shown promising results in term of elevating the function of NIS in thyroid cancer. Together these findings open avenues for NIS mediated therapy in cases with compromised NIS function for thyroid.

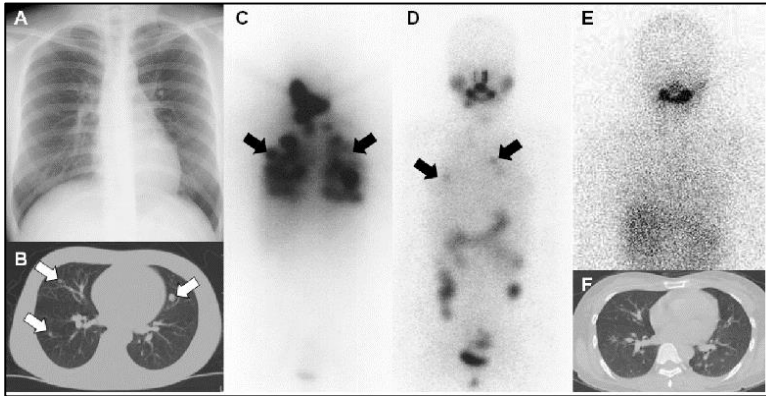


**Figure 1.10: Therapeutic application of NIS [75]:** Case report showing metastatic lesions of thyroid cancer in lungs from image A, which subsequently get cleared after repetitive cycles of  $^{131}\text{I}$  treatment as demonstrated by scintigraphy imaging in figure C,D and E.

### 1.11 NIS mediated gene therapy for non-thyroidal malignancies

Exogenous NIS gene mediated radioiodine therapy was applied to a number of cancers of non-thyroidal origin. Virus mediated approaches for gene delivery to tumour sites were achieved with the help of adenovirus, baculovirus and retrovirus transduction systems. Adenovirus mediated delivery of NIS gene *in vivo* for prostate cancer xenografts, using both human and rat NIS showed inhibition of tumour growth after intra-tumoural  $^{131}\text{I}$  administration [81]. Stable expression of adenovirus-NIS gene in prostate cancer cells, enhances the retention of  $^{131}\text{I}$  and causes 84% tumour ablation after a single dose of  $^{131}\text{I}$  [82]. Baculovirus mediated delivery of NIS gene to colon cancer cells also showed  $^{131}\text{I}$  induced cell death [83]. Similarly, adenovirus mediated NIS gene therapy was also demonstrated in ovarian cancer xenografts, which also showed tumour ablation effects [84]. Self-inactivating lentiviral constructs were developed for efficient gene delivery in a tissue specific manner with the help of suitable promoters such as immunoglobulin promoter for myeloma, alpha fetoprotein (AFP) for liver cancer [85, 86]. Although BC has endogenous NIS expression, its function is severely compromised, thus

exogenous NIS gene delivery has been attempted in BC. MUC1 promoter driven conditional adenoviral system was generated, where the virus would only replicate in MUC1 positive cells. T47D BC cells were used for the same and effective radio iodine therapy was demonstrated using this approach [87]. This NIS gene mediated radio-iodine therapy, could be further augmented by treating the BC cells with ATRA and gemcitabine [88]. Additionally, the use of non-replicative virus under human telomerase subunit promoters were also used, to achieve tumour specific expression. Non-viral methods of gene delivery like polyplexes coupled to an EGFR were used to target HCC [89], mesenchymal stem cell (MSC) mediated gene delivery to metastatic colon cancer and breast cancer [90], and extracellular vesicles (EV) are also being used for effective radio-iodine mediated killing of tumour cells [91].

### **1.12 Regulation of NIS in thyroid**

NIS regulation in thyroid is well characterized. TSH is the primary regulator of NIS function, membrane localization and stability in thyroid. TSH withdrawal from cells, leads to impaired membrane localization of NIS in cells, thereby reducing its functional ability. Also TSH treatment increases the stability of NIS from 3 days to 5 days in thyroid cells. TSH mediated induction of NIS include molecular regulators like PAX8, CREB/CREM which directly bind to the NUE and proximal promoter region of NIS, to enhance its transcription. cAMP activates PKA, which in turn activates ERK through Rap-1-MEK, p38 through Rac1-MKK and CREB transcription factor. P38, CREB and ERK show downstream activation of NIS transcription. PI3K pathway shows a negative regulatory effect on NIS expression unlike in case of BC, where PI3K acts as a positive modulator. Epigenetic modulators like HDAC inhibitors are known inducers of NIS in TC [2].

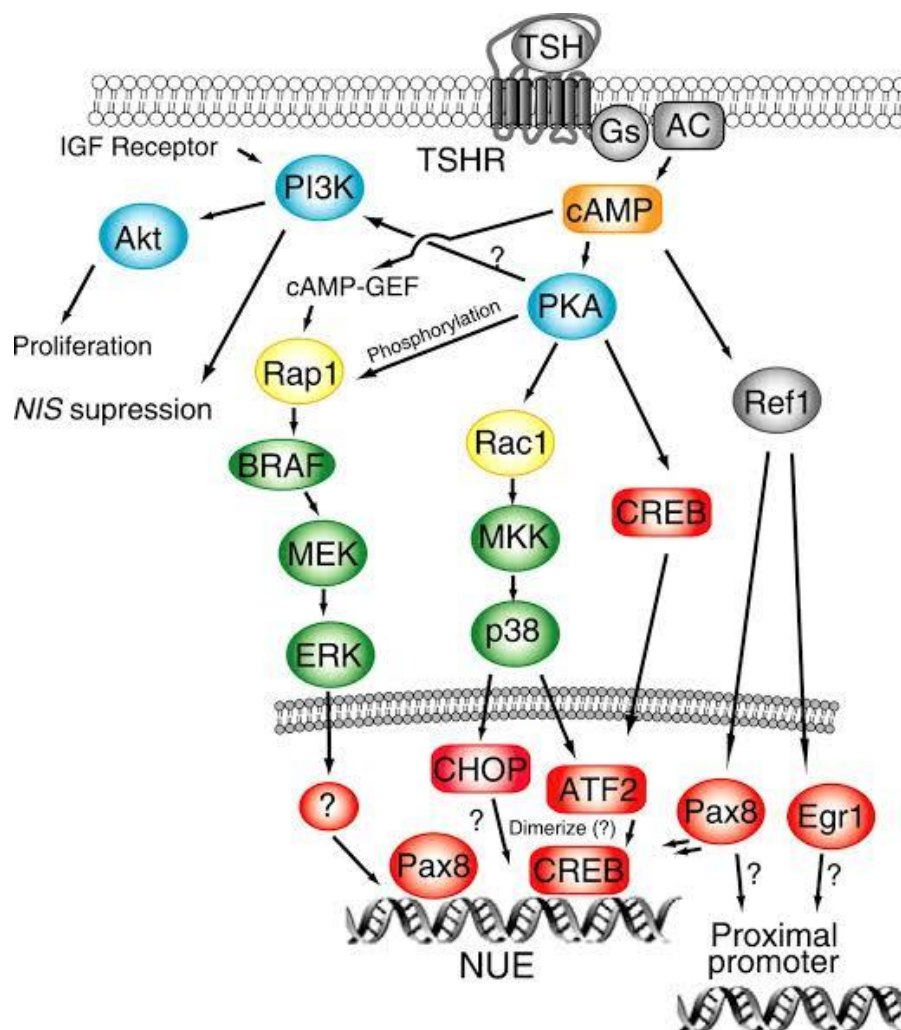


**Figure 1.11: Modulators of NIS expression in thyroid [2]:** TSH mediated signalling shows the role of cAMP-PKA pathway, MEK-ERK, CREB and Pax8 in regulating NIS expression in thyroid cells.

### 1.13 Expression of NIS in breast cancer

NIS expression in breast cancer (DCIS) was first demonstrated by Tazebay et al in 2000. Through this work, they also reported the presence of NIS in normal mammary glands during the lactation phase in mice. 80% BC cases tested, showed a positive staining of NIS [3].

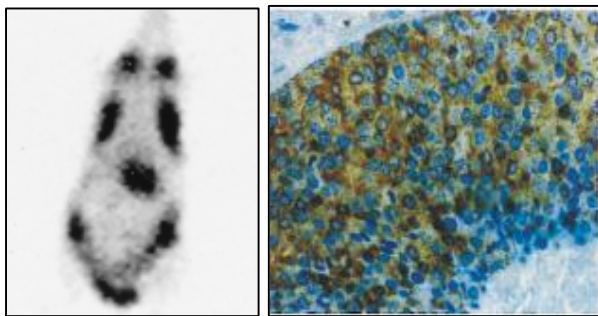


**Figure 1.12: NIS expression in lactating mammary gland of mice and breast cancer tissue [3]:** Autoradiography image of mammary fat pad of lactating mice showing NIS positivity (left), IHC image showing expression of NIS in breast tissues (right).

Later, many groups reported the presence of NIS in BC, but  $^{99m}\text{Tc}$  uptake study showed that only 4 of 24 patients had functional NIS [4]. Radio-iodine uptake detected by scintigraphy imaging, was seen in 25% of metastatic breast cancer tissues [6, 88]. This compromised function of NIS reported by several groups, correlates with a reduced expression of NIS on the cell surface [7, 92]. Detailed analysis of 202 patient samples from invasive and ductal in situ cases, revealed 76% and 88% NIS positive samples from invasive and DCIS respectively [93]. However, majority of them showed cytoplasmic staining of NIS. This fact was also confirmed by another group, where only 25% of the total patient samples analysed showed membranous NIS expression, while 75% showed cytoplasmic staining of NIS [57].

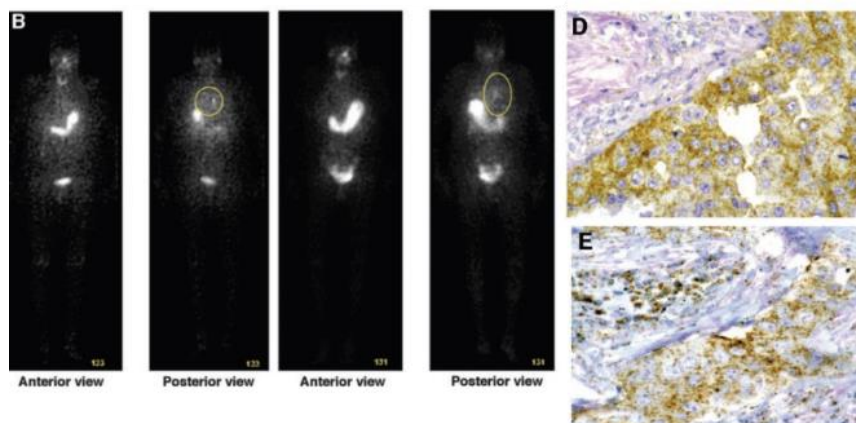


**Figure 1.13: Functional NIS expression in primary and metastatic BC [4]:** SPECT image showing the metastatic lesions of breast cancer, indicating the presence of functional NIS (left), IHC image showing NIS expression in primary and metastatic breast tumour samples.

Report from our own group in 2013, established a co-relation between the hormone receptor positive BC subtypes with NIS expression and found that the ER positive subtypes had higher NIS expression than ER negative subtypes. From this study also, it was observed that majority of the patient samples tested showed cytoplasmic localization of NIS with the same antibody which showed membrane staining of NIS in salivary gland or thyroid tissue. Even though 70% of the patient samples showed NIS positivity, only 30% of the cases showed high positive (2+/3+) score for NIS [7]. Thus from these studies, the clinical limitations of using NIS mediated therapy were noticed, of which defective localization of NIS to cytoplasm and insufficient expression of NIS, are the prime concerns. Thus studies attempting to understand the molecular defects associated would help resolve these limitations and take NIS mediated therapy to the bench for BC patients.

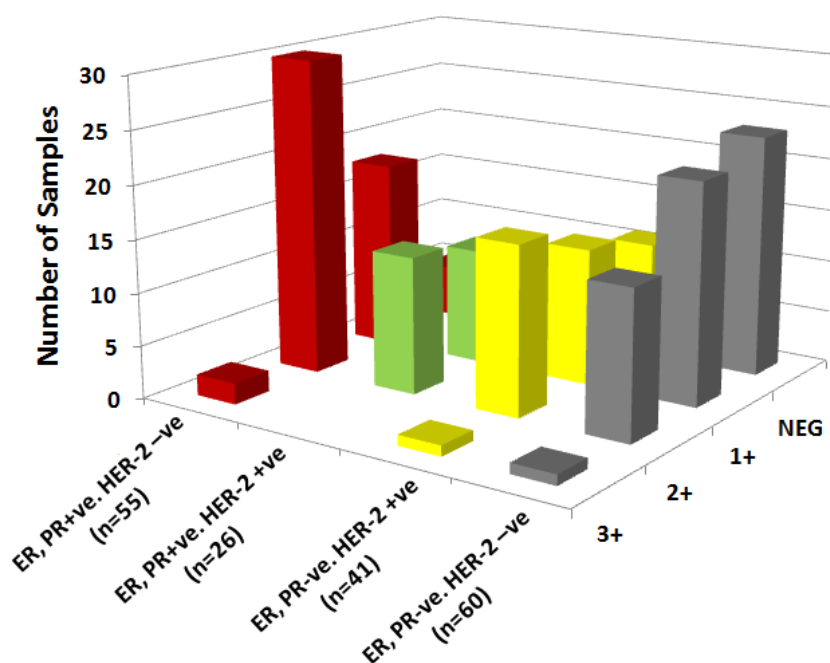


**Figure 1.14: Differential NIS expression across ER+ and ER- BC subtypes [7]:** Graph showing the differential expression of NIS across hormone negative and hormone positive breast tumour patient samples.

#### 1.14 Modulators of NIS in breast cancer

Lactogenic hormones like prolactin regulate NIS expression in breast cancer, which is also involved in modulating NIS expression in normal breast organ during lactation phase. Other physiologically important molecules like insulin, IGF and EGF have also shown positive regulatory role for NIS induction [10]. All Trans-retinoic acid (ATRA) is identified as an important regulator of NIS [94]. Trans retinoic acid and cis-9 retinoic acid bind to RAR and PXR group of nuclear receptors, which are the two predominant isoforms of nuclear receptors expressed in breast cancer cells, which downstream activate NIS expression [95]. This ATRA mediated induction of NIS was specific to receptor positive BC subtypes. Carbamazepine a PXR agonist, showed 1.8 fold increase in iodine uptake under the influence of ATRA in breast cancer cells [11]. The signalling pathway associated with RAR mediated induction of NIS was PI3K. The p85 subunit of PI3K binds to RAR beta for regulating NIS function [96]. Additionally, ATRA is known to induce the phosphorylation of p38- MAPK through Rac1 for elevating the NIS transcription [2]. Glucocorticoid agonists like dexamethasone and hydrocortisone show induction of NIS in MCF-7 cells [97]. Transcriptional modulators of NIS expression like Nkx2.5 and p53 have been identified for their opposing roles, where Nkx2.5 is a positive modulator and p53 is a negative modulator of NIS transcription in BC cells [12, 13]. Another aspect of gene regulation is through epigenetic control. Regulation of NIS gene through hypo acetylation has been proven for its effect on inducing NIS expression in thyroid and breast cancer cells. HDAC inhibitor (HDACi) LBH589 increased NIS expression and function in several breast cancer lines [14]. Six distinct chemical classes of HDACi tested in BC cell lines and *in vivo* tumour model, show significant enhancement of iodine uptake,

thereby increasing the therapeutic efficacy [15]. PTM like N-linked glycosylation also play an important role in regulating the intracellular trafficking of NIS in BC [16, 18]. Cyclic AMP (cAMP), is also suggested as mediator of NIS function augmentation in BC [10].

### 1.15 Molecular imaging

Understanding how a cell functions is a great challenge and to gain a deeper understanding into it, one must zoom into its biological functions at molecular and biochemical level in real time.

A cell is a complex entity with different molecular functions, a wide variety of signaling networks, proteins and their interactions and thus a thorough understanding of orchestral and complex systems can help resolve the molecular defects behind various disease conditions.

Various biochemical and genetic engineering techniques have been applied to understand biological functions, however these techniques fail to capture the dynamics of the cell processes in real time. Biological functions are not static therefore it demands understanding functions in real time and achieving spatial and temporal resolution[98].

This could be addressed using molecular imaging platforms. Molecular imaging provides a new dimension of visual representation, characterization and quantification of biological events, where images produced reflect cellular and molecular pathways [99].

Imaging strategies can be broadly classified into 3 main categories i.e.

- **Direct Imaging:** Direct imaging involves imaging of the target by probe-target interaction. The resultant image intensity of the probe is directly related to its interaction with the target.eg: imaging of dopamine, somatostatin receptors.
- **Indirect Imaging:** This method involves reporter gene technology, where imaging the level of reporter accumulated in cells provides indirect information on the level of gene expression or signalling/transcriptional regulation of that gene.

- Surrogate Imaging: Surrogate imaging strategies reflect downstream effects of one or more endogenous molecular-genetic processes. [100]

Reporter gene technology has been widely used and accepted. There are different kinds of reporter genes being used, which include radio nucleotide based reporters like HSV-TK, dopamine receptor 2, sodium iodide symporter (NIS), fluorescence based reporters like GFP, RFP, MRI reporter like ferritin receptor and bioluminescent reporters like luciferase [101].

An ideal reporter gene should not be endogenously expressed in the cell of interest, and it should be amenable to assays that are sensitive, quantitative, rapid, reproducible and safe.

Optical reporters are cost effective, rapid and high throughput as compared to other reporters which rely on PET, MRI. These include fluorescence and bioluminescence based reporters. Bioluminescence can be useful in monitoring biological functions *in vivo*. Bioluminescence imaging rely on light output generated by enzymes that catalyze the oxidation of substrates (in presence or absence of ATP) to generate photons [102].

There are various luminescent proteins isolated from natural organisms eg:

Luciferase	Organism	Substrate	Emission Wavelength
Firefly luciferase	<i>Photinus pyralis</i>	D-luciferin	569nm
Renilla luciferase	<i>Renilla reniformis</i>	Coelanzazine	480nm
Gaussia luciferase	<i>Gaussia princeps</i>	Coelanzazine	480nm
Vargulin luciferase	<i>Vargula hilgendorffii</i>	Sypridina luciferin	450nm

**Table 1.3: Natural bioluminescence sources:** Table showing the different bioluminescent proteins isolated from natural organisms, having different emission wavelengths and different substrates.

There are certain proteins like aequorin (isolated from luminous jellyfish *Aequorea aequorea*), which behave as natural reporters of calcium sensing. [99]. Advancements in luminescent proteins eg: red shifted (537nm) luciferase isolated from click beetle CBG99 , *Photinus pyralis* mutant Ppy RE8, which shows a shift in red spectrum to 618nm [103], mutants of *Renilla* luciferase i.e. RLuc8, RLuc 8.6, that show higher stability and enhanced photon output[104].

Bioluminescent reporters have been preferred over fluorescent reporters due to their property of providing background free signal, as they are not endogenously present in mammalian system, unlike certain aromatic amino acids which have inherent fluorescence properties which interfere with fluorescence imaging. BLI is considered the most sensitive method for optical imaging since it can detect low light output, from a few cm<sup>2</sup> depth. Additionally, BLI does not depend upon external illumination source which generally suffers quenching and phototoxicity drawbacks in live cells [105].

Thus optical reporter systems have provided a unique and strong platform for understanding various biological functions like gene expression, intracellular dynamic trafficking within organelles ,cell tracing and cell migration, promoter modulation (endogenous or stimulated), protein-protein interactions [106], tumor progression and metastasis, monitoring of different signaling pathways dynamics [107], apoptosis. Some specific examples include studies of viral gene expression [108], oncogene regulation [109], heat shock genes, genes involved in circadian clock rhythms [110], and genes involved in inflammation and various disease states [105].

Several different sensors have been developed for monitoring cellular functions which include TGF-  $\beta$  SMAD signaling sensors [111], TANGO assay for measuring GPCR signaling [112] and Estrogen receptor signaling [113], apoptosis sensors [101, 114], and secondary messenger induced activation sensor (cyclic AMP-PKA) [115].

### 1.16 Cerenkov luminescence imaging

Cerenkov imaging is an optical imaging platform, which was used since 1990 for assessment of sub atomic particles in physical studies and nuclear power plants. Cerenkov radiation (CR) was first explained by Pavel Cerenkov, who was awarded a Nobel Prize in 1958 for his discovery along with Ilya Frank and Igor Tamm. CR is polarized and is inversely proportional to the square of wavelength), which is observed as a blue colored glow in nuclear reactors [116]. When a charged particle travels in a dielectric medium faster than the speed of light in that medium, the randomly organized water molecules get polarized and aligned. These polarized molecules then come back to a relax state by releasing energy in the form of luminescence. The molecules that possess Cerenkov radiation phenomena are radioactive molecules which are either beta or alpha emitters like  $^{15}\text{O}$ ,  $^{13}\text{N}$ ,  $^{68}\text{Ga}$ ,  $^{89}\text{Zr}$ ,  $^{64}\text{Cu}$ ,  $^{225}\text{Ac}$ ,  $^{90}\text{Y}$ ,  $^{124}\text{I}$ , and  $^{74}\text{As}$  [117].

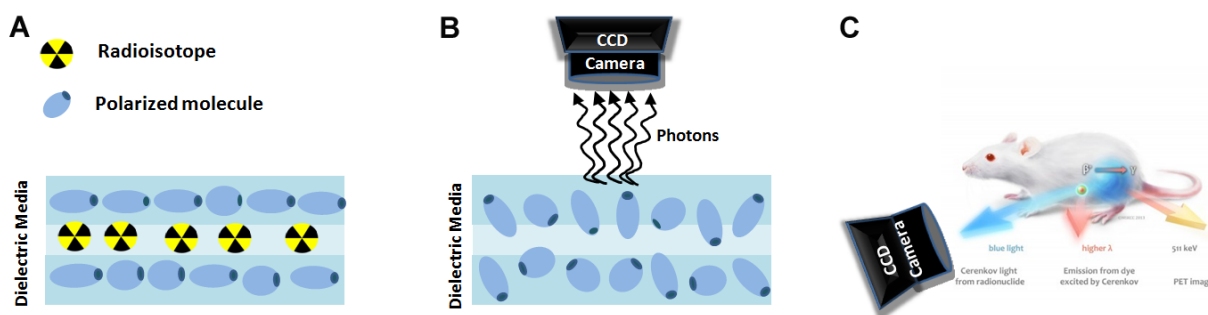


**Figure 1.15: Cerenkov luminescence principle:** **A:** Image showing the polarization of molecules after a charged radioisotope passes through the media. **B.** Emission of energy in the

form of photons, when the polarized molecules come back to relaxed state C. Detection of Cerenkov luminescence emitted from the animals, after injection of radioisotope, by EM-CCD camera.

Cerenkov luminescence can be detected using EM-CCD camera, which are used for recording the bioluminescence output [118].  $^{131}\text{I}$  and  $^{124}\text{I}$  can emit Cerenkov luminescence which can be detected by EM-CCD camera, thus making it possible to image the function of NIS on optical platforms thus reducing the dependency of NIS mediated imaging by SPECT/PET [69] [117]. NIS transgene expressing cells have been successfully imaged by this method using radioiodine [69]. CLI has also been applied for imaging the expression of rat NIS in A549 cells [119]. Beyond the *in vivo* imaging applications of CLI, its use in intraoperative surgery guidance imaging has also been demonstrated [120]. Thus, Cerenkov imaging can bridge optical (pre-clinical) and nuclear (clinical) imaging. However, CLI faces certain limitations like low tissue penetration, thereby restricting deep tissue imaging. Radioactive decay with time also reduces the Cerenkov luminescence output for time kinetic studies.

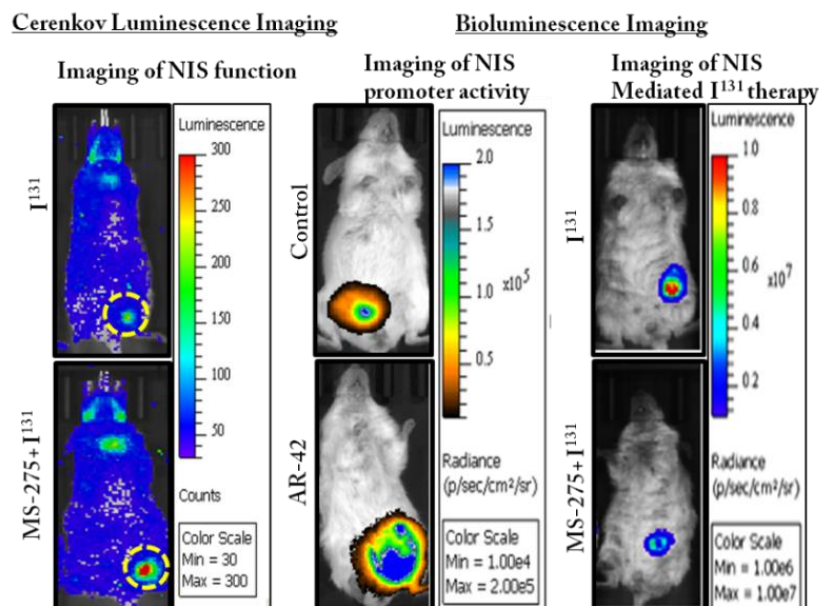


*Figure 1.16: Non-invasive imaging of NIS gene function and expression in vivo: Imaging of NIS function, promoter activity and its therapeutic implication by non-invasive real time bioluminescence and Cerenkov luminescence imaging platforms.*

### 1.17 Rationale of study

Although NIS expression is recorded in breast cancer tissues, the defective sub cellular localization and insufficient expression of NIS remains the bottleneck for successful translation of NIS gene therapy in breast cancer. Only 30% cases show 2+/3+ score for NIS staining, while majority of the positive cases are actually NIS low (1+). Hence studying the regulation of inherent NIS expression and subcellular localization may eventually help in finding a way to elevate NIS mediated uptake of iodine in cells.

Many studies in the past have attempted to identify regulators of NIS in BC, where one of the major well-studied regulators is all trans-retinoic acid (ATRA). ATRA binds to two nuclear receptors RAR/RXR to induce NIS expression. Glucocorticoid agonists like dexamethasone and hydrocortisone have been reported to augment NIS expression in MCF-7 cells [8]. Molecules like insulin, IGF-1, 2, ATRA and prolactin have also been proved as enhancers of NIS expression and function in MCF-7 cells [9] [10]. Carbamazepine, a PXR agonist, showed 1.8 fold increase in iodine uptake mediated through tRA in breast cancer cells [11]. A transcription factor Nkx2.5 was identified as a positive modulator of NIS in MCF-7 cells [12]. Recently, we also reported that p53 acts as a suppressor of NIS expression in breast cancer [13]. Cyclic AMP (C-AMP) pathway is very well characterized for positively regulating TSH mediated induction of NIS gene in thyroid cancer, however the modulatory role of cAMP response element binding protein (CREB) on NIS gene, in BC scenario remains elusive.

Inhibition of Histone deacetylase (HDAC) has also been a strategy used for stimulating NIS in several thyroid cancer cell lines. One HDACi candidate, LBH589, was used for inducing NIS expression and function in several BC lines [14]. Past work from our group has verified various chemical classes of HDACi for enhancing NIS expression, Iodine uptake, and thus increased therapeutic efficacy in BC cells

[15]. However, modulators which can induce the function of endogenous NIS specifically in BC, with minimal off target effects remains unknown. Another long-standing and important aspect appeared frequently in research literature is sub-cellular localization of NIS. This aberrantly overexpressed protein mostly found to be accumulated in the cytoplasm instead of plasma membrane [16]. Only a few reports so far have investigated on regulation aspects of NIS protein localization inside the BC cells. It has been shown that EGF mediates membrane targeting of NIS via MAPK pathway [17, 18]. Thus, identification of regulatory mechanisms involved in defective localization of NIS in BC cell is considered also here thinking that it may open new avenues for effective NIS function.

### **1.18 Aims and Objectives:**

Based on the current limitations pertaining to NIS mediated therapy in breast cancer, we have set the following objectives in an attempt to address the lacunae in our current understanding pertaining to the modulation of endogenous NIS in breast cancer:

**Objective 1:** To elucidate the role of HDACi (benzamide class) in regulating NIS expression and function in breast cancer as compared to thyroid cancer

**Objective 2:** Understanding the role of cAMP-PKA-CREB axis on regulating NIS expression

**Objective 3:** Investigating the role of glycosylation as a regulatory mechanism to control NIS cellular localization



## **CHAPTER 2:**

*To elucidate the role of HDACi (benzamide class) in  
regulating NIS expression and function in breast cancer as  
compared to thyroid cancer*

## 1.1 Introduction

The inherent heterogeneity of breast cancer (BC) is one of the major challenges for complete remission of the disease. Receptor negative subtype (Triple negative breast cancer or TNBC) still remains the most aggressive form of BC with limited treatment options. Apart from chemotherapy and targeted therapies, even radiation therapy faces challenges of Tumour relapse due to radiation resistance [121]. Gene therapy has evolved as a potential tool for cancer treatment. Although it has shown promising results in pre-clinical settings, successful translation of exogenous gene therapy still faces hurdles. Targeted delivery, efficiency, toxicity, ethical ramifications and immunogenic responses are major concerns associated [122]. Human sodium iodide symporter (NIS) has its reputation established in thyroid clinic as an effective therapeutic gene target for radio-ablation of thyroid cancer [75]. Physiologically, out of the vast number of solute carrier family of proteins, NIS is the sole candidate responsible for transporting iodine ions inside the thyroid follicular cells. NIS also functions in the mammary gland cells during lactation phase [3]. The major advantage of NIS in breast cancer settings is that it is endogenously expressed in BC tissues, thus nullifying the ethical and toxicity issues pertaining to exogenous gene delivery. Although NIS gene therapy mediated radio-ablation holds a great promise, there are practical clinical challenges associated with its application in BC patients : (i) Clinical studies have shown that 70-80% of the BC cases are NIS positive, of which around 30% cases show high intensity (2+/3+ score) [7]. Therefore, various ways to boost this endogenous gene expression has evolved to enhance the NIS mediated <sup>131</sup>I therapy effect [8, 15, 17]. (ii) Technetium-99m uptake studies and scintigraphy imaging have shown that only 27% of all NIS positive cases show functional NIS protein [4]. This fact can be co-related to reports showing lack of membranous staining of NIS in majority number of cases [5, 7, 16]. Several groups across the world are attempting to reveal the mechanisms by which NIS expression can be modulated in BC. The modulators of NIS

expression in case of thyroid cancer are well characterized, where thyroid stimulating hormone (TSH) is identified as a major inducer of functional NIS in thyroid cancer [123]. All trans retinoic acid (tRA) is known to induce NIS expression and function in BC through RAR/RXR receptors [124]. Glucocorticoid agonists like dexamethasone and hydrocortisone, lactogenic hormones, insulin, IGF-1, 2 are also reported as inducer of NIS expression in BC cells [8, 95, 125]. Pharmacological modulation of NIS by using HDAC inhibitors (HDACi) has also been proven efficacious for NIS gene mediated radio-iodine therapy [14, 15, 79]. As NIS gene expression and function is differently controlled in thyroid vs. breast cells, we further investigated for ways to specifically induce NIS in breast cancer cells, with minimum off target effects on thyroid cell. As currently there is no clinically relevant method to enhance the function of NIS specifically in BC cell with minimal or no effect on other organs, this study for the first time bring in evidence on that direction as a step forward for clinical realization of NIS gene targeted radio-iodine therapy. This study also establishes molecular basis of such tissue specific transcriptional modulation of NIS in BC.

## **1.2 Materials and Methods**

### **1.2.1 Chemicals and cell lines**

MCF-7 and ZR-75-1 BC cells (ATCC) maintained in RPMI-1640 media (Gibco, Invitrogen, USA), NPA and ARO (gifted by Mr. A. Chakraborty, BARC, India), were maintained in IMDM (Gibco, Invitrogen, USA) containing 10% FBS and 0.075% gentamycin solution. Benzamide class HDACi MS-275 (1590-1), Chidamide (2261), AR-42(2716-1) and CI-994 (1742-10) from biovision. EdU click-IT cell proliferation kit from thermo fisher scientific (C10340), EXPOSE HRP/DAB detection IHC kit from Abcam (ab80436), MTT (3-[4, 5-dimethylthiazol-2-yl] c-2, 5-diphenyltetrazolium bromide) (Sigma, USA). D-luciferin was procured from Biosyth chemistry and biology (L-8220), Luciferase Assay system from

Promega (E4030) , FOXA1 primary antibody from Abcam (ab-23738), H3 acetylation antibody (06-598, Upstate, USA), human Sodium Iodide Symporter antibody from Thermo Scientific (MA5-12308), alpha tubulin primary antibody from sigma (T9026),  $\gamma$  H2Ax (Pierce Biotechnology, USA) , anti-mouse HRP secondary antibody from AbCAM (ab6728), goat anti-rabbit HRP antibody from Thermo Scientific (31460), goat anti-mouse DyLight 633 secondary antibody from Thermo Scientific (35512). cDNA first strand synthesis kit (Invitrogen USA)

Group	Candidate	HDAC targets	Clinical Trial	Type of malignancy
	CI-994	Class 1 HDAC	Phase 2	Pancreatic cancer
<b>Benzamide</b>	Chidamide	Class 1,2 HDAC	Phase 2	Solid Tumours and lymphoma
	MS-275	Class 1 (HDAC 1,3)	Phase 2/1	Melanoma, Refractory Solid Tumours and lymphoma
	AR-42	Class 1,2 HDAC	Phase 1	Haematological malignancies

*Table 2.1: Benzamide class HDAC inhibitors selected for the study, showing their respective HDAC targets in the cell and the different clinical trials they belong as anti-tumour agents*

### 1.2.2 Luciferase assay

The luciferase assay was performed as per recommended protocol from promega firefly reporter kit. Protein lysates were prepared using the reporter lysis buffer provided in the kit. 10 $\mu$ l lysates were added with 50  $\mu$ l LARII substrate in a white well plate. The relative light output (RLU) was normalized with the respective protein concentrations of the lysates.

### **1.2.3 Quantitative real time PCR**

After the cells were treated with HDACi for 48 hours, RNA was extracted using RNeasy kit (QIAGEN, USA). cDNA was synthesized using the first strand cDNA synthesis kit (Invitrogen, USA). Quantitative real-time PCR was performed using TaqMan probe mix on the 7900HT PCR cycler (Applied Biosystems, USA). The TaqMan probes for human NIS and GAPDH with assay IDs Hs00166567\_m1 and Hs02758991\_g1 respectively were used (Applied Biosystems, USA). RT-PCR reactions were set in triplicate for each sample. The comparative  $\Delta\Delta C_t$  method was used to calculate relative gene expression.

### **1.2.4 Western blotting and Immunofluorescence**

Cells were lysed using RIPA buffer containing protease inhibitor cocktail. Equal amount of protein from control and transfected/treated cells were resolved in 7.5% SDS-PAGE gel and transferred onto a nitrocellulose membrane by semi-dry blotting apparatus. After blocking with 5% non-fat dry milk, membranes were probed with anti-human NIS antibody, anti- $\alpha$ -tubulin, FOXA1. The blots were then probed with HRP-conjugated secondary antibodies and developed using a Chemidoc system. For IF, cells were fixed with 4% paraformaldehyde for 10 minutes at 37 degree Celsius. Blocking was done with 2% BSA. Primary antibody was incubated overnight at 4 degree Celsius, followed by 1 hour incubation with secondary Dylight 633 antibody. Fluorescence micrographs were captured using Carl Zeiss LSM 780 confocal microscope. The magnification used was 63x objective, with a numerical aperture of 1.3 and pinhole restricted to 1 AU (1AU=0.7 $\mu$ m).

### **1.2.5 Intracellular staining and flow cytometry**

FACS buffer was made by adding 0.01% sodium azide and 2% FBS in 1XPBS. 0.25% saponin for 15 minutes at room temperature was used for permeabilisation of the cells. 1:70 dilution of

primary NIS antibody was used, with an incubation of 45 minutes on ice, followed by anti - mouse FITC (Sigma US) secondary antibody for 45 minutes on ice. Protocol discussed in detail in appendix section.

### **1.2.6 MTT cell cytotoxicity assay**

To evaluate cytotoxicity of various HDACi, MCF-7 and MDA-MB-231 ( $5 \times 10^3$ ) cells were seeded in 96 well plates (Corning, USA). Cells were exposed to different concentrations of HDACi for 48 hours. Cell viability was assessed using the MTT (3-[4, 5-dimethylthiazol-2-yl]-2, 5-diphenyltetrazolium bromide) reagent (Sigma, USA). IC<sub>30</sub> or lower concentrations of bHDACi were used in the study, which were as follows: 10 $\mu$ M CI-994, 1 $\mu$ M Chidamide, 5 $\mu$ M MS-275 and 500nM AR-42.

### **1.2.7 Non-radioactive iodine uptake assay**

Iodide uptake and efflux study was performed as described previously [102, 169]. After 48 hours of treatment with indicated HDACi, cells were incubated with 10 $\mu$ M NaI in uptake buffer [Hank's Balanced Salt Solution (HBSS) supplemented with 10mM HEPES (pH 7.3)]. To determine NIS-specific iodide uptake, cells were incubated with 30 $\mu$ M KClO<sub>4</sub> in uptake buffer for one hour prior to addition of 10 $\mu$ M NaI. After 30 minutes incubation with NaI at 37°C, cells were washed with ice-cold uptake buffer. Then 10.5mM ammonium cerium (IV) sulphate solution and 24mM sodium arsenite (III) solution were added. The plate was incubated at room temperature (RT) in dark for 30 minutes and the absorbance at 420nm was recorded. Using logarithmic conversion and standard equation of iodide standards, amount of nanomoles (nmoles) of iodide uptake was calculated from absorbance read-outs.

### **1.2.8 In vitro long term survival assay using $^{131}\text{I}$**

The in vitro clonogenic assay was performed as described by Mandell et al [[126](#)]. MCF-7, ARO and NPA were incubated with 50  $\mu\text{Ci/ml}$   $^{131}\text{I}$  and ZR-75-1 was incubated with 100  $\mu\text{Ci/ml}$   $^{131}\text{I}$  for 5 hours. After which the cells were washed with ice cold HBSS and then seeded in equal numbers (1000 cells/well).

### **1.2.9 In vivo orthotopic breast cancer model development and drug treatment**

The experimental protocol was approved by Institutional Animal Ethics Committee (IAEC) at ACTREC and performed in accordance with the guidelines for the Care and Use of the Laboratory Animals with the help of ACTREC animal house and Molecular Imaging facilities. ZR-75-1 cells labeled with Fluc2.Turbo fusion gene were used to generate an orthotopic breast cancer model in female BALB/c SCID mice. The mice were divided in 3 groups i.e. the  $^{131}\text{I}$  group (intraperitoneal injection of 1mCi Na- $^{131}\text{I}$ ), AR-42, MS-275 +  $^{131}\text{I}$  group (3 doses of 5 mg/kg of AR-42, 10mg/kg of MS-275 every alternate day followed by 1mCi Na- $^{131}\text{I}$ ) and the control group (saline). After the tumour was initiated, all the groups received a daily intraperitoneal injection of T3, T4+Methimazole for blocking the uptake of iodine in the thyroid glands for 21 days. Following which, AR-42(5mg/kg) /MS-275 (10mg/kg) were given to AR-42/MS-275+  $^{131}\text{I}$  group mice at a total of 3 doses, every alternate day. 1mCi  $^{131}\text{I}$  /mouse was then administered to  $^{131}\text{I}$  and AR-42/MS-275+  $^{131}\text{I}$  groups. Data were analyzed using Living Image version 4.4 software.

### **1.2.10 Immunohistochemistry**

For immunohistochemistry (IHC), tumours and organs from drug (MS-275, AR-42) treated and control group were harvested and fixed in 10% formalin. The detailed procedure is

discussed in appendix section. Since the primary antibody was raised in mouse, an additional step of mouse serum blocking was performed to prevent non-specific binding of antibody on mouse tissues. For digital scoring of IHC slides, the IHC profiler plugin for ImageJ (software) was used, which was developed by our group. IHC staining for NIS was performed as described in the following paper [[127](#)]

#### **2.2.11 In vivo non-invasive bioluminescence imaging**

Bioluminescence imaging was performed using IVIS-Spectrum (Caliper Life Sciences) after I.P injection of 30 mg/ml of D-luciferin. Mice were anesthetized with isofluorane and placed in the imaging chamber with continuous 2% isofluorane administration via nasal cone.

#### **2.2.12 TF profiling and promoter binding array**

We performed a TF activation and promoter binding array for 96 different TF (FA2002, Signosis, USA) as per the manufacturer's guideline. MCF-7 and ARO cells were treated with CI-994 for 48 hours and nuclear lysates from both control and treated cells were isolated using standard procedure. For analysing promoter binding, the nuclear lysates were incubated with oligo-binding mix along with NIS-promoter DNA fragment. Comparing luminescence in presence or absence of competitor human NIS promoter, binding of various TFs were predicted.

#### **2.2.13 Cloning of shRNA and generation of lenti-viral mediated FOXA1 knockdown stable cell model**

The shRNA sequence of FOXA1 was designed and cloned into a PLL3.7 Lenti-Lox vector by xho1 and xba1 restriction enzymes. The colonies were screened by colony PCR by primer

against U6 promoter. Positive colonies were confirmed by restriction digestion of xho1 xba1 double digest product and verification of the loss of Hpa1 site. Sanger sequencing was done for further verification. The positive clone for shFOXA1 was then co-transfected along with PMDG and PACS viral packaging vectors in HEK-293FT cells for the production of lenti-virus containing the shFOXA1 DNA (GFP positive). The virus were concentrated by high speed ultra-centrifugation and transduced in MCF-7 NF cells. GFP positive cells were selected over passages and amplified.

#### **2.2.14 Cerenkov luminescence imaging**

CLI was performed using the same IVIS spectrum system. For *in vivo* Cerenkov imaging, animals in the <sup>131</sup>I alone or VPA+<sup>131</sup>I group were injected with 1mCi of <sup>131</sup>I intraperitoneally. Animals were placed in a light-tight chamber under isoflurane anesthesia. Cerenkov imaging was performed after 24 and 72 hours of <sup>131</sup>I injection. The detailed procedure is given in the appendix section.

#### **1.2.15 Statistical analysis**

All data are expressed as mean  $\pm$  SE and are representative of at least two separate experiments. Statistical significance was analyzed by Student t-test using GraphPad Prism 6 (GraphPad Software, La Jolla, CA). P values of  $\leq 0.05$  were considered statistically significant.

## 1.3 Results

### 2.3.1 Non-toxic dose profiling of benzamide class HDAC inhibitors (bHDACi) on breast and thyroid cancer cells.

Four drug inhibitors belonging to benzamide class of HDAC inhibitors (bHDACi) were selected in this study, and all of which are at different stages of clinical trials as anticancer agent (**Table 2.1**). Since we aimed to use them as transcriptional modulators of NIS, a non-toxic dose (i.e. IC-30 equivalent or lower) was determined using breast cancer (BC) cell lines MCF-7, ZR-75-1 and a thyroid cancer cell line (ARO). 10 $\mu$ M CI-994, 1 $\mu$ M Chidamide, 5 $\mu$ M MS-275 and 500nM of AR-42 used in the study are non-toxic to BC and TC cells tested (**Figure 2.3.1 A-D**).

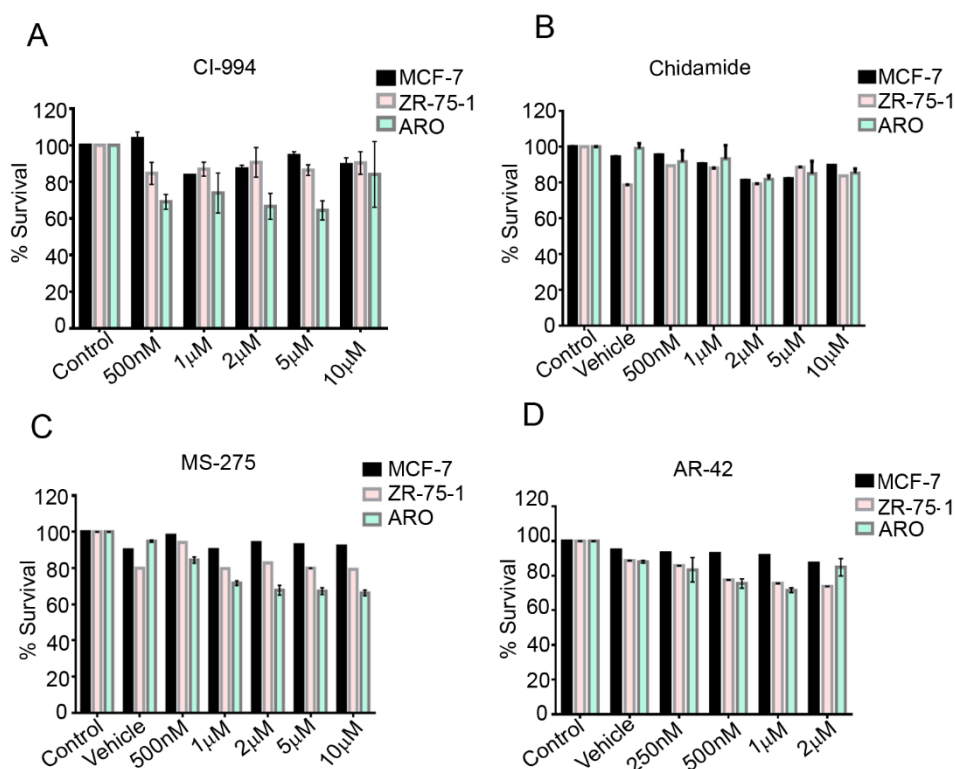


**Figure 2.3.1** Cytotoxicity measurement of bHDACi on breast and thyroid cancer cells

**2.3.1A-D:** Charts showing the percent cell survival (y-axis) on exposure to different

concentrations of CI-994, Chidamide, MS-275 and AR-42 respectively on MCF-7, ZR-75-1 and ARO cells, as measured by MTT assay.

### 2.3.2 Benzamide class HDACi show anti-proliferative effect on BC cells and are able to induce acetylation of its substrate

As established from literature, all classes of HDACi have an anti-proliferative effect on cancer cells. Thus to confirm this drug function, live cell proliferation was measured by EdU assay. All four bHDACi drugs in use show anti-proliferative effect on MCF-7 cells (**Figure 2.3.2A**). The quantification of the number of EdU positive cells from control and bHDACi treated samples show decrease in the number of actively proliferating cells (**Figure 2.3.2B**). Further validation of the functional activity of HDACi i.e. acetylation of its primary substrate histone H3, shows increased acetylated status after all bHDACi treatment, confirming specific HDACi action in MCF-7, ARO and NPA cells (**Figure 2.3.2C**).

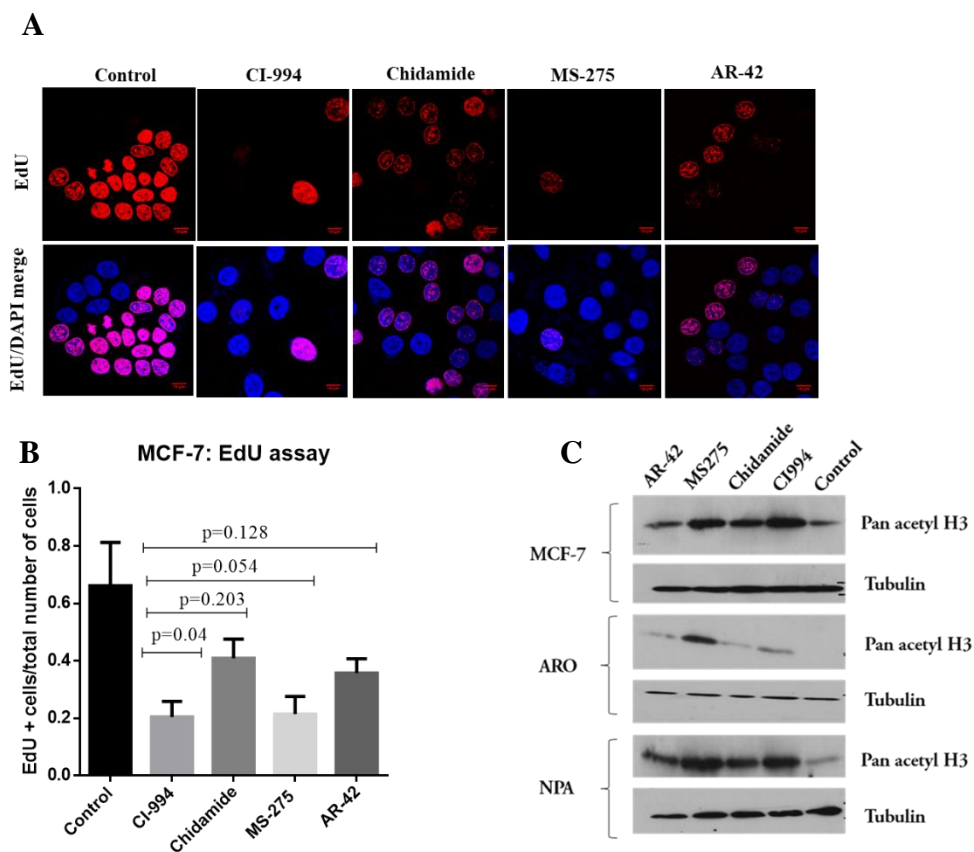


**Figure 2.3.2 Effect of bHDACi on cell proliferation and histone acetylation** **2.3.2A:** Immunofluorescence images showing EdU positive cells (red) stained with Alexa Fluor 647 and nucleus (blue) indicating DAPI stain. Scale bar represents 10 $\mu$ m distance. **2.3.2B:** Graph showing the quantification of EdU positive cells among the total number of cells. Error bar indicate SEM calculated from 50 cells. **2.3.2C:** Western blot showing the increase in pan acetylation of histone H3 after bHDACi treatment in MCF-7, ARO and NPA cells. Tubulin used as endogenous loading control.

### **2.3.3 Benzamide class HDACi differentially modulate NIS promoter activity in breast cancer cells**

After validating the activity and cytotoxicity of bHDACi, we sought out to study their effect on NIS promoter modulation. A previously developed stable reporter system in the lab was used, where NIS promoter drives the reporter construct i.e. firefly luciferase fused to turbo fluorescent protein (pNIS-FL2.turbo), in MCF-7, ZR-75-1 and ARO cell (**Figure 2.3.3A**). Treatment of these engineered BC cells with bHDACi shows approximately 6-8 fold higher reporter gene expression ( $p \leq 0.0001$ ), except for chidamide drug where about 3-fold increase is recorded (**Figure 2.3.3B**). However, in ARO cell line, the same drug candidates show only 3-fold or lesser reporter activity ( $p = 0.1863$ ) (**Figure 2.3.3B**).

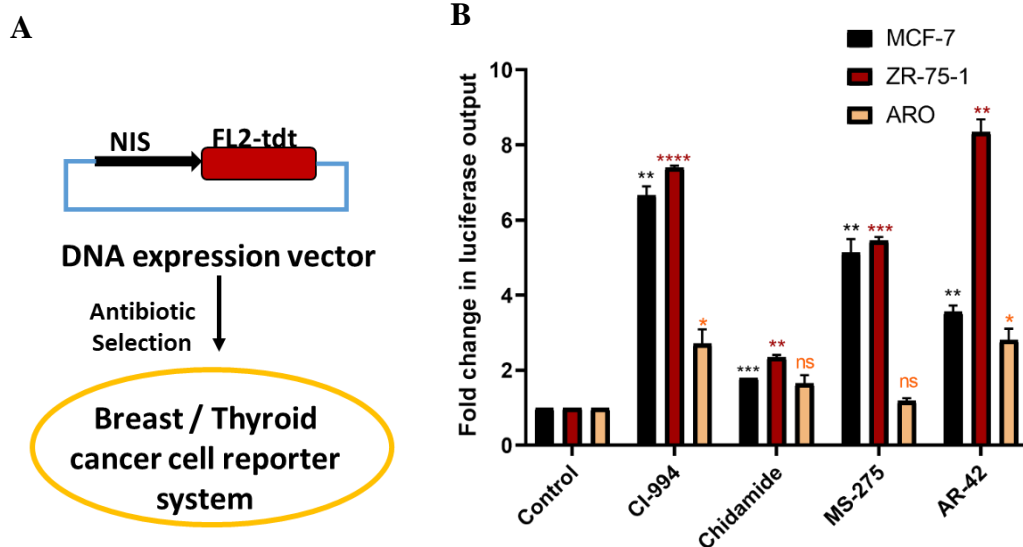


**Figure 2.3.3 NIS promoter activity is specifically enhanced in breast cancer cells**

**2.3.3A:** Schematic demonstrating the engineered BC, TC cell models overexpressing pNIS-FL2.Turbo constructs. **2.3.3B:** Graph showing NIS promoter activity after bHDACi treatments for 24 hours in MCF-7 NF, ZR-75-1 NF and ARO NF cells respectively. Error bar represents SEM, significance determined by t-test. \*\* indicates  $p \leq 0.01$ , \*\*\* indicates  $p \leq 0.001$ .

### 2.3.4 bHDACi enhance endogenous NIS expression preferentially in BC cells

bHDACi were capable of modulating NIS promoter activity, thus we took the next step to test the effect of these epigenetic modifiers on endogenous NIS transcription and translation.

As measured by quantitative real time PCR, we observed a significant ( $P < 0.05$ ) up regulation of NIS transcription in response to bHDACi treatment in MCF-7 and ZR-75-1 cells. CI-994 shows around 30 fold increase in NIS expression in BC cells and MS-275 leads to 15 fold increase in both BC cell lines tested. However, these same drugs show lower level of NIS transcript induction across TC (ARO) cell tested (**Figure 2.3.4A**). Next, in order to check if the transcription of NIS could lead to successful translation, we measured the NIS protein levels

on 3 different platforms i.e. western blotting, flow cytometer based assessment and immunofluorescence based staining of NIS protein. bHDACi treatment to MCF-7 cells shows an enhanced NIS expression when measured western blotting (**Figure 2.3.4B**). Intracellular staining of NIS protein show increased NIS positive population by CI-994, Chidamide, MS-275 and AR-42 treatments in both BC cell lines MCF-7 and ZR-75-1. However, TC cell ARO shows no increase in NIS positive population with the same bHDACi treatment (**Figure 2.3.4C**). We have also tested if bHDACi treatment can modulate NIS protein translation in a normal breast cell line MCF-10A, in addition to BC/TC cells. Therefore, IF staining was performed in MCF-7, ZR-75-1, MCF-10A, ARO and NPA cells, where only the MCF-7 and ZR-75-1 cells show enhanced NIS expression after bHDACi treatment, while MCF-10A or ARO, NPA cells display unaltered NIS expression (**Figure 2.3.4D**). The specificity of bHDACi drug effect on BC cells is further demonstrated by using sodium butyrate (NaB) which is a short chain fatty acid class of HDACi. NaB treatment shows enhanced NIS protein in ARO and NPA (**Figure 2.3.4E**), unlike bHDACi, whose effect was more inclined towards BC cell types.

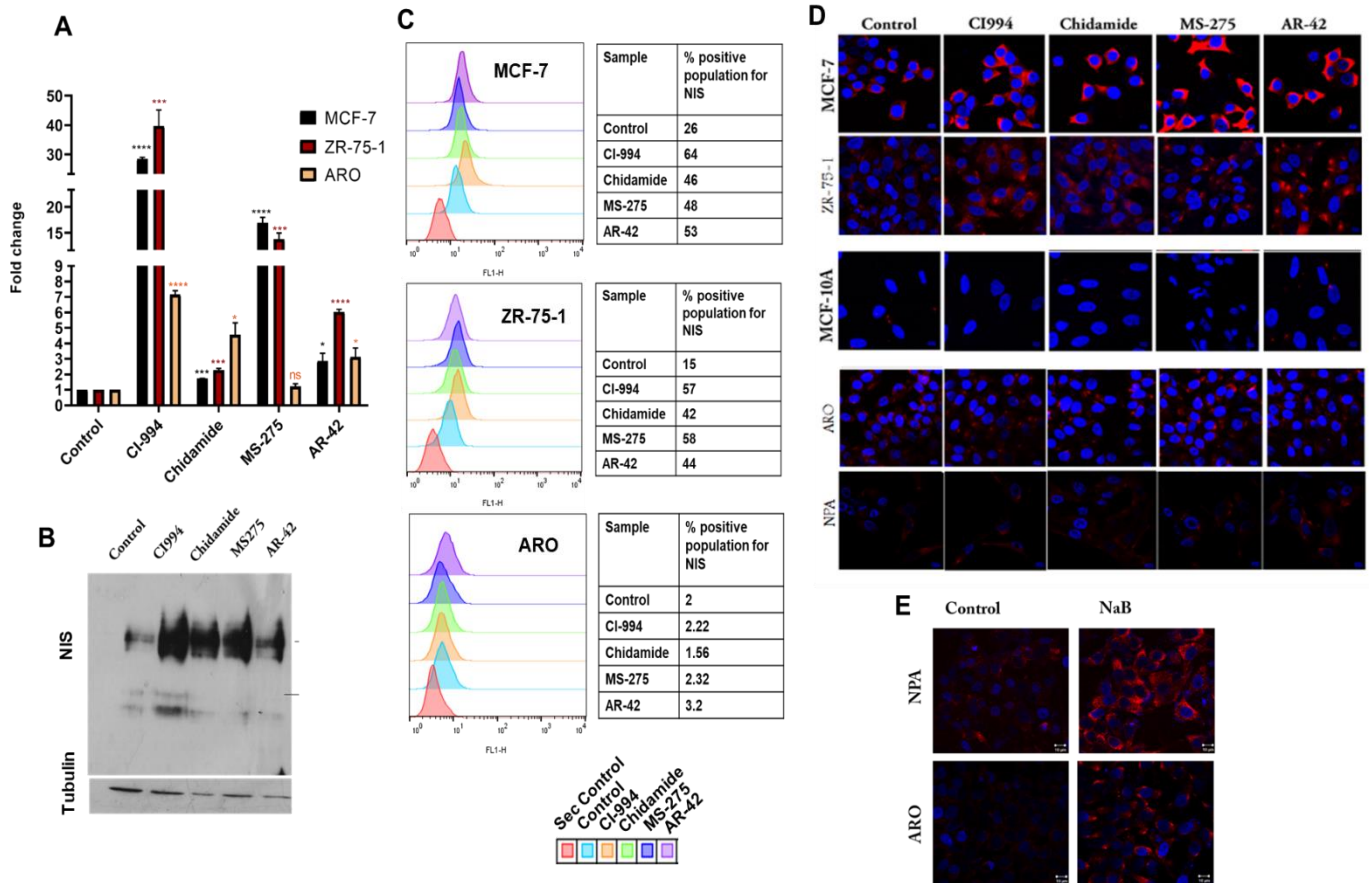


**Figure 2.3.4** *bHDACi* positively regulate NIS expression in breast and thyroid cancer cells, in a differential manner **2.3.4A**: Graph showing increase in NIS transcript expression after 24 hours of *bHDACi* treatment as compared to their untreated counterparts in ZR-75-1, MCF-7 and ARO cells respectively. Error bar represents SEM, significance determined by *t*-test. \*\* indicates  $p \leq 0.01$ , \*\*\* indicates  $p \leq 0.001$ , ns indicates non-significant. **2.3.4B**: Western blot image indicating increased NIS expression (100kDa) post *bHDACi* treatments. Tubulin was used as an endogenous loading control. **2.3.4C**: Flow cytometry assay charts showing NIS positive population in MCF-7, ZR-75-1 and ARO cells on FITC channel (FLH-1) on x-axis and the counts of individual events on y-axis. **2.3.4D**: Images obtained by Immunofluorescence assay, showing NIS protein expression (red), stained by Dylight 633 in MCF-7, ZR-75-1, MCF-10A, ARO and NPA cells respectively. Blue indicates DAPI. **2.3.4E**: Immunofluorescence

images showing NIS protein staining (red), pre and post 48 hours NaB treatment on NPA and ARO cells. Blue indicates DAPI. Scale bar shows 10 $\mu$ m distance.

### 2.3.5 Benzamide class HDACi significantly enhance NIS function in breast cancer cells

Corroborating the above findings, we tested whether the enhanced NIS expression correlates with its function. Thus a non-radioactive iodine uptake assay was performed, where bHDACi treated MCF-7 and ZR-75-1 cells show significantly ( $p < 0.05$ ) higher iodine uptake as compared to their untreated counterpart (**Figure 2.3.5A**). Further, when the same drugs were tested on thyroid cancer cell lines ARO and NPA, there was no significant change in the amount of iodine uptake seen (**Figure 2.3.5B**).

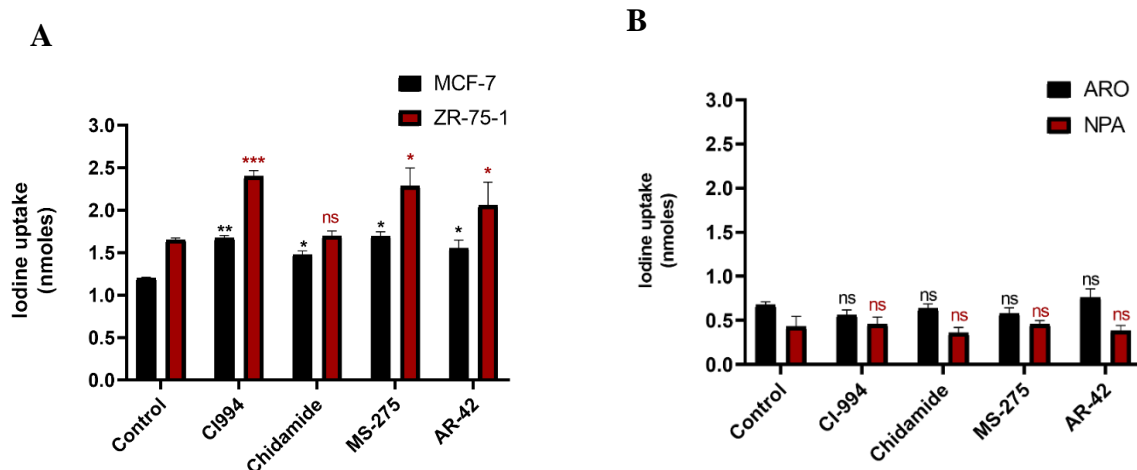


**Figure 2.3.5 bHDACi differentially enhance the function of NIS in BC cells 2.3.5A-B:**

Graphs indicating iodine uptake post 48 hours (nano-moles y-axis) in MCF-7, ZR-75-1, ARO and NPA cells respectively. Error bars indicate SEM

### 2.3.6 Depletion of HDAC1 from MCF-7 cells leads to an increase in NIS expression

Most HDACi act by inhibiting class 1, class 2 HDAC candidates. HDAC1 and HDAC2 serve as important HDACs, since they are a part of majority of repressor complexes. Also, HDCA1 is a

prime target of MS-275, thus in order to mimic the bHDACi mediated effect by genetic knockdown strategy, we created a HDAC1 knock down system in MCF-7 cells (**Figure 2.3.6A**). Depletion of HDAC1 in MCF-7 leads to an increase in NIS expression, as measured by flow cytometry analysis showing an enhanced intensity of NIS (**Figure 2.3.6B-C**). Further, validation by another assay i.e. immunofluorescence (IF), a significant ( $p < 0.0001$ ) increase in NIS expression is noted after HDAC1 knockdown (**Figure 2.3.6D-E**). Thus we prove that HDAC1 is a negative regulator of NIS expression in MCF-7 cells.

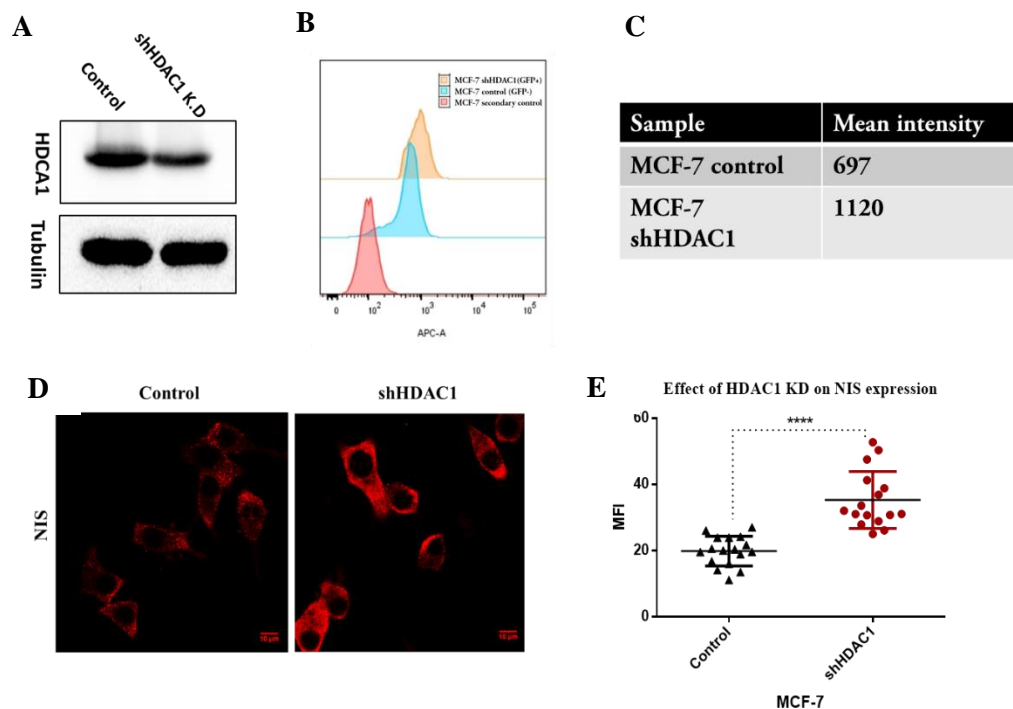


**Figure 2.3.6 HDAC1 is a negative regulator of NIS expression in BC cells 2.3.6A:** Western blot indicating knockdown of HDAC1 in shHDAC1 stable cells. Tubulin used as an internal loading control. **2.3.6B-C:** Flow cytometry data showing the increase in NIS expression in MCF-7 shHDAC1 cells as compared to parental cells. **2.3.6D-E:** Immunofluorescence data indicating an increase in NIS (red) expression in MCF-7 shHDAC1 cells. Scale bar marks

10 $\mu$ m distance. Graph shows mean fluorescence intensity (MFI) on Y-axis. \*\*\*\* indicates  $p < 0.0001$ . Error bar indicate SEM.

### **2.3.7 Transcription factor (TF) profiler array reveals differential TF activated by CI-994 in MCF-7 and ARO**

HDACi induce acetylation which help in opening up the chromatin structure, facilitating transcription factor binding to genes for driving their transcription. Thus in order to gain mechanistic insights into differential induction of NIS in BC versus TC, we performed a high throughput transcription (TF) factor profiling array for 96 global TFs. **Figure 2.3.7A** shows the TFs activated or inhibited post CI-994 treatment, represented as a fold change compared to their un-treated counterparts. Further screen reveals the TFs which are positively modulated by CI-994, in a differential manner across MCF-7 and ARO cells. A set 22 TF are identified from the array i.e. AP3, CDF, CREB, EGR, ELK, FOXA1, FOXO1, FOXOF2, HOXA5, PAX3, PAX8, PIT, PXR, STAT5, STAT6, NF-1, FOXC1, TCF/LEF, NKX3.2, PBX1, RB and XBP (**Figure 2.3.7B**). PAX8, which is a well reported TF for thyroid shows higher activation in ARO as compared to MCF-7. FOXA1 shows maximum difference in activation post CI-994 treatment in MCF-7. Further, using a competition assay for understanding TF binding to promoter, purified NIS promoter DNA was used in the promoter binding array. All 22 TFs screened above show binding to NIS promoter, as reflected by a reduced ratio (below 1) of

chemiluminescence output from CI-994+NIS promoter samples/CI-994 samples (Figure 2.3.7C).

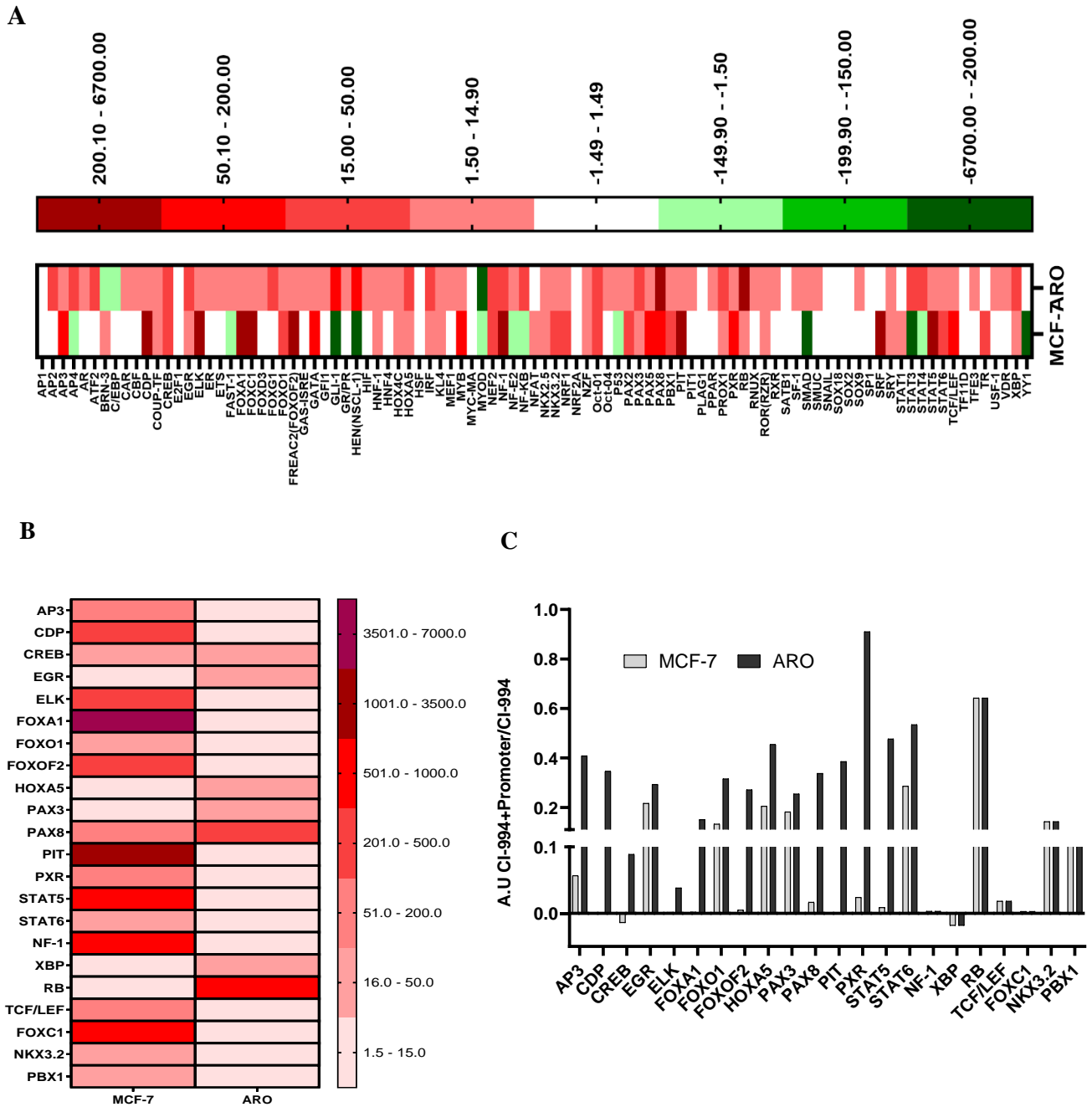


**Figure 2.3.7 TF profiler and promoter binding array unfolds differential TF activation and binding in MCF-7 cells** 2.3.7A: Heatmap indicating the differential modulation (fold change with respect to untreated condition) of 96 different transcription factors (TFs) in response to CI-994 treatment in MCF-7 and ARO cell lines. Shades of red indicate positive modulators

( $<1.5$  fold) and green indicates negative modulators. **2.3.7B:** Heatmap showing the positive modulators activated after CI-994 treatment, differentially in MCF-7 and ARO cells. **2.3.7C:** Graph showing the chemiluminescence signal output (A.U) on y-axis, of the TFs (CI-994+NIS promoter/CI-994).

### **2.3.8 FOXA1 expression is higher in breast cancer in contrast to thyroid cancer**

FOXA1 is selected from the array, since FOXA1 shows maximum differential regulation post CI-994 treatment in MCF-7 cells. Retrospective TCGA analysis reveals a sharp difference in the expression of FOXA1 towards the higher side in BC patients (METABRIC data set, n=2509) in contrast to TC patients (cell 2014 dataset, n=496). (**Figure 2.3.8A**). Thus, we further analyzed the expression of FOXA1 in MCF-7 and ARO cells. FOXA1 expression significantly increases after CI-994 treatment in MCF-7 cells but not in ARO, and also the basal expression of FOXA1 in ARO is lower than MCF-7 cells (**Figure 2.3.8B**). Western blot analysis also shows enhanced FOXA1 expression post CI-994 treatment in MCF-7 cells specifically (**Figure 2.3.8C**).

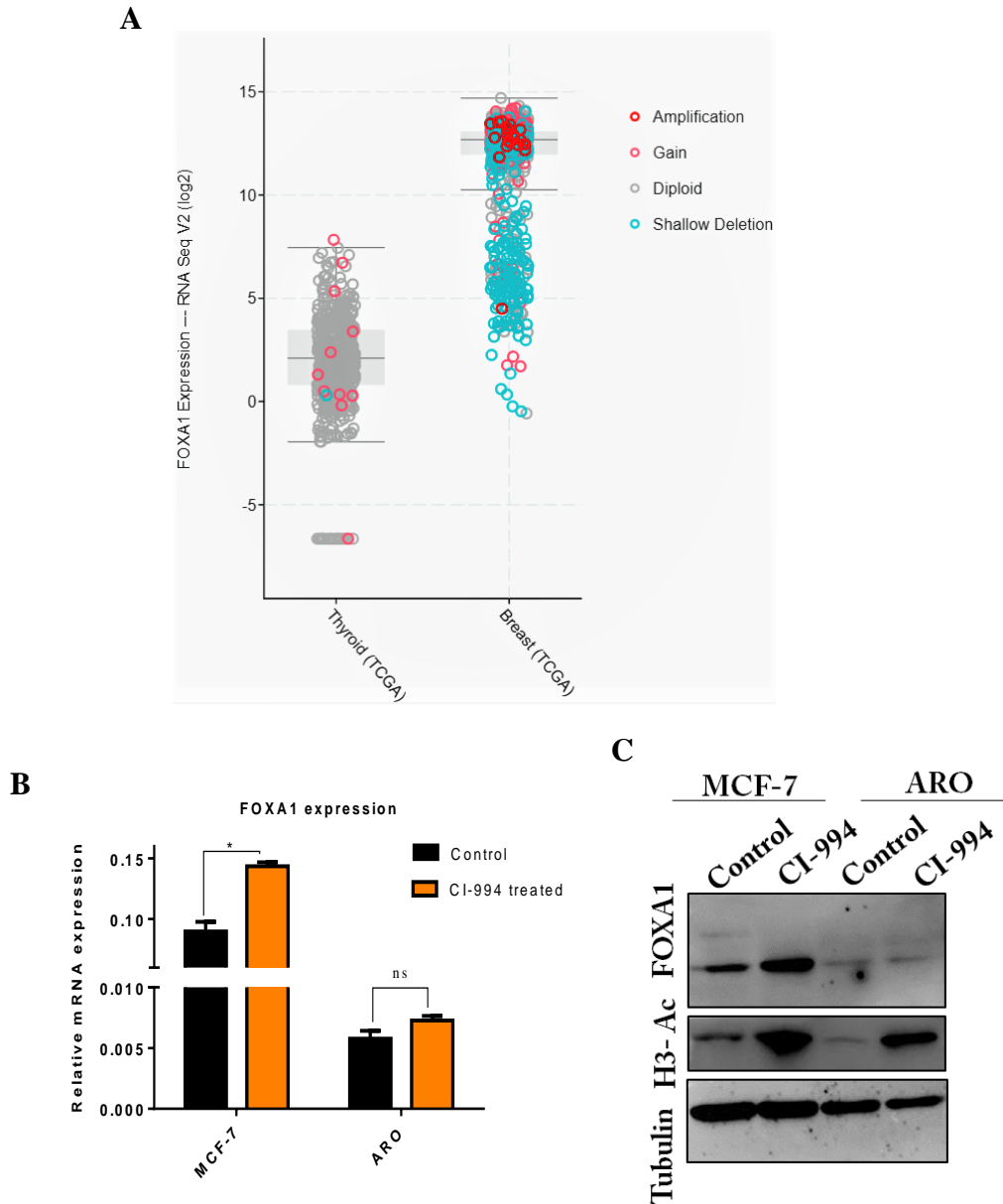
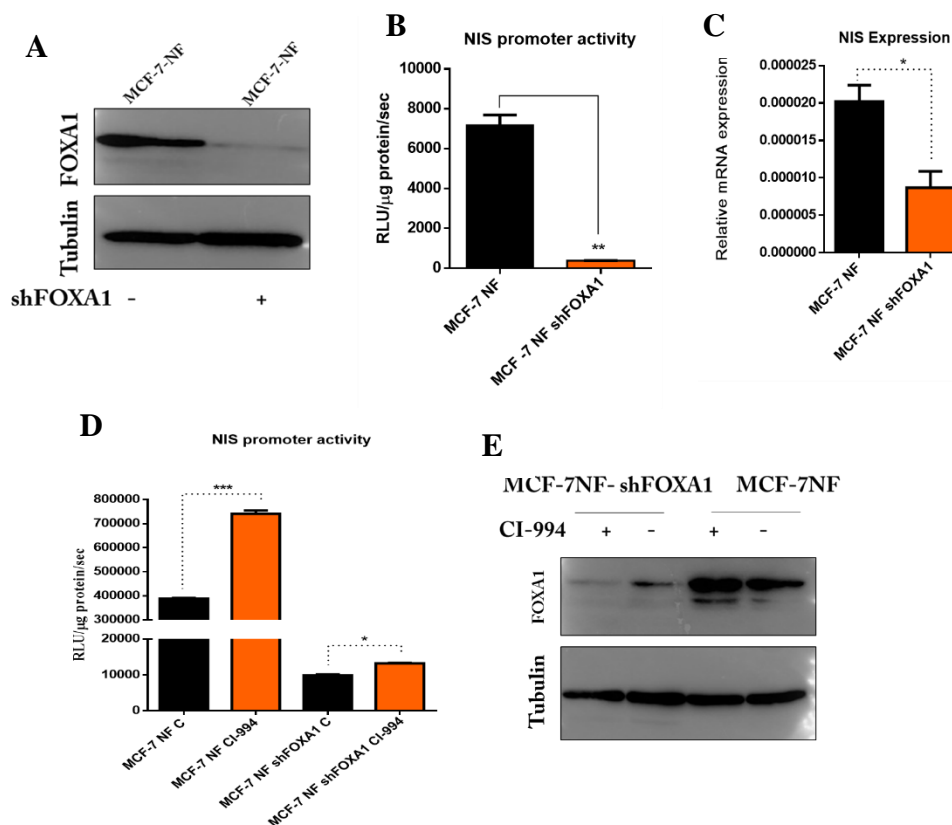


**Figure 2.3.8 FOXA1 shows differential expression in breast versus thyroid cancer**

**2.3.8A:** Retrospective TCGA data analysis showing the RNA sequencing expression values of FOXA1 on y-axis. **2.3.8B:** Graph showing real time PCR data for FOXA1 in MCF-7 and ARO cells. Y-axis shows relative mRNA expression. GAPDH is used as an internal loading control. \* indicates  $p < 0.05$ . Error bar shows SEM. **2.3.8C:** Western blot showing the expression of FOXA1 under 48 hours of CI-994 treatment in MCF-7 and ARO cells. H3Ac is used to measure the functional activity of HDACi, tubulin used as an internal loading control.

### 2.3.9 FOXA1 is a positive transcriptional modulator of NIS expression in breast cancer

Using the FOXA1 knockdown stable system (**Figure 2.3.9A**), we tested the effect of FOXA1 depletion on NIS promoter activity. **Figure 2.3.9B** shows a significant ( $p < 0.01$ ) decrease in NIS promoter activity under FOXA1 knockdown condition (shFOXA1 MCF-7 NF). The similar finding was validated by measuring the NIS transcript levels in shFOXA1 MCF-7 NF cells. A significant ( $p < 0.05$ ) drop in NIS mRNA expression is recorded in FOXA1 knockdown cells as compared to parental MCF-7 NF cells (**Figure 2.3.9C**). Since HDACi can globally regulate the transcriptional status of genes through various TFs, we tested the effect of CI-994 treatment on shFOXA1 MCF-7 NF cells. Interestingly we found that CI-994 treatment is not able to enhance NIS promoter activity in FOXA1 knockdown background, thus highlighting the dominance of FOXA1 for NIS modulation in MCF-7 cells (**Figure 2.3.9D**). Assessment of FOXA1 expression in shFOXA1 MCF-7 NF cells, also showed that CI-994 could enhance FOXA1 expression only in the parental MCF-7 NF cells and not in shFOXA1 MCF-7 NF model (**Figure 2.3.9E**).

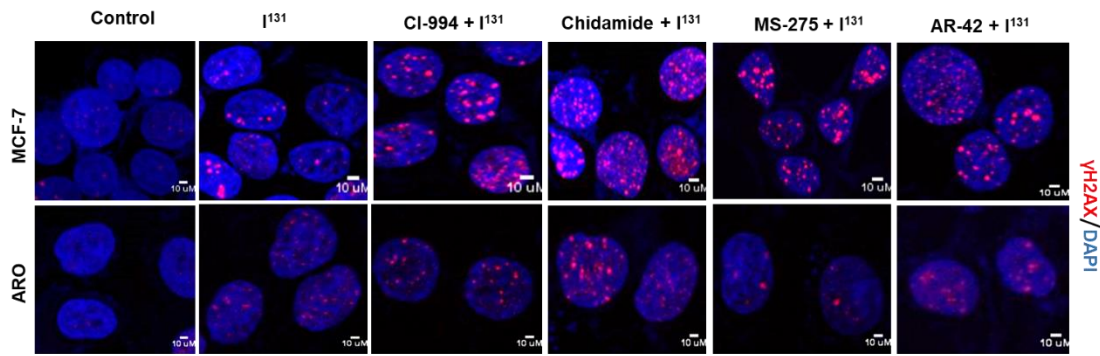


**2.3.9 FOXA1 positively modulates NIS expression in MCF-7 cells** **2.3.9A:** Western blot showing FOXA1 expression in MCF-7 NF and MCF-NF shFOXA1 cells. Tubulin was used as loading control. **2.3.9B:** Graph showing NIS promoter activity in terms of relative light output, normalized by protein concentration (RLU/ $\mu$ g/s) as indicated on y-axis. Error bar indicates SEM. \*\* indicates  $p \leq 0.01$ . Relative light output (RLU). **2.3.9C:** Graph showing the relative mRNA expression of NIS (y-axis) in parental and shFOXA1 MCF-7 NF cells. **2.3.9D:** Chart showing NIS promoter activity in MCF-7 NF parent and MCF-NF shFOXA1 cells with 24 hours CI-994 treatment. \*\* indicates  $p \leq 0.01$ . **2.3.9E:** Western blot showing the change in FOXA1 expression post CI-994 treatment in MCF-7 NF and MCF-NF shFOXA1 cells. Tubulin was used as loading control.

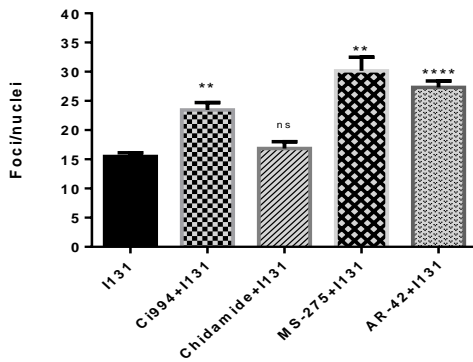
### **2.3.10 Enhanced function of NIS in BC, leads to significant induction of DNA damage in response to $^{131}\text{I}$**

Increase in NIS function would lead to a higher accumulation of iodine in cells, thus for testing the therapeutic implication of enhanced NIS function, we exposed MCF-7 and ARO cells to radio-active isotope of iodine  $^{131}\text{I}$ .  $^{131}\text{I}$  is known to cause double stranded DNA breaks in the cell, hence we applied a classical approach to check DSB i.e.  $\gamma\text{H2AX}$  foci measurement. MCF-7 cells treated with bHDACi at IC30 equivalent or lower concentrations, show a significant increase in the number of  $\gamma\text{H2AX}$  foci (**Figure 2.3.10A-B**), whereas the thyroid cancer cell line ARO show no significant change in the number of foci, indicating no change in DSB (**Figure 2.3.10A,C**).

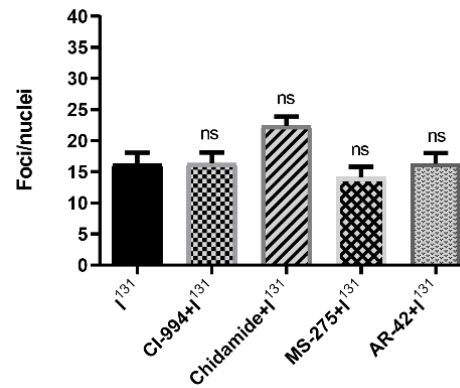
**A**



**B**



**C**

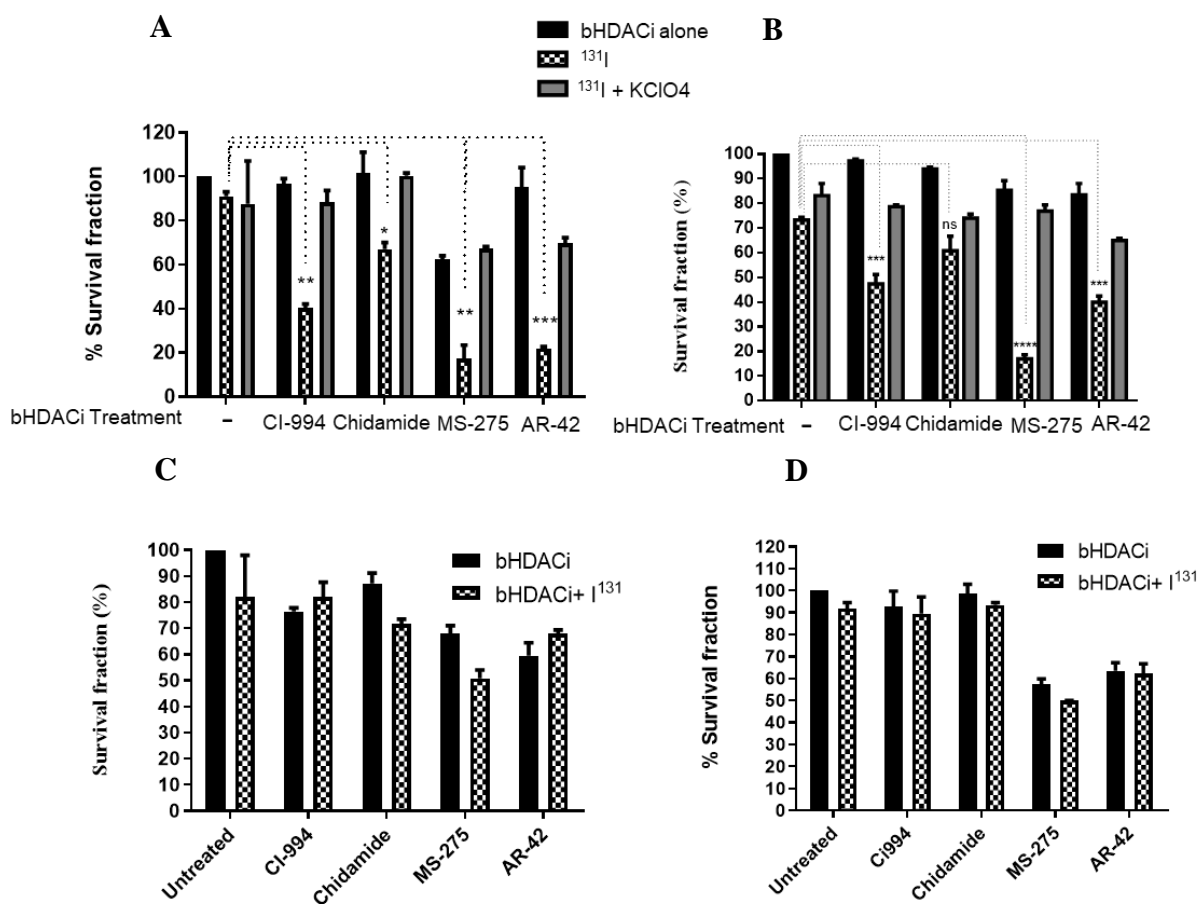


**2.3.10 Enhanced NIS function leads to an increase in  $^{131}\text{I}$  mediated DSB in breast cancer cells. 2.3.10A:** Immunofluorescence images showing  $\gamma\text{H2AX}$  foci stained in red and nucleus stained with DAPI in blue. Scale bar indicating  $10\mu\text{m}$  distance. **2.3.10B-C:** Graphs showing the quantification of  $\gamma\text{H2AX}$  foci per nucleus in MCF-7 and ARO cells respectively. Error bar indicates SEM. \* indicates  $p < 0.05$ , ns means non-significant.

### 2.3.11 bHDACi reinforces the $^{131}\text{I}$ mediated radio ablation effect differentially in breast cancer cells

Since bHDACi treatment to breast cancer cells can enhance the NIS mediated uptake of  $^{131}\text{I}$  and cause significant damage to DNA, we tested its therapeutic implication by *in vitro* long term cell survival assay. As seen from **Figure 2.3.11A-B**,  $^{131}\text{I}$  and bHDACi treatments individually did not have any cytotoxic effect on the long term survival of breast cancer cells

(MCF-7 and ZR-75-1). However, when the bHDACi (IC30) are combined with  $^{131}\text{I}$ , a significant ( $p < 0.05$ ) reduction in the cell surviving fraction is observed. The effect was most profound under CI-994, MS-275 and AR-42 treatment for both MCF-7 and ZR-75-1 cell lines. CI-994 combination with  $^{131}\text{I}$  leads to around 60% cell death in BC cells, while MS-275 combination with  $^{131}\text{I}$  causes 80% cell death in both MCF-7 and ZR-75-1 cells. This  $^{131}\text{I}$  mediated cell death is NIS specific, since the inhibition of NIS function by potassium perchlorate ( $\text{KClO}_4$ ) could rescue the  $^{131}\text{I}$  mediated cell death, showing 70-80% cell survival, which is almost at par with only bHDACi treated cells. The thyroid cancer cell lines ARO and NPA, treated with bHDACi and a combination of bHDACi +  $^{131}\text{I}$ , show no change in cell death, which goes in line with our earlier findings, showing no change in NIS function in TC after bHDACi treatment (**Figure 2.3.11C-D**).



### 2.3.11 <sup>131</sup>I mediated radio ablation effect is differentially enhanced in breast cancer cells.

2.3.11A-D: Graphs depicting the fraction of cells surviving on a long term after <sup>131</sup>I treatment in the presence or absence of bHDACi in MCF-7, ZR-75-1, ARO and NPA cells respectively. Potassium perchlorate – KClO<sub>4</sub> (30μM) was as a negative control for NIS function. Error bar represents SEM (\*\*indicates  $p \leq 0.01$ ).

### 2.3.12 Low dose AR-42 and MS-275 boost NIS expression *in vivo*

For validating our *in vitro* findings under *in vivo* settings, we used engineered ZR-75-1 (CMV-FL2.Turbo reporter expressing) BC cells, for generating orthotopic BC model. The mice were divided into treated and un-treated groups for standardizing the drug treatment dose and schedule. Immunohistochemistry (IHC) analysis of NIS from tumours treated with AR-42 (5mg/kg) and MS-275 (10mg/kg), show enhanced staining of NIS post treatment as compared to untreated tumours, indicating elevated expression of endogenous NIS (**Figure 2.3.12A-B**). Haematoxylin eosin (H&E) staining confirms tumour morphology.

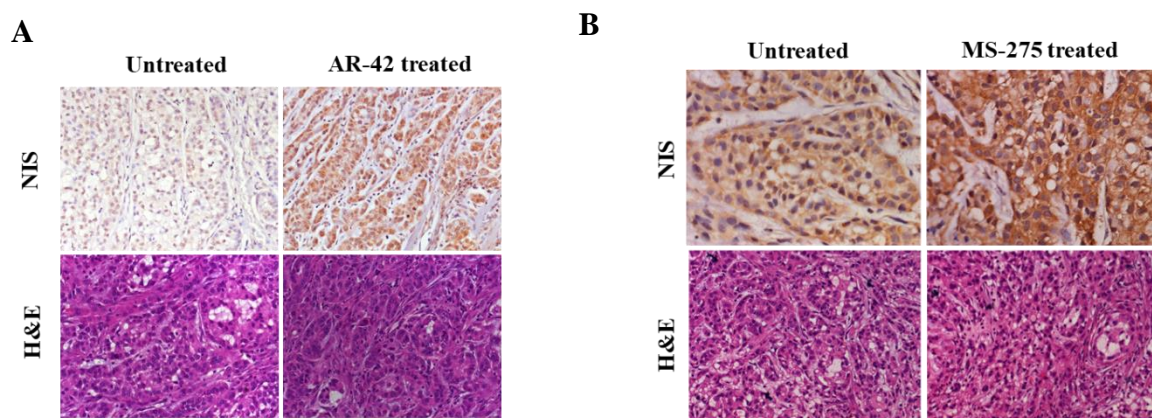


**Figure 2.3.12 MS-275 and AR-42 induce NIS expression in *in vivo* breast tumour model**

2.3.12A-B: Images of Immunohistochemistry (IHC) analysis of NIS (brown DAB stain) expression from tumours of treated (AR-42, MS-275 respectively) and untreated groups. Haematoxylin and eosin (H&E) staining shows the tumour morphology.

### **2.3.13 AR-42 elevates NIS promoter activity in breast tumour *in vivo***

Further, the modulatory effect of bHDACi on NIS promoter activity was also verified *in vivo*. Breast cancer cells (ZR-75-1) overexpressing pNIS-FL2.Turbo construct (ZR-75-1 NF) were used to develop orthotopic BC model in mice. AR-42 treatment at 5mg/kg, for 3 alternate doses was given to the treated group by intraperitoneal route. The treated group shows a significant ( $p \leq 0.05$ ) increase in NIS promoter activity *in vivo* (**Figure 2.3.13A-B**), as compared to control. The tumour volumes measured from mice belonging to both control and treated groups show no significant change in tumour growth over the treatment time span (**Figure 2.3.13C**). Thus implying that the change in BLI signal is contributed majorly by NIS promoter activity (luciferase signal), rather than change in tumour volume. However, we also observed that low doses of AR-42(5mg/kg) and MS-275(10mg/kg) selected for NIS mediated radio iodine therapy, did not impart anti-tumour effect themselves (**Figure 2.3.13D-E**). Quantification of BLI signal shows that tumours from control and AR-42, MS-275 treated group keep growing with time, thus implying that AR-42 and MS-275 at sub optimal doses do not have anti-tumour activity (**Figure 2.3.13E**).

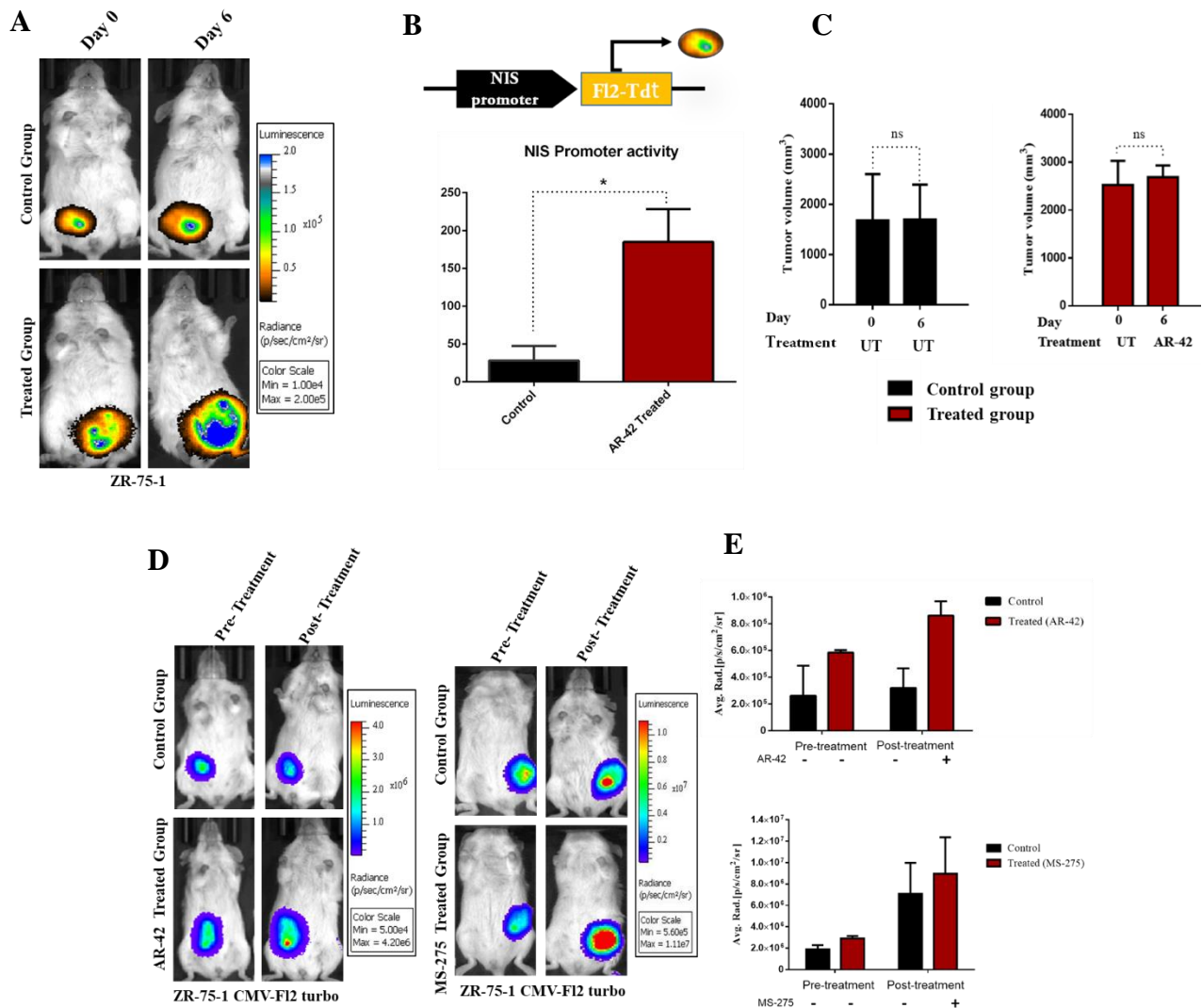
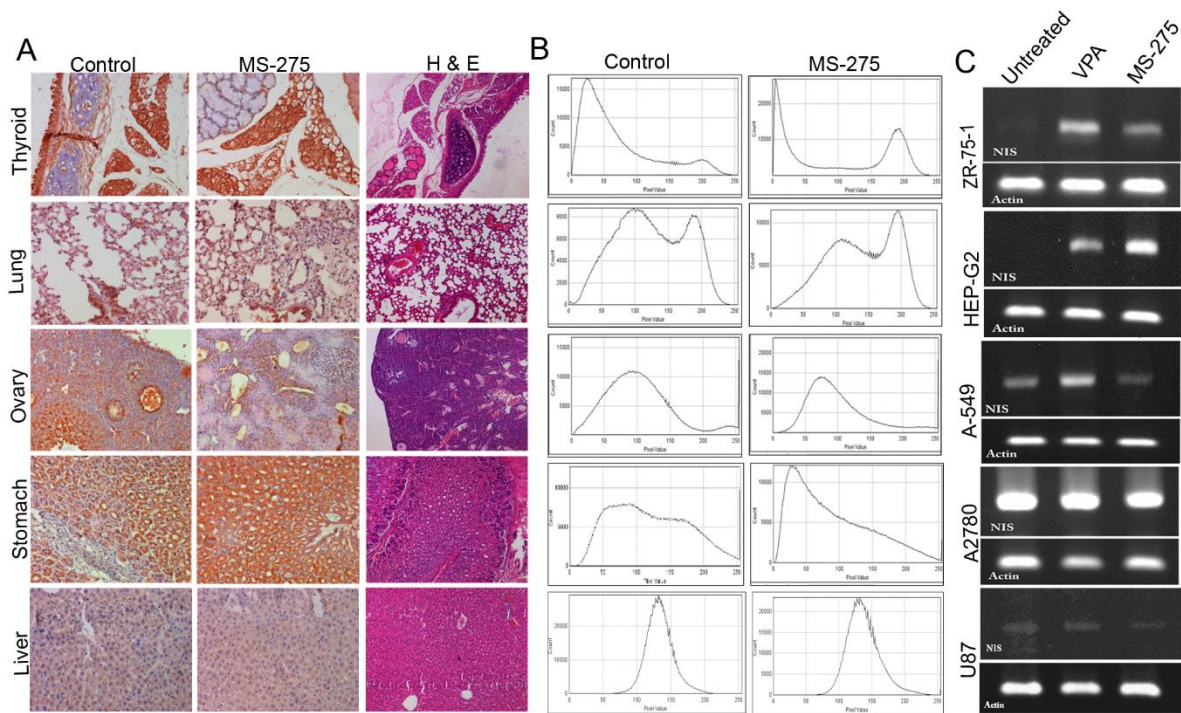


**Figure 2.3.13 AR-42 induce NIS promoter activity at non tumorigenic sub optimal dose in breast tumour model in vivo** **2.3.13A:** Images representing the change in NIS promoter activity as measured by bioluminescence (BLI) signal, coming from orthotopic ZR-75-1 NF (pNIS-FL2.Turbo) tumour. **2.3.13B:** Representation showing the NIS promoter driven construct design and graph showing quantification of the BLI signal post AR-42 treatment in control and treated groups, normalized to their respective pre-treatment signals. Error bar indicates SEM from 2 mice. \* indicates  $p \leq 0.05$ , as calculated by student's t-test. **2.3.13C:** Graph showing the tumour volume (mm<sup>3</sup>) measurement from control and treated groups on day 0 and day 6 of AR-42 treatment. **2.3.13D-E:** BLI images and their quantification

*obtained from control and AR-42, MS-275 treated tumours harboring the stable CMV-Fl2.Turbo constructs for reporting tumour growth.*

#### **2.3.14 NIS expression is differentially regulated in non-breast organs and cells**

Further, to establish the differential modulatory effect of bHDACi *in vivo*, IHC profiling of NIS expression was done across different organs isolated from mice treated with MS-275 (10mg/kg). Organs that have a basal expression of NIS like stomach, ovary, liver and thyroid were considered for the study. MS-275 treatment enhances NIS expression in stomach, but is ineffective for inducing NIS expression in other organs. Most importantly, NIS expression in thyroid remains unaltered after MS-275 treatment, which goes in line with the *in vitro* data showing bHDACi do not modulate NIS expression in thyroid cancer cells (**Figure 2.3.14A-B**). Further, we also compared the modulatory effect of bHDACi candidate MS-275 with aliphatic acid class HDACi candidate VPA, across breast carcinoma (ZR-75-1), hepatocellular carcinoma (HEP-G2), lung (A-549), ovarian carcinoma (A2780) and glioblastoma (U87) cell lines. Both the drugs induce NIS expression in BC cell line ZR-75-1 and hepatocellular carcinoma cell line HEP-G2. Whereas, bHDACi (MS-275) mediated induction of NIS in ovarian cancer, glioblastoma and lung cancer cell lines is absent. Interestingly neither VPA nor MS-275 could augment NIS expression in glioblastoma (U87) and ovarian carcinoma (A2780) cell line tested (**Figure 2.3.14C**).



### 2.3.14 MS-275 differentially regulates NIS expression in non-breast organs and cells

**2.3.14A:** Images obtained by Immunohistochemistry staining of NIS expression (brown) depicted by DAB stain from thyroid, lung, ovary, stomach and liver. (H&E) staining shows the architecture of the respective normal organs. **2.3.14B:** Graphs showing the quantification of NIS expression by IHC profiler. X-axis shows the intensity and y-axis shows counts. Peaks closer to 0 indicate highest intensity, following a decreasing trend towards 250. **2.3.14 C:** Semi-quantitative PCR gel images of NIS transcript expression. Actin was used as housekeeping control.

### 2.3.15 bHDACi mediated elevation of NIS, leads to a potential radio ablation effect on orthotopic breast tumour *in vivo*

Since, bHDACi candidates MS-275 and AR-42 were capable of inducing endogenous NIS expression *in vivo*, we sought out to study the therapeutic benefit of augmented NIS levels in breast tumours. Mice bearing orthotopic breast tumours were divided into 3 groups i.e. control,  $^{131}\text{I}$  and bHDACi+ $^{131}\text{I}$ . The uptake of  $^{131}\text{I}$  in thyroid was blocked by giving a 25 days treatment

of T3, T4 and methimazole (MMZ) combination, prior to  $^{131}\text{I}$  therapy. Tumours from AR-42 +  $^{131}\text{I}$  treated mice show a significant ( $p < 0.05$ ) reduction in reporter signal, as compared to  $^{131}\text{I}$  treated and untreated control tumours. The BLI signal from AR-42 +  $^{131}\text{I}$  treated tumours show regression till day 2 post  $^{131}\text{I}$  injection, and the remnant tumour mass starts re-growing after day 2, however the tumours of control and  $^{131}\text{I}$  treated mice continue to grow at every measured point. (Figure 2.3.15A-C). The similar trend was observed with MS-275 as well. MS-275 +  $^{131}\text{I}$  combination groups show a decrease in tumour growth at day 1 and day 2 after  $^{131}\text{I}$  injection, whereas the tumours from  $^{131}\text{I}$  and control group continued to grow (Figure 2.3.15B-D).

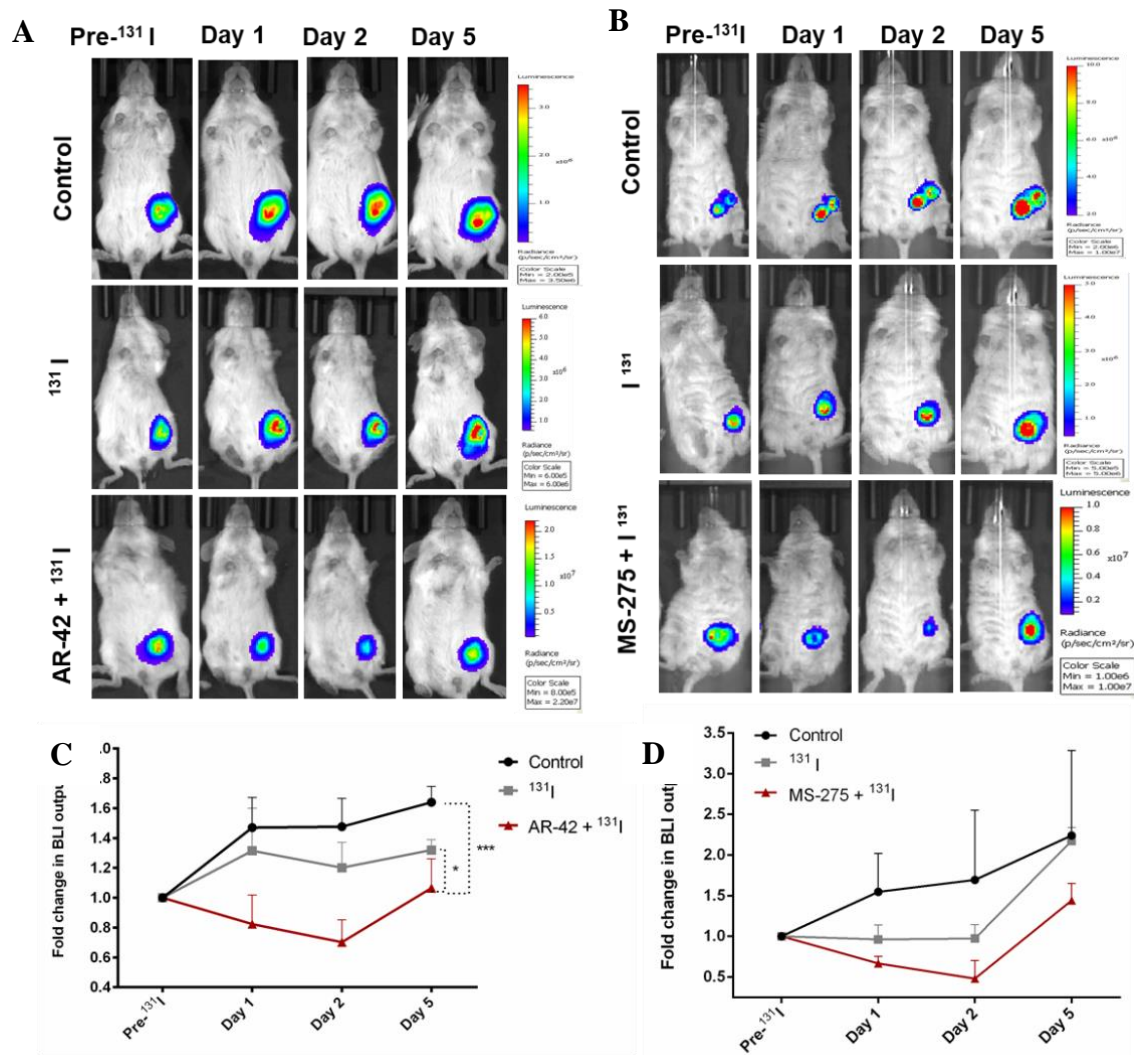


**Figure 2.3.15: bHDACi augments NIS mediated  $I^{131}$  therapy in breast tumours. 2.3.15 A, B:** Mice images indicating bioluminescence (BLI) signal as a measure of tumour growth, from Control,  $^{131}\text{I}$  and AR-42, MS-275+ $^{131}\text{I}$  groups. Scale bar indicates the minimum and maximum BLI output in terms of radiance. **2.3.15C, D:** Graphs showing the percent change in BLI signal with respect to their pre  $^{131}\text{I}$  treatment signal. Error bar indicates SEM calculated from 3 mice per group.

### 2.3.16 $^{131}\text{I}$ accumulation in tumour is higher in MS-275+ $^{131}\text{I}$ group

Since  $^{131}\text{I}$  poses the inherent property of emitting Cerenkov radiance, we utilized this phenomena to image the distribution of  $^{131}\text{I}$  in tumour and thyroid. Interestingly we found that the accumulation of  $^{131}\text{I}$  was higher in MS-275+  $^{131}\text{I}$  tumours than only  $^{131}\text{I}$  treated tumours, thus explaining the reduction of tumour growth in MS-275+  $^{131}\text{I}$  groups seen from previous data (**Figure 2.3.16A-B**).

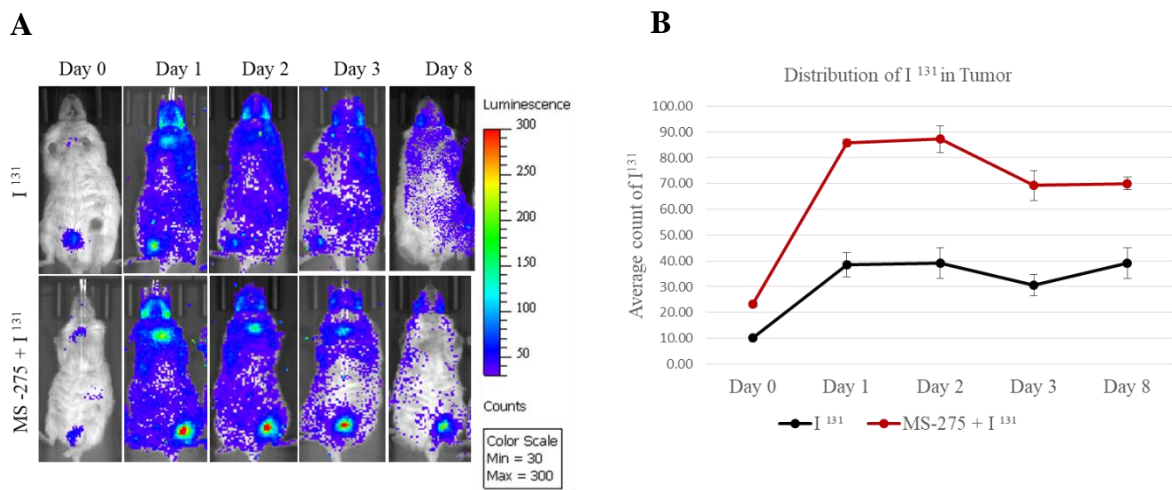


**Figure 2.3.16** MS-275+<sup>131</sup>I treated breast tumours have a higher accumulation of <sup>131</sup>I

**2.3.16A:** Mice images showing Cerenkov luminescence (CLI) signal at different time points post <sup>131</sup>I injection in <sup>131</sup>I and MS-275+<sup>131</sup>I groups. Scale bar shows the CLI signal in terms of counts of photons. **2.3.16B:** Graph indicating the photon counts of Cerenkov luminescence generated by <sup>131</sup>I on y-axis, over a time span in <sup>131</sup>I and MS-275+<sup>131</sup>I groups.

## 1.4 Discussion

Over a time span of 19 years, several groups have reported the expression of NIS in breast cancer and breast cancer metastasis to brain and lymph nodes [3-7, 93]. NIS mediated radioablation therapy is a promising approach in the pursuit for alternate therapies to breast cancer. However, due to the clinical limitations pertaining to low expression of endogenous NIS and defective membrane localization in breast cancer, NIS mediated gene therapy is still far from clinical trials. Significant efforts in the past have helped us understand some molecular regulators of NIS, where tRA is the major enhancer of NIS function in breast cancer [94]. The association of NIS gene expression to epigenetic silencing by hypo acetylation has been well established in thyroid cancer. HDAC inhibitors also enhance NIS expression and function in breast cancer [14, 15]. We show that HDAC 1 is an important mediator of NIS induction, where viral mediated stable knock down of HDAC1 in MCF-7 cells, lead to a significant enhancement in NIS expression. Report from our lab has demonstrated the effect of various HDACi belonging to 6 different chemical class of HDACi on augmenting NIS function *in vitro* and *in vivo* [15]. As HDACi have a global effect on modulating gene expression in cells, we would expect that they can induce NIS expression in all cell types showing endogenous NIS staining. To our surprise, we found that benzamide class HDACi could elevate NIS expression and function in BC but failed to enhance NIS expression in the thyroid cancer cells and normal

breast MCF-10A cells. Further, the effect of MS-275 (benzamide class HDACi) on elevating NIS expression in normal thyroid was investigated at *in vivo* setting. We found that MS-275 did not change the endogenous levels of NIS in thyroid gland, but could successfully enhance NIS expression in the tumour tissue from the same mice tested. In a quest to understand the mechanistic basis for this differential modulation of NIS across two tumour types, we performed a high throughput assay for determining the activation of 96 different transcription factors (TF) post CI-994 treatment in MCF-7 (BC cell) and ARO (TC cell). We found 22 differentially regulated TF across MCF-7 versus ARO. Pax8 and CREB are known regulators of NIS in thyroid cancer, whereas AP3, CDF, CREB, EGR, ELK, FOXA1, FOXO1, FOXOF2, HOXA5, PAX3, PAX8, PIT, PXR, STAT5, STAT6, NF-1, FOXC1, TCF/LEF, NKX3.2, PBX1, RB and XBP are novel TF identified. FOXA1 showed maximum induction specifically in breast cancer cell. Interestingly, from retrospective TCGA data analysis, we found that FOXA1 expression is higher in breast cancer patients as compared to thyroid cancer patients. Also, FOXA1 shows amplification in breast cancer patients, which is absent in TC patients. Human protein expression atlas also reports higher expression of FOXA1 in breast cancer as compared to thyroid cancer. We investigated the role of FOXA1 on regulating NIS gene expression in our system. The basal endogenous levels of FOXA1 show a differential trend in MCF-7 and ARO, where FOXA1 is higher in MCF-7 cells, thus corroborating the patient sample data from TCGA. CI-994 is capable of inducing the expression of FOXA1 in MCF-7 but not in ARO cells. Further stable knockdown of FOXA1 in MCF-7 cells expressing NIS promoter driven firefly luciferase (shFOXA1 MCF-7 NF), showed a significant reduction in NIS promoter activity and NIS gene expression. Thus we identify a novel transcriptional regulator of NIS which positively regulates NIS expression. Interestingly, when we treated the shFOXA1 MCF-7 NF cells with CI-994, we found that it failed to induce FOXA1 and NIS

expression. As CI-994 can up regulate various other TFs in MCF-7 cells, it is important to note that the loss of FOXA1 itself abrogates the effect of CI-994 to induce NIS in MCF-7.

Benzamide class HDAC inhibitors used in the study are in phase 2/phase 1 clinical trials for various solid tumours and refractory tumours [[128-131](#)]. However, HDACi at high doses show adverse effects and toxicities. Use of low dose HDACi can be used to repurpose them as mediators of NIS mediated radio-iodine therapy. Cytotoxicity assay from our data shows that the effective concentrations of the benzamide class HDACi used in the study are non-toxic to cells.

Drug alone or  $^{131}\text{I}$  alone do not abate the tumour growth, while MS-275 and AR-42 in combination with  $^{131}\text{I}$  (single 1mCi dose) could effectively reduce the tumour burden by 40%. It is appreciable that a single systemic dose of  $^{131}\text{I}$  along with MS-275 and AR-42 can cause a reduction in tumour growth. As in clinical settings, for thyroid cancer patients repeated doses of TSH followed by  $^{131}\text{I}$  are administered systemically, for complete tumour remission, a similar schedule for breast cancer treatment could be established in pre-clinical models. As reported earlier that NIS is expressed in the brain and lymph node metastasis of breast tumours [[6](#)], NIS mediated radio-ablation therapy in metastatic setting needs further warrant. Hence our study lays the base for pre-clinical radio-ablation gene therapy by re-purposing the benzamide class HDACi in breast cancer. These bHDACi especially MS-275 and AR-42 can be extended for clinical trials in future after establishing preclinical dosing for breast cancer. Benzamide class HDACi is more clinically worthwhile compared to other chemical class of HDACi since they show breast cancer specific modulation of NIS, whilst not tampering the NIS expression profile in normal breast cells and thyroid.

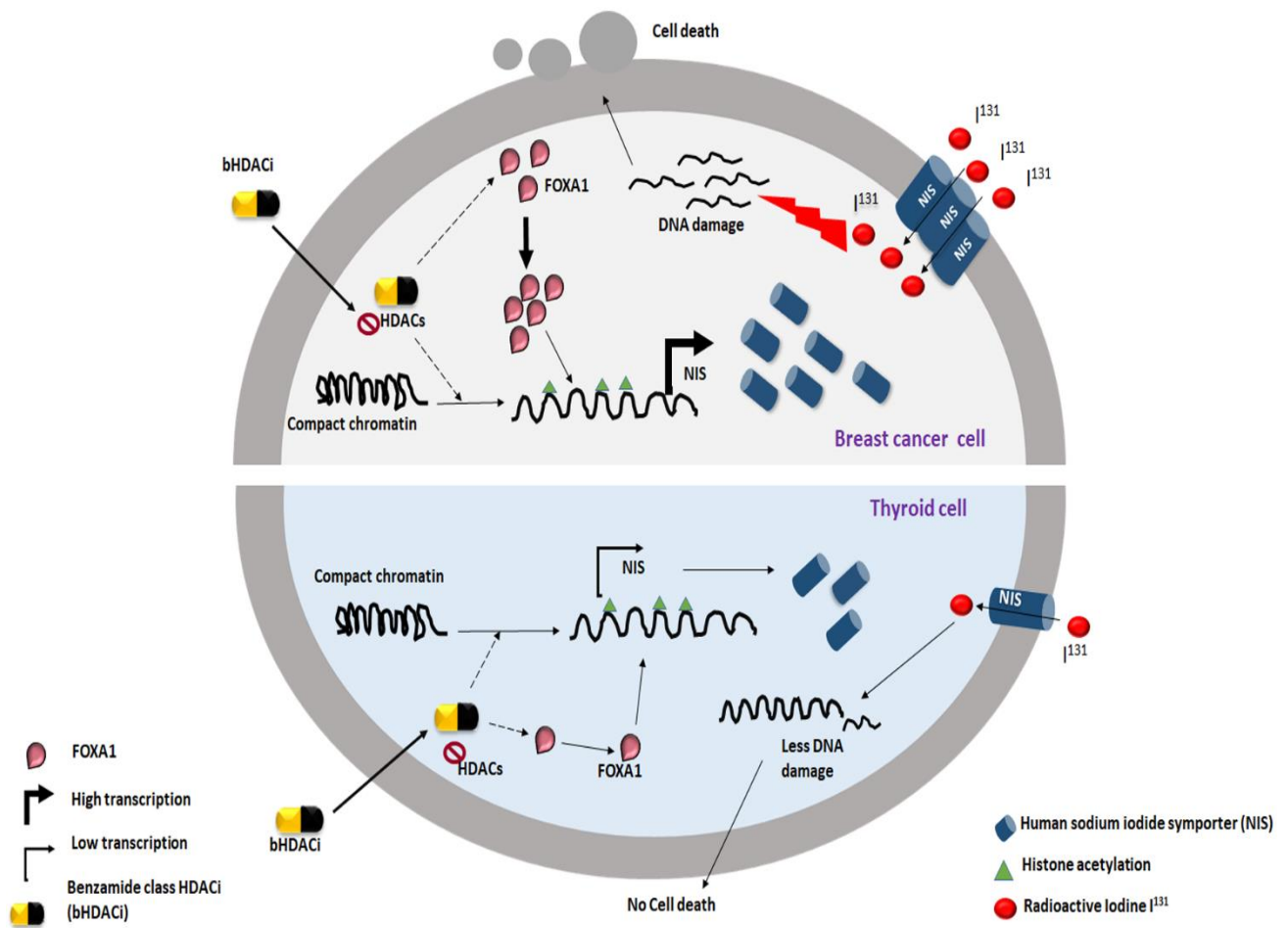


*Figure 2.4.1 Schematic illustrating the bHDACi mediated regulation of NIS across breast and thyroid cancer cells*

**CHAPTER 3:**

*Understanding the role of cAMP-PKA-CREB axis on  
regulating NIS expression*

### 3.1 Introduction

Human Sodium Iodide Symporter (NIS) is a transmembrane glycoprotein which uses an electrochemical gradient from Na<sup>+</sup>/K<sup>+</sup> pump to symport 2 sodium ions along with 1 iodine ion into the thyroid follicular cells [53]. The physiological role of NIS in thyroid cancer is established for the production of thyroid hormones T3 and T4. The distinct ability of thyroid to concentrate iodine due to the presence of functional NIS, has made the treatment of thyroid cancers remarkably successful in clinics [132]. NIS could serve as an ideal therapeutic gene target for organs which inherently express this protein. Lactating mammary glands are known to express functional NIS in plasma membrane for efficient uptake of iodine in colostrum [3]. However, the first report indicating the presence of NIS in breast cancer (BC), has opened new avenue for applying NIS based radio ablation therapy in BC. Successful use of radio ablation therapy in thyroid cancer (TC) clinics relies majorly on the understanding of the regulatory pathways for functional NIS. Thyroid stimulating hormone (TSH) regulates NIS expression by a cAMP dependant pathway in thyroid [1]. The use of NIS mediated radio ablation therapy in breast cancer faces some clinical limitations like insufficient expression of protein i.e. only 30% cases show 2+/3+ score for NIS and defective subcellular localization of NIS [7, 16]. Thus a deeper understanding of the modulators of NIS in BC can help in enhancing NIS expression in BC. Trans retinoic acid (tRA) is identified as an important enhancer of NIS function [95]. Hydrocortisones, lactogenic hormones and purinergic signals are also capable of enhancing NIS expression in a tRA dependant fashion in MCF-7 cells [1]. Since cAMP has a pivotal role in modulating NIS in thyroid, studies have attempted to understand its role in breast cancer. But, cAMP mediated regulation of NIS in BC had contradictory reports. One group reports that cAMP has inhibitory effects on NIS transcription in combination to tRA [133]. While on the other hand, cAMP enhanced the expression of NIS in BC [134], however it had no significant

effect on NIS function in MCF-7. cAMP is an important secondary messenger which not only regulates cell signalling through transcriptional activation of genes, but is also reported as a potential regulator of N-linked glycosylation [18]. The use of cAMP in BC lead to an increase in the translocation of NIS to plasma membrane. cAMP response element binding protein (CREB) is a transcription factor which gets activated through different kinases, importantly protein kinase A(PKA), mediated by a secondary messenger cyclic AMP(cAMP). PKA phosphorylates CREB at serine 133 residue, leading to homo dimerization of CREB [135]. This activated CREB dimer then binds at CRE sites on gene targets to induce their transcription. Since 1996, when NIS was cloned and characterized, it is known that NIS has CRE sites in the upstream enhancer region (NUE) in thyroid [63]. However, the role of CREB in modulating NIS expression in BC remains unaddressed. This study elucidates the role of activated CREB in modulating NIS expression in BC and also provides evidence that CREB is a direct regulator of NIS gene expression.

## **3.2 Materials and methods**

### **3.2.1 Reagents and antibodies**

KT-5720(sc-3538), 8-Br-cAMP (sc-201564), Forskolin (F3917), CREB monoclonal antibody from Abcam (ab32515), pCREB (ab32096), PKA(ab108385), pPKA(ab75991), human Sodium Iodide Symporter antibody from Thermo Scientific (MA5-12308), alpha tubulin primary antibody from sigma (T9026), anti-mouse HRP secondary antibody from AbCAM (ab6728), goat anti-rabbit DyLight 488 secondary antibody from Thermo Scientific (35552), goat anti-rabbit HRP antibody from Thermo Scientific (31460), goat anti-mouse DyLight 633 secondary antibody from Thermo Scientific (35512).

### **3.2.2 Luciferase assay**

The protocol suggested by Promega was followed for performing the assay. NIS promoter driven engineered cells were lysed by reporter lysis buffer provided and luciferase activity was measured in a luminometer (BMG Labtech), using LARII substrate. The relative light output (RLU) was normalized with the respective protein concentrations of the lysates.

### **3.2.3 Immunoblotting**

RIPA buffer along with protease inhibitor cocktail was used for cell lysis. 10 % SDS-PAGE gel was used to resolve the proteins and then transferred onto a nitrocellulose membrane by semi-dry blotting apparatus. 5% non-fat dry milk was used to block the non-specific sites on the membrane, and then the membranes containing proteins were probed with respective primary antibodies, followed by HRP- conjugated secondary antibodies in blocking solutions.

### **3.2.4 Immunofluorescence**

4% paraformaldehyde for 10 minutes incubation at RT was used for fixing the cells. 2% BSA was then used for blocking, followed by overnight exposure at 4°C to NIS, pPKA antibodies. Anti-mouse/anti-rabbit Dylight 633 secondary antibody was used. Image acquisition was done by LSM780 confocal system, using a 63x oil objective, with a numerical aperture of 1.3 and pinhole restricted to 1 AU (1AU=0.7µm). Sequential scanning was done to capture images with two independent channels.

### **3.2.5 Real Time PCR**

RNA extraction was done using RNeasy kit. First strand cDNA synthesis kit was then used for preparing the cDNA from the RNA obtained under different experimental setups. Taqman

chemistry was applied for real time quantitation of NIS transcripts, by 7900HT PCR cycler (Applied Biosystems, USA). Technical and biological replicates were run for the experiments.

### 3.2.6 Chromatin Immunoprecipitation

RIPA lysis buffer was used to lyse the cells. Sepharose G beads were blocked by salmon sperm DNA. Low SDS (0.01%) RIPA buffer served as CHIP dilution buffer. 2 $\mu$ g primary CREB, pCREB antibodies along with blocked beads and chromatin fragments were incubated overnight under rotation at together overnight at 4°C, for immunoprecipitation. DNA was isolated from the pull down product and purified by ethanol wash. CHIP products were then verified by PCR assay for determining the binding of CREB, pCREB to NIS promoter region. The detailed protocol is discussed in appendix section. The primers used and PCR conditions were as follows:

CRE site on NIS promoter	Sequence
Forward primer	TCAAAGTCCTCCTGGGTCC
Reverse primer	GGGAGAAAGTCTACTGGGG

*Table 3.1: CREB binding sites on NIS promoter sequence*

PCR step	Temperature	Time
Initial denaturation	95°C	10 min
Denaturation	95°C	30 sec
Primer annealing	55°C	30 sec
Primer Extension	72°C	60 sec
Final extension	72°C	10 min
Hold	4°C	Infinity

**Table 3.2: PCR conditions for CHIP- PCR for CRE amplification on NIS promoter****3.3 Results****3.3.1 NIS promoter activity is positively regulated by CREB in breast cancer cells**

Forskolin and 8-Br cAMP are positive modulators of protein kinase A (PKA), which phosphorylates CREB at serine 133, thereby activating CREB. Forskolin and 8 Br cAMP activate CREB at 10 $\mu$ M and 1 $\mu$ M concentrations respectively, as demonstrated by an increase in phosphorylated CREB (pCREB) after Forskolin and 8 Br cAMP treatment to MCF-7 cells (**Figure 3.3.1A**). To study the effect of CREB activators on NIS promoter activity, we developed a NIS promoter driven firefly luciferase (pNIS-FL2.Turbo overexpressing) reporter model in ZR-75-1 cells (ZR-75-1 NF) previously in lab. 24 hours treatment of Forskolin and 8-Br cAMP to ZR-75-1 NF cells lead to a significant ( $p < 0.0001$ ) increase in the NIS promoter activity (**Figure 3.3.1B-C**).

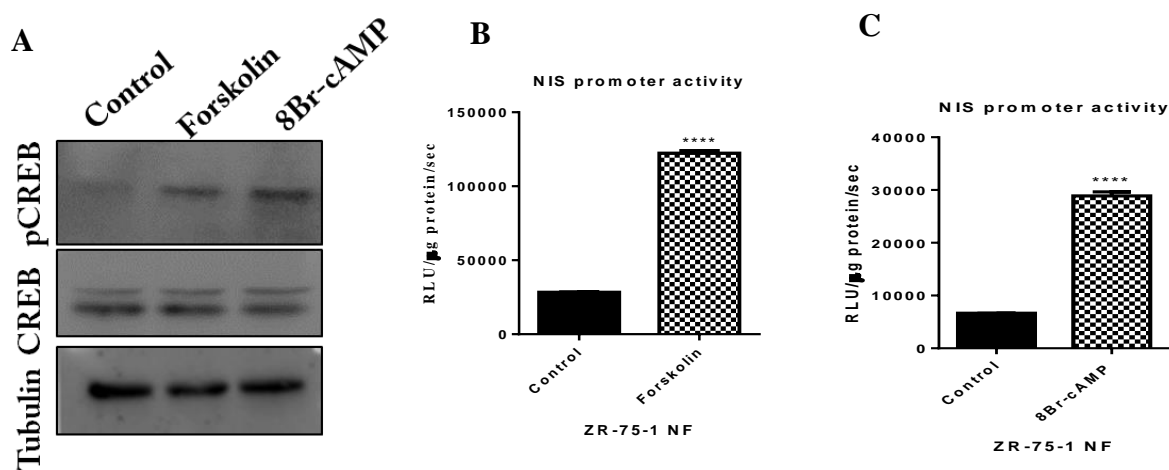


**Figure 3.3.1 CREB activation leads to elevation of NIS promoter activity 3.3.1A:** Western blot showing the increase in pCREB expression post Forskolin and 8 Br cAMP treatment.

*Tubulin is used as an internal loading control. **Figure 3.3.1B-C:** Graphs showing induction of NIS promoter activity post Forskolin (fsk) and 8 Br cAMP treatment. Y-axis shows relative light output from luciferase signal normalised to protein concentration. \*\*\*\* indicates  $p < 0.0001$ .*

### **1.3.2 Activation of CREB can induce NIS expression in breast cancer cells**

Forskolin and 8-Br cAMP also enhance the NIS transcript levels, in MCF-7 and ZR-75-1 cells, as tested by quantitative real time PCR. Forskolin treatment triggers a 5 fold induction of NIS in MCF-7 and 2.5 fold in ZR-75-1 cells (**Figure 3.3.2A-B**). Also, 8 Br cAMP leads to 7 fold induction in NIS transcript levels in MCF-7 and ZR-75-1 cells (**Figure 3.3.2C-D**). Immunofluorescence staining of NIS protein in MCF-7 and ZR-75-1 cells shows that activation of CREB mediates an increase in the NIS protein levels in both MCF-7 and ZR-75-1 cell lines (**Figure 3.3.2E**). The induction of NIS translation post Forskolin and 8 Br cAMP treatment was also verified by performing an intracellular staining of NIS from MCF-7 and ZR-75-1 cells. Forskolin treatment enhances the expression of NIS from 9.8 to 12.4 in MCF-7 cells and 2.8 to 7.4 in ZR-75-1 cells. While 8 Br cAMP elevates NIS expression to 11.72 from 9.71 in ZR-75-1 cells (**Figure 3.3.2F**).

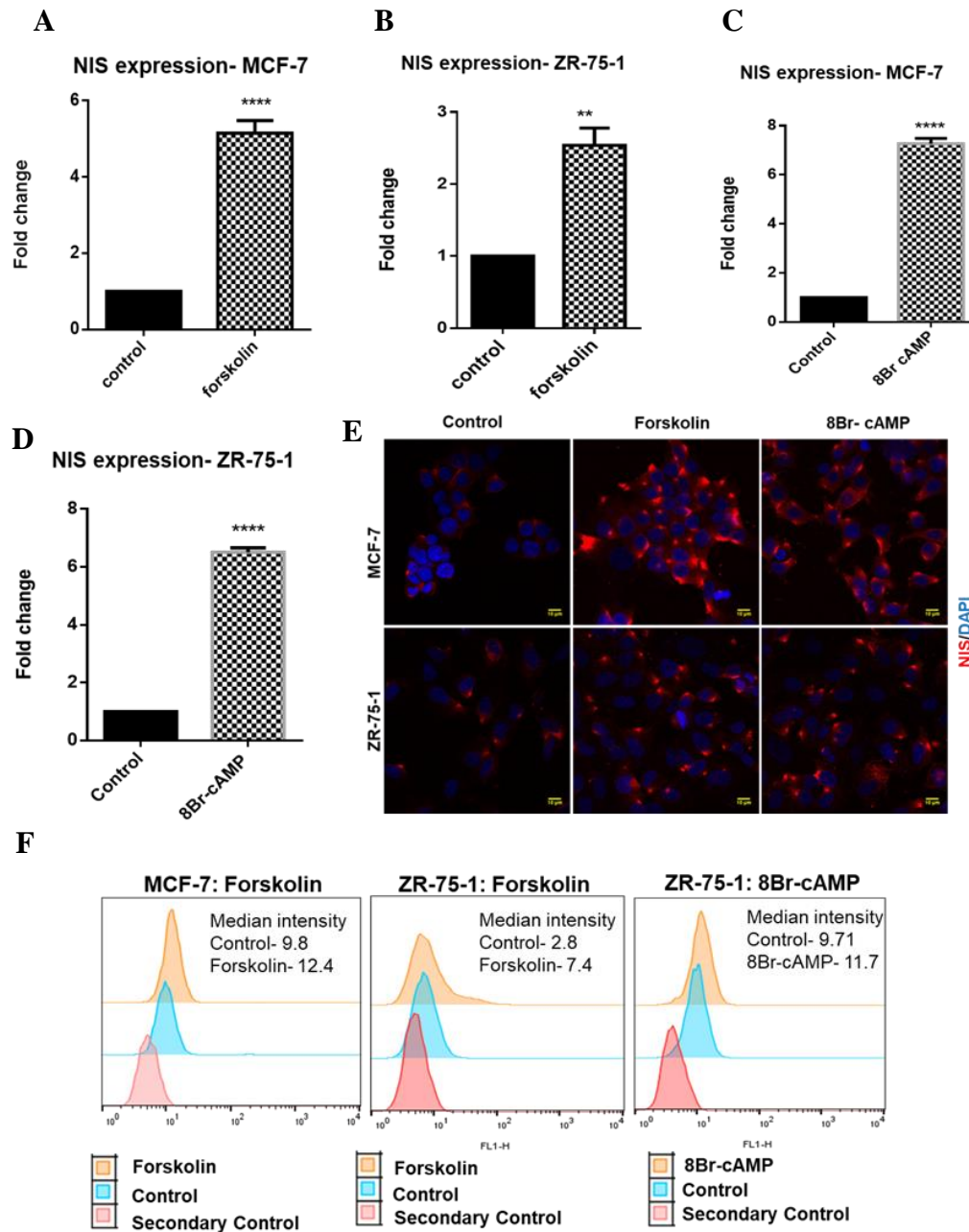


**Figure 3.3.2: Activated CREB enhances endogenous NIS expression in breast cancer cells**

**3.3.2A-D:** Charts indicating the change in mRNA expression of NIS after 24 hours of Forskolin and 8-Br cAMP treatment, in MCF-7 and ZR-75-1 cells. \*\*\*\* indicates  $p < 0.0001$ . Y-axis shows fold change values of treated samples/control. **3.3.2E:** Images from immunofluorescence assay showing NIS positive cells (red) stained with Dylight 633 and blue

showing nuclei stained with DAPI. Scale bar represents 10 $\mu$ m distance. **3.3.2F**: Intracellular staining of NIS in ZR-75-1 and MCF-7 cells, by anti -mouse FITC, as measured by FACS. Sec control represents the peaks with only FITC, whereas the rest of the samples indicate FITC signal in presence of primary NIS antibody.

### 3.3.3 Inhibition of PKA attenuates NIS expression

KT-5720 (KT) is an inhibitor of protein kinase A (PKA). As PKA is an important kinase for CREB activation, inhibition of PKA should effect the activation status of CREB. Thus we monitored the expression of pCREB in response to KT-5720. Dose dependent decrease in the activation of CREB is observed upon treatment with KT-5720 (KT) in MCF-7 cells (**Figure 3.3.3A**). Further, inhibition of CREB activation, leads to a significant ( $p < 0.001$ ) decrease in the NIS mRNA expression, thus highlighting the importance of this activated TF for regulating NIS gene expression (**Figure 3.3.3B**). Activation of CREB leads to its homo dimerization, which then binds to promoters of various targets and drives transcription. Thus, we studied the effect of inhibiting CREB activation upon NIS promoter activity. A significant ( $p < 0.0001$ ) reduction in NIS promoter activity is seen after KT-5720 treatment (**Figure 3.3.3C**). Immunofluorescence analysis for NIS protein expression also shows decreased NIS levels, post KT-5720 treatment in ZR-75-1 cells. The activation of PKA was also measured in the same experiment, which shows a decrease in pPKA levels as well (**Figure 3.3.3D**). The decreased NIS protein expression after KT treatment was also validated on another platform i.e. flow cytometry based intracellular staining for endogenous NIS, where a profound decrease in the median intensity of NIS is seen in KT treated cells as compared to control (**Figure 3.3.3E**).

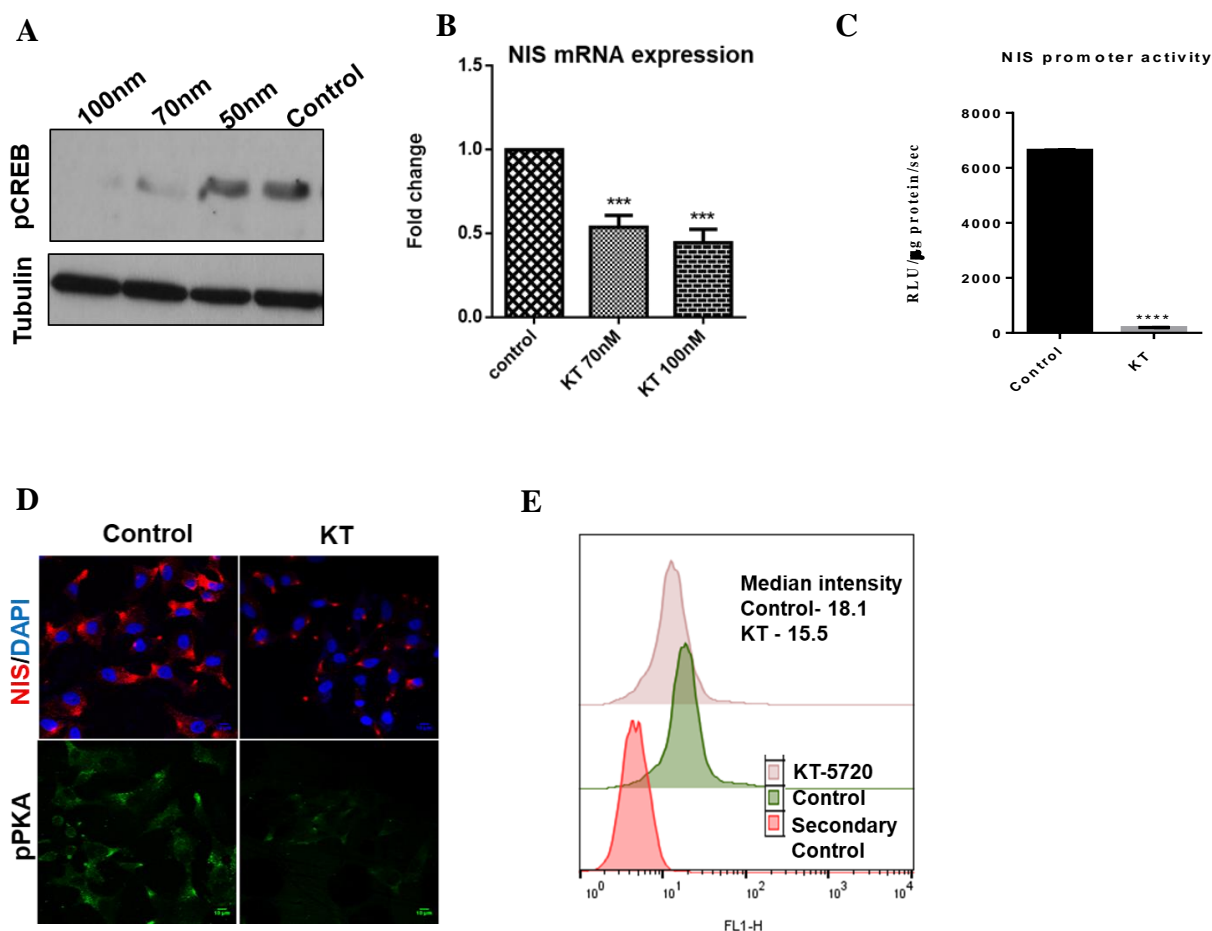


**Figure 3.3.3: Inhibition of PKA decreases NIS expression.** 3.3.3A: Western blot showing decrease in pCREB expression post KT-5720 treatment. Tubulin is used as an internal loading control. 3.3.3B: Graph showing the fold change in mRNA expression of NIS post KT-5720 treatment with respect to untreated control (y-axis). \*\*\* indicates  $p < 0.001$ . 3.3.3C: Graphs showing reduction of NIS promoter activity post KT-5720 treatment. Y-axis shows relative light output from luciferase signal normalized to protein concentration. \*\*\*\* indicates  $p < 0.0001$ . 3.3.3D: Immunofluorescence assay showing NIS positive cells (red) stained with Dylight 633 and blue shows nuclei stained with DAPI. Green indicates pPKA expression stained with Dylight 488. Scale bar represents  $10\mu\text{m}$  distance. 3.3.3E: Intracellular staining of NIS in ZR-75-1 cells, by anti -mouse FITC, as measured by flow cytometry. Sec control

*represents the peaks with only FITC, whereas the rest of the samples indicate FITC signal in presence of primary NIS antibody.*

### **3.3.4 CREB is directly recruited to NIS promoter, in order to regulate NIS gene expression**

CREB binds to its target promoters at CREB response element (CRE) sites, upon activation. Bioinformatics analysis of NIS promoter reveals 5 different CRE sites on the promoter as shown in **Figure 3.3.4A**. The primer was designed against the middle two sites as reflected in the illustration of Figure 3.3.4A. The primer was validated by performing a semi quantitative PCR using purified NIS promoter DNA as template, which shows amplification (**Figure 3.3.4B**). Further, the binding of CREB to NIS promoter was tested by CHIP-PCR from DNA bound to both CREB and pCREB pull down product. CRE site on NIS promoter show amplification from CHIPed DNA isolated from CREB pull down product (**Figure 3.3.4C**). The binding of pCREB to NIS promoter is enhanced after Forskolin treatment, as reflected from **Figure 3.3.4D-G**. GAPDH was used as an internal negative control to verify specific binding of CREB to its target promoter. Since CREB does not bind to GAPDH, there is no band seen in I.P from control and forskolin treated lysates (**Figure 3.3.4H**).

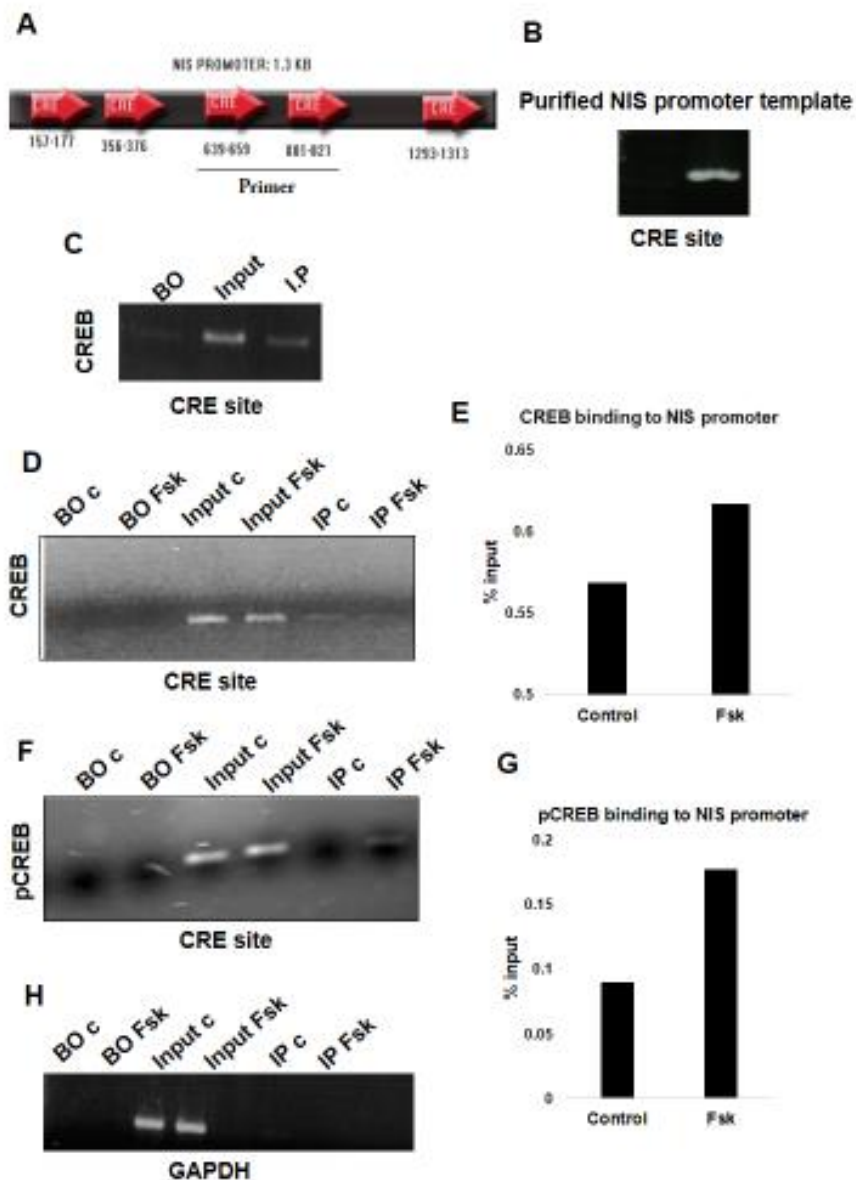


**Figure 3.3.4: pCREB physically interacts with NIS promoter.** 3.3.4A: Schematic indicating CRE sites on NIS promoter. 3.3.4B: Agarose Gel image showing the amplification of CRE site from purified NIS promoter template. 3.3.4C: Gel image for CRE site amplification of NIS promoter from CREB bound DNA template. BO indicates bead only control, I.P. indicates Immuno precipitated sample. 3.3.4D, F: Gel images for CRE site amplification of NIS promoter from CREB and pCREB bound DNA template respectively with Forskolin treatment. BO indicates bead only control, I.P. indicates Immuno precipitated sample, fsk stands for

*Forskolin treatment. 3.3.4E, G: Graphs showing the binding of CREB, pCREB to NIS promoter, calculated as percentage of input (y-axis). 3.3.4H: Gel image for GAPDH amplification from CHIP assay with CREB antibody. BO indicates bead only control, I.P indicates Immuno precipitated sample*

### **3.4 Discussion**

PKA-CREB pathway plays an important regulatory role for NIS expression in thyroid tissues. The presence of CRE elements (CREB binding sites) on NIS promoter suggests a potential role of CREB for NIS regulation. Thus we studied the effect of CREB on NIS gene modulation in BC scenario. cAMP inducers like forskolin have been used on MCF-7 cells in the past where it has shown contradictory reports, where one study showed an enhanced NIS function after forskolin treatment [134] and one study showed a decreased function of NIS [133]. However, whether cAMP induced activation of CREB directly controls NIS gene expression remains elusive. Our findings suggests that cAMP-PKA axis modulates CREB activation, which can positively modulate NIS expression in breast cancer cells. Treatment of MCF-7 and ZR-75-1 BC cells with forskolin (cAMP inducer) and 8-Br-cAMP (cAMP analog) leads to a significant ( $p < 0.0005$ ) increase in NIS promoter activity, NIS transcript expression and NIS protein expression.

In order to further verify if this induction of NIS is dependent on PKA mediated activation of CREB, we inhibited PKA activation by KT-5720 [136]. PKA consists of regulatory subunit and catalytic subunit. Upon activation, the catalytic subunit gets phosphorylated and dissociates from the regulatory subunits. This activated catalytic subunit then phosphorylates CREB at serine 133 position, which upon phosphorylation forms a homo-dimer and translocate to nucleus to induce target gene expression [135]. Inhibition of PKA activation, impeded the activation of CREB thus implying the dependence of CREB activation majorly on PKA pathway. Inhibition of CREB activation, further lead to a significant ( $p < 0.0005$ ) decrease in

the NIS promoter activity, NIS transcription and NIS protein levels. Further, we also established that activated CREB can directly bind to NIS promoter, thus acting as a direct modulator of NIS gene transcription. NIS promoter has 5 putative CRE elements present, of which two sites tested show efficient binding of activated CREB.

cAMP not only activates CREB to induce NIS expression in BC, but is also capable to induce N-linked glycosylation [137]. As discussed in chapter 4, N-linked glycosylation is an important mediator for the trafficking of NIS to plasma membrane in BC cells. As reported previously, cAMP could aid the translocation of NIS to plasma membrane, thus making cAMP an important modulator of NIS in BC [18]. cAMP can itself enhance N-linked glycosylation process and also elevate endogenous NIS expression through PKA-CREB pathway. Studies towards these lines could help in circumventing some important clinical limitations pertaining to NIS in BC.

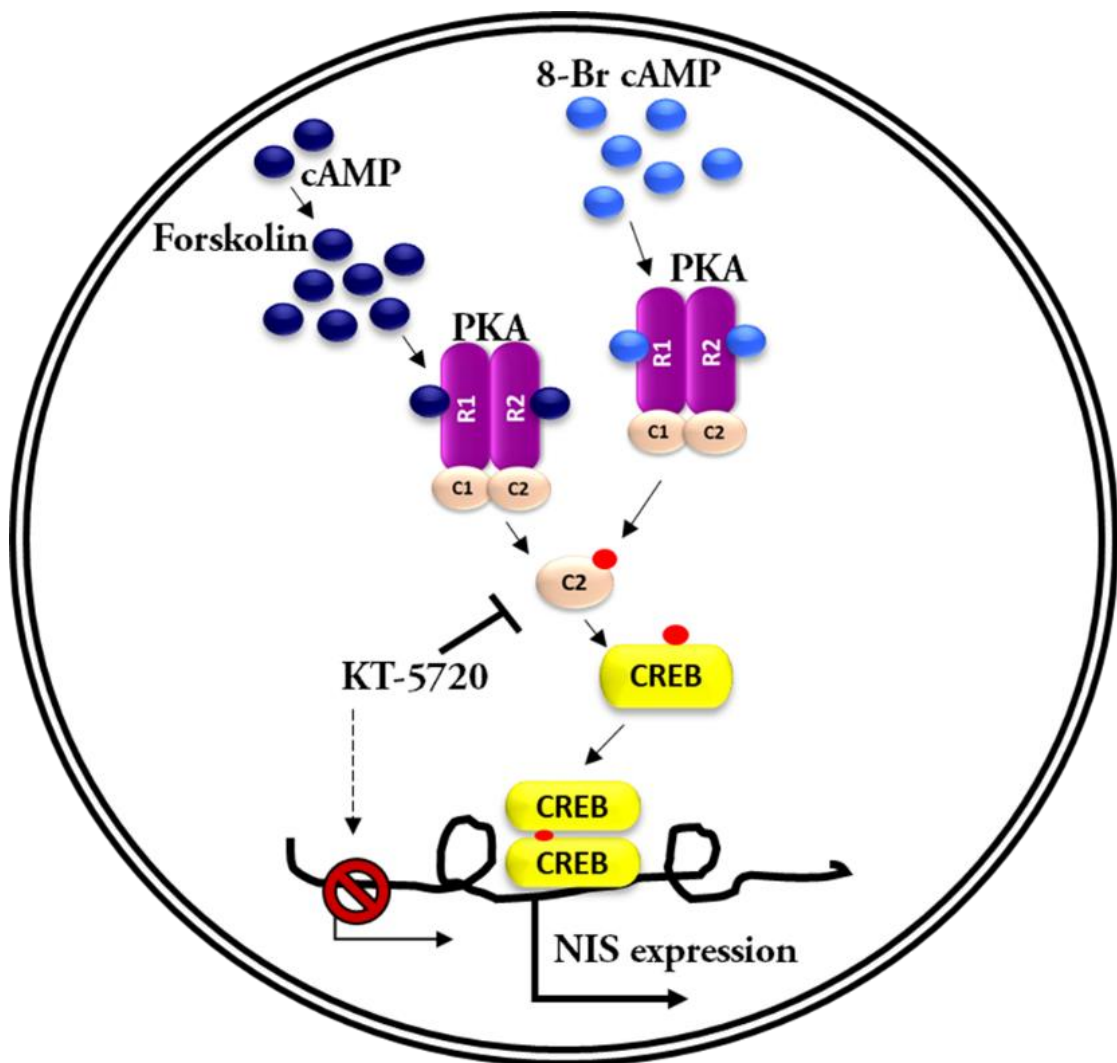


*Figure 3.4.1: Diagrammatic representation of the modulatory role of cAMP-PKA-CREB pathway for NIS gene regulation in BC cells*



## **CHAPTER 4:**

*Investigating the role of glycosylation as a regulatory  
mechanism to control NIS cellular localization*

## 4.1 Introduction

Human sodium iodide symporter (NIS) is an ion transporter protein, which is majorly found in thyroid tissue, where it transports iodine across the cell to the lumen of follicular cells. NIS expression is also reported in non-thyroidal tissues like lactating mammary glands, gastric organs, salivary gland [138]. NIS is a member of solute carrier family of proteins and thus its localization to plasma membrane is important for effective functioning. NIS is a membrane glycoproteins with 3 putative N-linked glycosylation sites at 225, 485, and 497 amino acid positions, which could most likely govern its function [52]. Although NIS is not expressed in normal breast during non-lactating phase, its expression was reported in breast cancer condition by various groups [3, 7, 9, 93], raising a hope for utilizing NIS gene for targeted delivery of radio-active iodine in the breast cancer cells and achieve a targeted tumour ablation [132]. However the localization of NIS was found to be cytoplasmic in most of the cases, which gave rise to a major disappointment for the clinical use of NIS in BC clinic, since defective localization of NIS hampered its function[7]. Out of majority of the patients samples which showed NIS positive expression, only 27% had membrane localized NIS [57]. Their study also co-related the defective sub cellular localization of NIS to poor iodine uptake, where only 15-20% patients showed visible amount of iodine uptake in the tumour [4]. The similar observation was confirmed by several groups, including our own group [5, 7].

There have been studies which have tried to address the localization defect of NIS in the past, however the underlying cause and the molecular regulators remain unsettled [18, 28]. Glycosylation is an important PTM which regulates biological processes like protein folding, stability and subcellular localization [139]. Several membrane glycoproteins, rely on effective glycosylation process for proper localization to the plasma membrane [140]. ER and Golgi are the organelles where the glycoproteins are processed until maturation, after which they are marked for exit from the ER or Golgi compartments towards their target destination. Biological

chaperons such as calnexin and calreticulin assists the proteins in ER for folding and ensure accurate glycan processing [141-143]. Thus, every step of glycosylation process is important for ensuring correct folding and maturation of a protein, as it moves from one organelle to the next. Thus defective localization of NIS in BC made us follow the basic cellular path of NIS across the organelles of secretory pathway.

EGF-ERK pathway has been demonstrated to lead NIS to plasma membrane in T47D breast cancer cells in the past [17]. Apart from positive regulators of NIS localization, negative modulator of NIS localization to membrane has also been elucidated like PI3K, overexpression of which, can lead to the enhanced accumulation of NIS in the cytosol [144]. The role of glycosylation as a mediator of NIS localization in BC has been suggested by reports where tunicamycin treatment could cause an accumulation of the de-glycosylated form of NIS which migrates at 55kDa in immunoblot [18, 97]. This has been confirmed previously by a group which demonstrated a 50% reduction of NIS function upon mutation of the putative N-linked glycosylation sites in rat [53], which was even more reduced in human breast cancer condition. A staurosporine-related protein kinase inhibitor (KT5823), could also lead to enhanced hypo-glycosylated NIS [97]. Thus emphasizing on the dependence of NIS function on glycosylation [18]. Certain mutations like R124H of NIS, render NIS accumulation in the ER and hamper its transit to Golgi, thus this mutant form of NIS expressed in COS cells, was majorly found localized in the cytoplasm. [145]. Although glycosylation is an important PTM modulating NIS function in BC, the actual cause behind cytoplasmic localization of NIS, in breast cancer still remains a mystery. Hence we aim at understanding whether there is some basic cellular defect in the trafficking of NIS in BC cells. Further our study also thoroughly investigates the role of N-linked glycosylation and their key effectors, on NIS localization in BC.

## **4.2 Materials and Methods**

### **4.2.1 Reagents and antibodies**

Brefeldin A(BFA) from Sigma, (B7651) , Deoxymannojirimycin (DMM) and tunicamycin from Sigma (D9305, T7765,), Glycosylation RT-PCR array from Qiagen (PAH546Z) ,Silencer select siRNA smartpools from Life Technologies, (4392426), CellLight ER-GFP Bacmam from Thermo Fisher scientific (C10590 ), HER3 monoclonal antibody from CST(12708S), human Sodium Iodide Symporter antibody from Thermo Scientific (MA5-12308), EGFR primary antibody from Cell signaling technologies(CST) (4267S), Calnexin from CST (C5C9), alpha tubulin primary antibody from sigma (T9026), anti-mouse HRP secondary antibody from AbCAM (ab6728), goat anti-rabbit DyLight 488 secondary antibody from Thermo Scientific (35552), goat anti-rabbit HRP antibody from Thermo Scientific (31460), goat anti-mouse DyLight 633 secondary antibody from Thermo Scientific (35512).

### **4.2.2 Generation of NIS overexpressing stable cell line**

Attb-CAG NIS-IRES-FL2.turbo plasmid DNA was introduced in MCF-7 cells by lipid based method (Lipofectamine 2000) [[146](#)] . The plasmid positive cells were selected and maintained under 600µg/ml G418 antibiotic. The positive clones were screened by luciferase assay for reporter positive cells and further the expression of NIS was cross checked by immunofluorescence (IF).

### **4.2.3 Luciferase assay**

The promega catalogue guided protocol was followed for performing the assay. Clonal cells were lysed by reporter lysis buffer provided and luciferase activity was measured in a luminometer (BMG Labtech), using LARII substrate. The relative light output (RLU) was normalized with the respective protein concentrations of the lysates.

### **4.2.4 Immunoblotting**

RIPA buffer along with protease inhibitor cocktail was used for cell lysis. 7.5% SDS-PAGE gel was used to resolve the proteins and then transferred onto a nitrocellulose membrane by semi-dry blotting apparatus. 5% non-fat dry milk was used to block the non-specific sites on the membrane, and then the membranes containing proteins were probed with respective primary antibodies, followed by HRP- conjugated secondary antibodies in blocking solutions.

#### **4.2.5 Immunofluorescence**

4% paraformaldehyde for 10minutes incubation at RT was used for fixing the cells. 2% BSA was then used for blocking, followed by overnight exposure at 4°C to NIS, HER3, Calnexin antibodies. Anti-mouse/anti-rabbit Dylight 633 secondary antibody was used. Image acquisition was done by LSM780 confocal system, using a 63x oil objective, with a numerical aperture of 1.3 and pinhole restricted to 1 AU (1AU=0.7µm). Sequential scanning was done to capture images with two independent channels.

#### **4.2.6 Real Time PCR**

RNA extraction was done using RNeasy kit. First strand cDNA synthesis kit was then used for preparing the cDNA from the RNA obtained under different experimental setups. SyBr green chemistry was applied for real time quantitation of transcripts, by 7900HT PCR cycler (Applied Biosystems, USA). Technical and biological replicates were run for the experiments.

#### **4.2.7 Iodine uptake assay**

Iodine uptake assay protocol was followed as per the method described before for non-radioactive assessment of amount of iodine present in the cells [15]. Also discussed in chapter 2.

#### **4.2.8 Immunoprecipitation and lectin western blot**

RIPA lysis buffer was used to lyse the cells. 250µg protein of each sample was used for IP. Sepharose G beads were used for pull down assay which were pre-blocked with 2% BSA. Low SDS (0.01%) RIPA buffer served as an IP dilution buffer. 2µg primary NIS antibody along with blocked beads and lysates were incubated overnight under rotation at together overnight at 4°C, for immunoprecipitation of NIS. The elution of NIS was done using urea buffer as per Abcam protocol for IP. Purified NIS obtained after immunoprecipitation, were run on SDS-PAGE gel, transferred to a nitrocellulose membrane and probed with 15µg/ml in TBST of Biotynylated concavalin A (conA) and biotin labelled L-PHA lectins for 1 h at RT. The blot was exposed with streptavidin HRP-conjugated secondary antibody at 1:30,000 dilution.

#### **4.2.9 Statistics**

All data were presented as standard error mean. Statistical significance was done with the help of GraphPad Prism 6 software (GraphPad Software, La Jolla, CA). Student t-test and 2 way anova (Tukey's multiple comparison test) were applied in the study. P values of  $\leq 0.05$  were considered statistically significant, Confidence Interval was set at 95%. ClustVis software was used for generating heatmap and cluster analysis of the RT-profiler array datasets obtained for 84 key genes for Glycosylation process.

## 4.3 Results

### 4.3.1 Standardization of Golgi deformation and reformation time kinetics, post BFA treatment

In order to study the intracellular trafficking of NIS in breast cancer cell model, we first standardised the Golgi deformation kinetics by brefeldin A (BFA) treatment. Disruption of Golgi would lead to the accumulation of NIS in the Endoplasmic Reticulum (ER) and when Golgi would reform after rescue from BFA treatment, the trafficking of NIS from ER to the Golgi could be tracked by co-localization of NIS and the respective organelle markers. Live cell imaging of Golgi marker (GalNacT2- GFP) at every 2 minutes time interval, over a span of 30 minutes shows gradual disruption in Golgi structure over time (**Figure 4.3.1A**). 30 minutes time point was fixed for looking at disrupted Golgi structure for further experiments. Further, the rescue period for Golgi reformation after withdrawal of BFA was standardised at 6-12 hours, time points (**Figure 4.3.1B**).

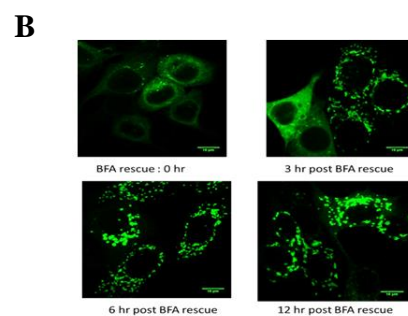
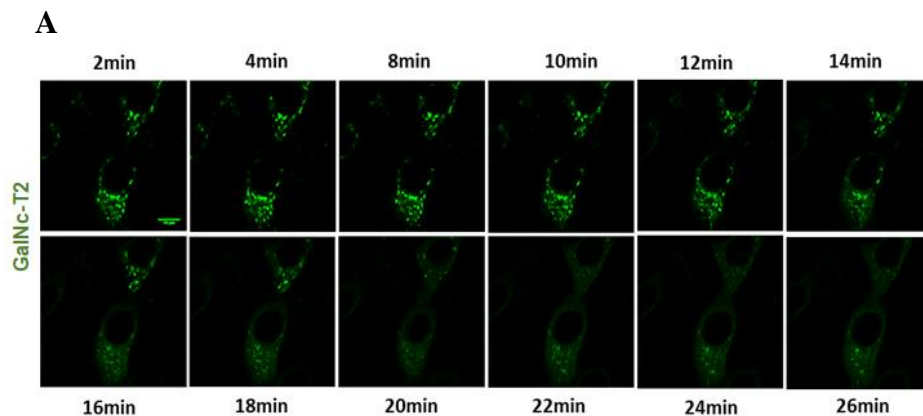


**Figure 4.3.1 Effect of BFA on Golgi morphology** **4.3.1A:** Live cell images captured at different time points post BFA treatment over 26 minutes time span. Green indicates GalNacT2-GFP marker staining Golgi. **4.3.1B:** GalNacT2-GFP (Green) showing the reformation of Golgi post BFA treatment rescue.

### **4.3.2 MCF-7 cells show defective NIS trafficking through secretory pathway**

After standardizing the Golgi deformation/re-formation kinetics in MCF-7 cells using BFA, we sought out to study the co-localization of NIS with ER (KDEL-GFP), ER exit site (ERES:Sec16B-GFP) and Golgi (GalNacT2-GFP) markers tagged to reporter over 0, 6 and 12 hours post BFA rescue. At 0 hour time point, when the Golgi is completely disrupted, the Golgi resident cargo move to ER through retrograde transport. Thus, staining of Golgi (GalNacT2-GFP) in **Figure 4.3.2A** resembles the ER structure, and NIS co-localization to this compartment is found to be 0.6. This reduces dramatically ( $p=0.0001$ ) as Golgi structure reforms (**Figure 4.3.2B**), thus indicating that NIS trafficking to Golgi is highly diminished. However NIS can travel from ER to ERES in MCF-7 cells (**Figure 4.3.2B**).

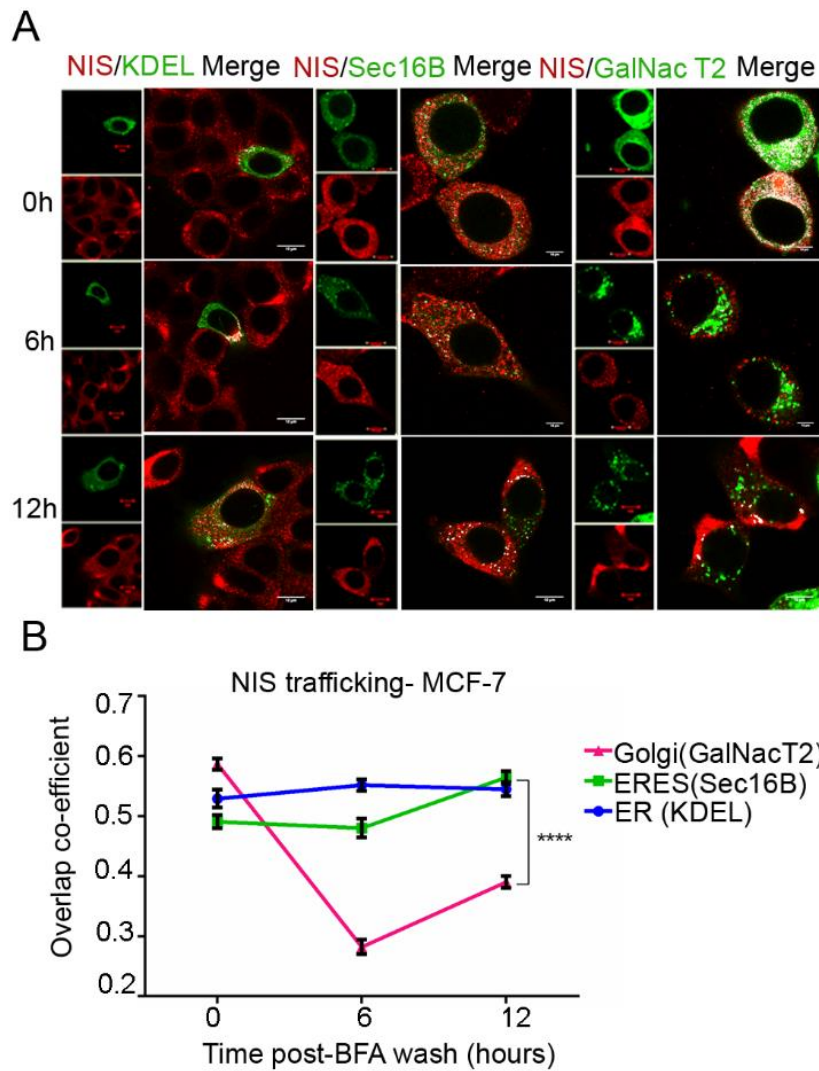
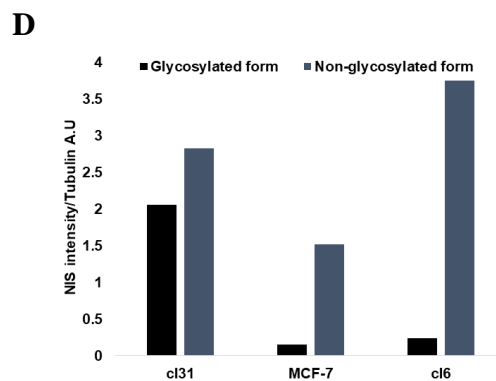
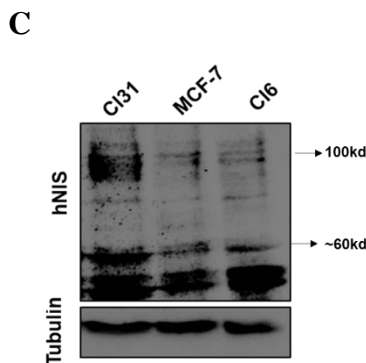
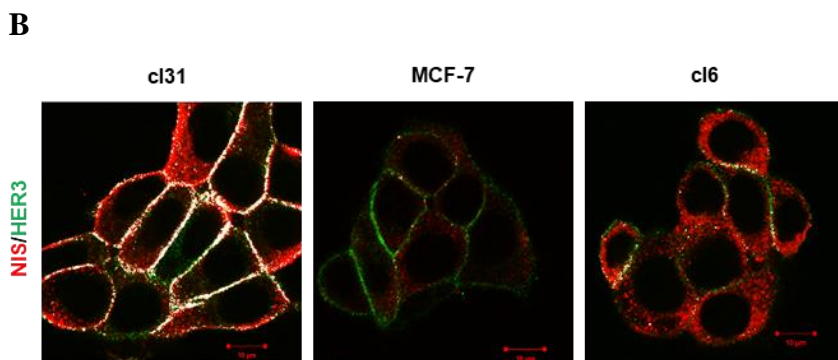
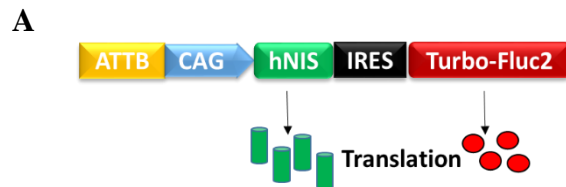


**Figure 4.3.2 Breast adenocarcinoma cells show impaired trafficking of NIS through cellular compartments.** **4.3.2A:** Immunofluorescence images showing the Co-localization of NIS (red) with green: ER (KDEL-GFP), ERES (Sec-16B-GFP) and Golgi (GalNac T2-GFP) respectively. 0 hours, 6 and 12 hours indicate the time spans of Golgi reformation post BFA rescue. White spots on the merge channel show points of co-localization between the two channels. The scale bar represents 10 $\mu$ m. Images were acquired with 63x objective. **4.3.2B:** Graph showing the overlap co-efficient (y-axis) of NIS (red) with GalNac T2, KDEL and Sec-16B (green) at 0, 6 and 12 hours post BFA withdrawal (x-axis). Error bars indicate SEM. \*\*\*\* indicate  $p < 0.0001$ .

### **4.3.3 Overexpression of NIS gene in MCF-7 cells, reveals two distinct type of clones with karyotype heterogeneity**

We used a previously developed (in house) NIS overexpressing MCF-7 cell model containing a bi-cistronic plasmid construct i.e. ATTB-CAG driving human NIS-IRES-Turbo.Fluc2 DNA sequence, to understand the underlying defect in the intracellular localization of NIS. NIS translation happens in the cap dependant manner and the reporter gets translated in a cap independent manner, thus aiding in simultaneous expression of NIS and the fusion reporter genes (**Figure 4.3.3A**). Strikingly, the overexpression of NIS in MCF-7 cells had given rise to 2 distinct clonal populations with differential localization of NIS at cell surface. One set of clones showed plasma membrane localization (cl31) while majority others localized to cytoplasm (cl6) like parental MCF-7 cells. The localization of NIS on the plasma membrane was verified by cross staining with HER3 (endogenous membrane protein). Co-staining for NIS and HER3 shows co-localization of NIS with HER3 in cl31 cells only, thus indicating the presence of NIS on membrane in this clone (**Figure 4.3.3B**), and thereby making these clonal cells an ideal model system for studying the differential sub cellular localization of NIS. Biochemical analysis of the glycosylation status of NIS across these clones was done by western blotting, where a 100kDa fraction indicates completely glycosylated mature form of NIS and 55-60kDa indicates the un-glycosylated form. NIS was found to migrate at 100kDa in cl31 cells, whereas parental MCF-7 and cl6 showed highly diminished levels of 100kDa NIS (**Figure 4.3.3C**). The semi-quantitative analysis of the intensity of NIS in glycosylated and non-glycosylated forms also shows that the glycosylated form is maximum in cl31 cells (**Figure 4.3.3D**). Further, to understand whether there is clonal heterogeneity within the clones derived from the same parent, we did a karyotype (GTG banding) analysis of parental MCF-7 and clonal cell variants. There were some similarities and differences observed within these cells as depicted in **Figure 4.3.3E**. Triploidy, derivative chromosome 1 and isochromosomes

of 7 and 11 were the similarities noted. However, apart from resembling the parental karyotype, the clones showed differences, such as deletions and extra copies of some chromosomes. However, no alteration was seen on chromosome 19 where NIS is located, across the three cell types tested.



**E**

Cell line	MCF-7 parent	cl31	cl6
<b>Ploidy</b>	Triploidy	Triploidy	Triploidy
<b>Similar abnormalities</b>	<ul style="list-style-type: none"> <li>Derivative chromosome 1 due to inversion and duplication of chromosome</li> <li>Isochromosomes of q arm of chromosome 7 and 11</li> </ul>	<ul style="list-style-type: none"> <li>Derivative chromosome 1 due to inversion or duplication of chromosome</li> <li>Isochromosomes of q arm of chromosome 7 and 11</li> </ul>	<ul style="list-style-type: none"> <li>Derivative chromosome 1 due to inversion or duplication of chromosome</li> <li>Isochromosomes of q arm of chromosome 7 and 11</li> </ul>
<b>Differential abnormalities</b>	Deletion in p/q arm of chromosome 1,2,3,6,11,17  Extra copies of chromosomes 7,8,9,10,11,13,14,15,16,17	Deletion in p/q arm of chromosome 1,6,8,11,17  Extra copies of chromosomes 4,5,7,8,9,10,11,13,15,16,17,20,22	Deletion in p/q arm of chromosome 1,2,3,6,8,11,17  Extra copies of chromosomes 4,5,7,8,9,10,11,13,14,15,16,17,20

**Figure 4.3.3 NIS overexpression in MCF-7 cells leads to clonal heterogeneity and differential sub cellular localization of NIS** **4.3.3A:** Cartoon depicting the bi-cistronic vector used for NIS overexpression clones in MCF-7. **4.3.3B:** Immunofluorescence assay showing the co-staining of NIS (red) and HER3 (green) in cl31, MCF-7 and cl6 cells. White spots indicate the points of co-localization between the two proteins tested. **4.3.3C:** Western blot showing the glycosylated (100kDa) and non-glycosylated (55-60kDa) forms of NIS in cl31, MCF-7 and cl6 cells. Tubulin used as an endogenous loading control. **4.3.3D:** Graph showing the quantification of the different forms of NIS from above western blot across cl31, MCF-7 and cl6 cells. **4.3.3E:** Table showing the summary of karyotype data analysis from MCF-7, cl31 and cl6 cells.

#### **4.3.4 NIS follows classical intracellular trafficking path in membrane clones**

Since we had two unique model systems in hand, with one depicting the ideal scenario of membrane localized NIS and the other showing the defective pattern of cytoplasmic NIS, we studied the intracellular trafficking of NIS in these two clonal types. Using a similar strategy like parental MCF-7, NIS co-localization with ER, ERES and Golgi markers was quantified after BFA rescue. NIS trafficking to ER was maintained at 0.55 overlap co-efficient. However, unlike MCF-7 cells, cl31 cells show a significant increase in Golgi localized NIS at 6 and 12 hours. The localization of NIS in ERES was drastically reduced in this case, indicating that the localization of NIS in membranous NIS expressing cells, follows a traditional path from ER to Golgi (**Figure 4.3.4A-B**). In contrast, the cytosolic clone (cl6) cells show a localization pattern similar to parental MCF-7 cells, where the trafficking of NIS from ER to ERES is maintained, but its localization to Golgi is significantly reduced, thus indicating a defective sub cellular localization of NIS in Golgi (**Figure 4.3.4D-E**). The comparison of NIS trafficking pattern across major organelles across cl6 and cl31 are depicted in **Figure 4.3.4C**, where we see that

as the Golgi structure is reformed at 6 and 12 hours post BFA rescue, NIS is capable of reaching Golgi only in cl31 cells. However, this transit from ER to Golgi in the cytosolic clone is perturbed.

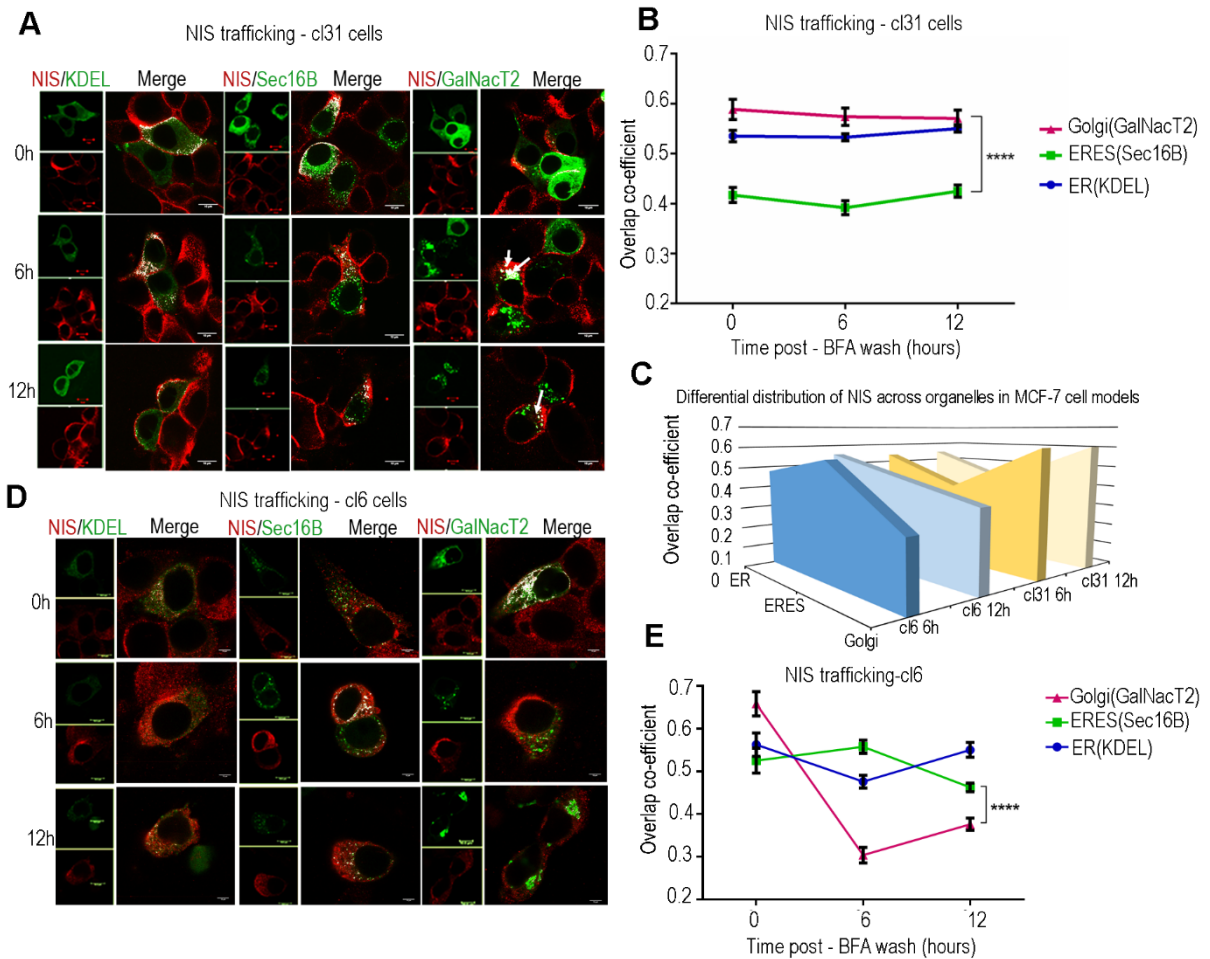


**Figure 4.3.4 NIS follows differential sub cellular trafficking path in MCF-7 and its clones**  
**4.3.4A,D:** Images showing the co-staining of NIS (red) with ER(KDEL), ERES(sec-16B), Golgi(GalNac T2) (green) in cl31 and cl6 cells respectively. White spots show points of co-localization between the red and green channels. The scale bar represents 10 $\mu$ m. White arrows indicate co-localization of NIS and Golgi marker in cl31. **4.3.4B, E:** Graphs showing overlap co-efficient (y-axis) between NIS and organelle specific markers at 0, 6 and 12 hours post BFA wash in cl31 and cl6 cells respectively. The middle plane was used for quantification.

*Error bars indicate SEM. 4.3.4C: Graph showing the overall distribution of NIS across secretory pathway organelles (y-axis) in cl31 and cl6 cells over 6 and 12 hours of Golgi re-formation (x-axis), z-axis shows the average overlap co-efficient value.*

#### **4.3.5 EGFR can cross ERES and reach Golgi in MCF-7 parent and clonal cells**

Since intracellular trafficking path from ER to Golgi is taken by most membrane glycoproteins, we investigated this process for another N-linked glycoprotein like NIS i.e. EGFR. The localization of EGFR in breast cancer cell (MCF-7) is on the cell surface, thus we could expect the trafficking pattern similar to NIS in cl31 cells. Following a similar strategy, the localization of EGFR to ER, ERES and Golgi was studied. **Figure 4.3.5A** shows the presence of EGFR (white spots) in ER, ERES and Golgi. Quantification of overlap co-efficient of EGFR (red) with organelle specific markers (green) indicates the presence of EGFR in Golgi at 6 and 12 hours' time points, where there is a significant increase in co-localization in Golgi as compared to ERES (**Figure 4.3.5B**). Further, when we compared the localization of EGFR in Golgi from cl31 and cl6 cells, we observed a significant increase in the co-localization co-efficient at 6hours in cl31 cells (**Figure 4.3.5C**).

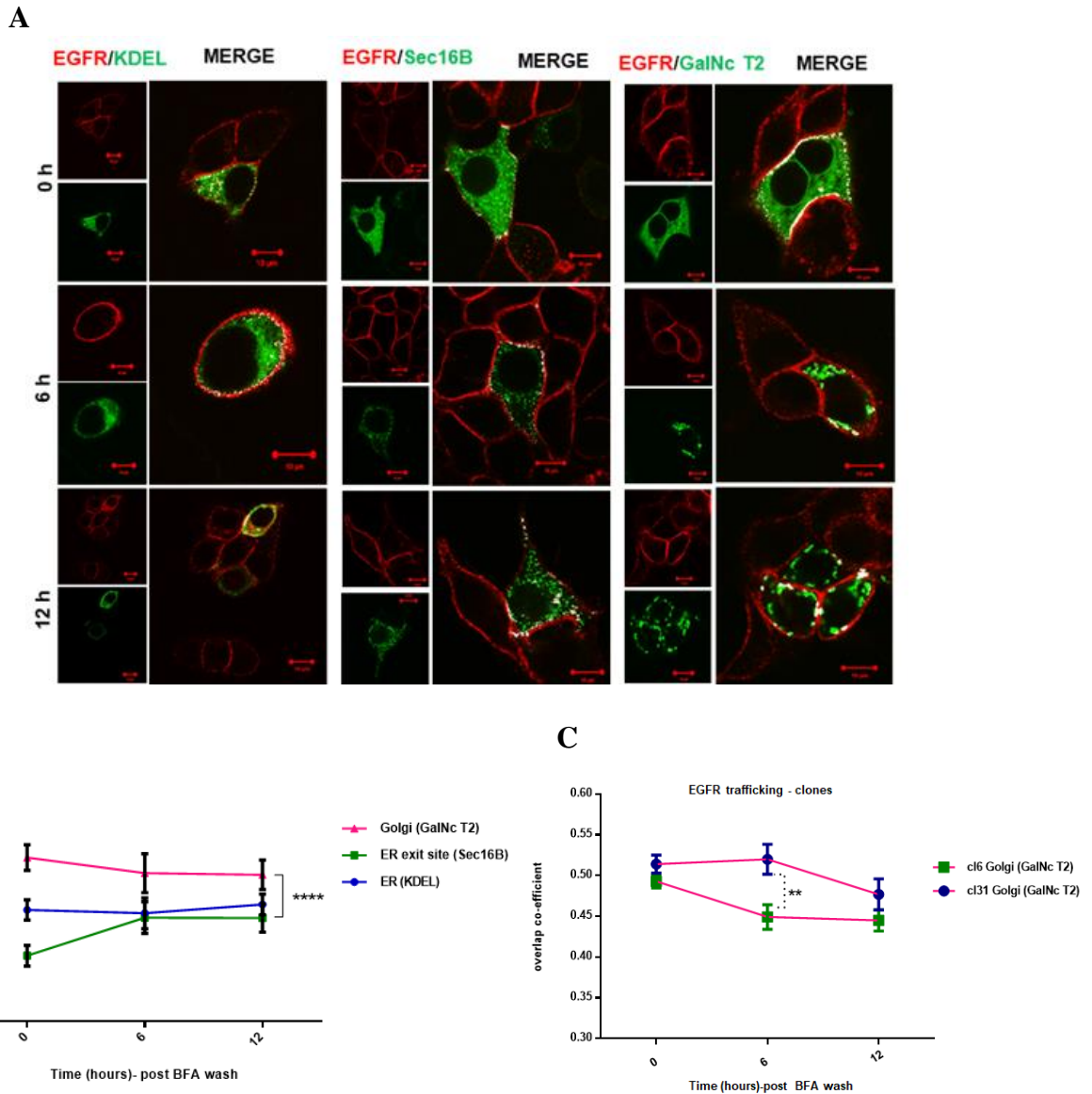


**Figure 4.3.5 EGFR follows conventional trafficking pathway in MCF-7 cells** 4.3.5A: Images showing the co-staining of EGFR (red) with ER(KDEL), ERES(sec-16B), Golgi(GalNac T2) (green) respectively in MCF-7 cells. White spots show points of co-localization between the red and green channels. The scale bar represents 10 $\mu$ m. 4.3.5B: Graph showing overlap co-efficient (y-axis) between EGFR and organelle specific markers at 0, 6 and 12 hours post BFA wash in MCF-7 cells. The middle plane was used for quantification. Error bars indicate SEM.

*4.3.5C: Graph showing overlap co-efficient (y-axis) between EGFR and organelle specific markers at 0, 6 and 12 hours post BFA wash in cl6 and cl31 cells.*

#### **4.3.6 NIS shows a higher association with calnexin in cells with trafficking defect**

Newly synthesising proteins rely on their interaction with ER resident chaperons like calnexin to detect their folding competency. Once the proteins are folded properly or their subsequent quality is met, the 3 terminal glucose moieties get cleaved and calnexin leaves the protein. Thus the association of NIS with calnexin was studied to gain insights into its folding state and quality in ER, because we saw a defect in ER to Golgi transit in MCF-7 and MCF-7 based cytoplasmic clones earlier. In order to capture the association of nascent NIS with calnexin, we first treated the cells with cyclohexamide (chx) followed by a short rescue and then studied the overlap between calnexin and nascent NIS. Dual IF experiment showed that the association of NIS with calnexin was significantly ( $p < 0.05$ ) lower in cl31 cells, as compared to cl6 and MCF-7 cells, indicating NIS present in folding competent state in cl31 cells, thus justifying the membrane localization of NIS in these cells (**Figure 4.3.6A-B**). The treatment of chx shows the loss of mature form of NIS from 12 hours, whereas the non-glycosylated NIS remains unaffected (**Figure 4.3.6C**). Importantly, when we checked the expression of endogenous calnexin in cl31, cl6 and MCF-7 cells, we see that the levels of calnexin is maintained across these cells (**Figure 4.3.6D**), thus indicating that only the calnexin/NIS association dissociation cycle is different in cl31 versus cl6 and MCF-7.

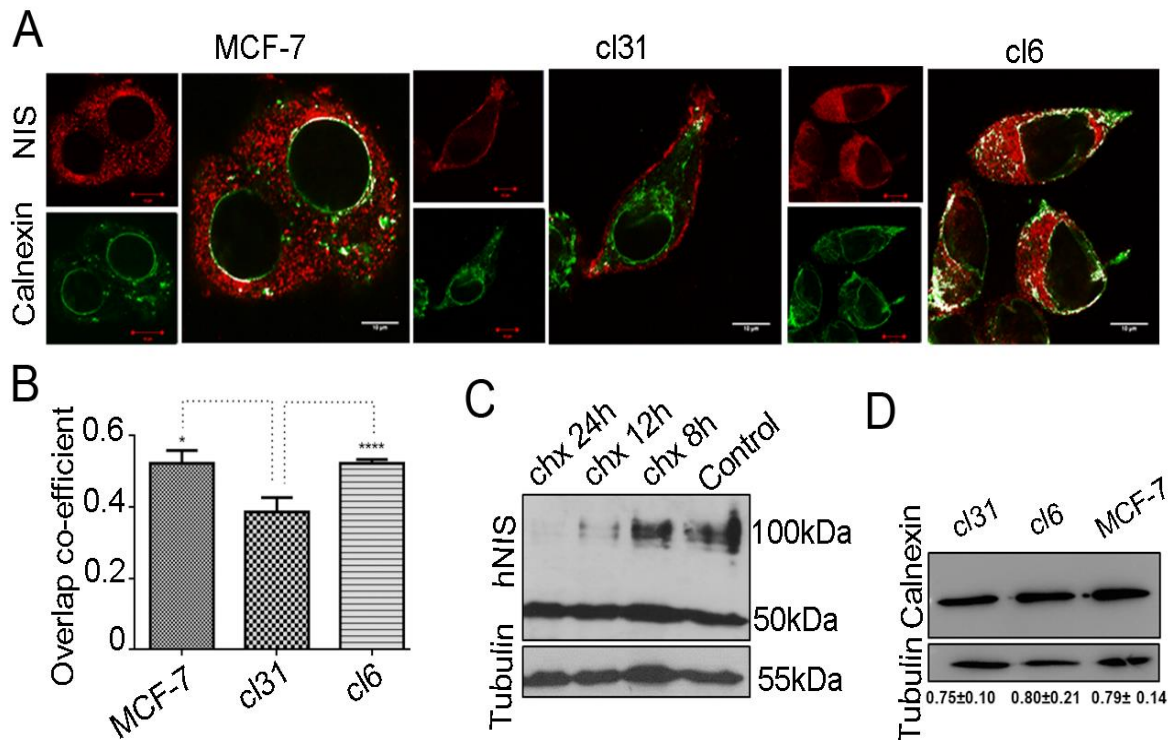


**Figure 4.3.6: NIS association with calnexin is lower in cells with membranous NIS expression 4.3.6A.** Immunofluorescence images depicting the co-localization of calnexin (green) with NIS (red) in cl31, cl6 and MCF-7 cells. White spot indicate points of co-localization between NIS and calnexin. Scale bars represent 10 $\mu$ m. **4.3.6B.** Graph showing the overlap co-efficient between NIS and calnexin. The association of NIS/calnexin in cl6 is significantly higher ( $p < 0.0001$ ) than cl31. Error bars represent SEM. **4.3.6C.** Western blot showing the expression of NIS after chx treatment at different time points. Tubulin was used as endogenous loading control **4.3.6D.** Western blot showing calnexin levels in cl31, cl6 and MCF-7 cells. Tubulin was used as loading control.

#### 4.3.7 N linked Glycosylation is an important PTM that regulates the sub cellular localization of NIS

As, N-linked glycosylation is an important PTM which dictates the sub cellular localization of proteins in a cell, we sought out to study if this PTM has any direct implication on NIS trafficking in the breast cancer cell. We selected 3 different N-linked glycosylation inhibitors

i.e tunicamycin which inhibits the first step of N-linked glycosylation, deoxymannojirimycin (DMM) and swainsonine which affect the later steps of glycosylation process (**Figure 4.3.7A**). Cytotoxicity assessment of these drugs show that the selected concentrations (highlighted in blue on the graph) of all three drugs are in the non-toxic range (**Figure 4.3.7B**). Treatment of cl31 cells with these inhibitors (48 hours) show that DMM and tunicamycin have a profound effect on NIS localization in cl31 cells, and display a vivid loss of NIS from cell surface (**Figure 4.3.7C**). Swainsonine treatment shows a partial loss of membrane localized NIS at 48 hours, whereas a prolonged treatment up to 120 hours causes a complete loss of membrane localized NIS (**Figure 4.3.7D**). Further, we also observe a reduction in the glycosylated mature form of NIS (100kDa band) after 48 hours of DMM and tunicamycin treatment in cl31 cells (**Figure 4.3.7E**). The reduction in membrane localised NIS, has direct implication on its function, thus we measured the amount of iodine uptake post glycosylation inhibitor treatment. A significant reduction in the function of NIS is observed at 48 and 72 hours post DMM and tunicamycin treatment. Also, the tunicamycin treated samples show reduced iodine uptake in cl31 cells which is comparable to cl6 (which has cytosolic NIS expression) (**Figure 4.3.7F**). As these inhibitors have a global effect on all glycoproteins, we tested the EGFR glycosylation status as an additional control for drug specificity. Western blot data indicated that DMM and swainsonine treatment for 48 and 120 hours causes a loss of glycosylated form of EGFR as well, indicated by a 35kDa shift in molecular weight of EGFR from 170kDa to 135kDa (**Figure 4.3.7G**).

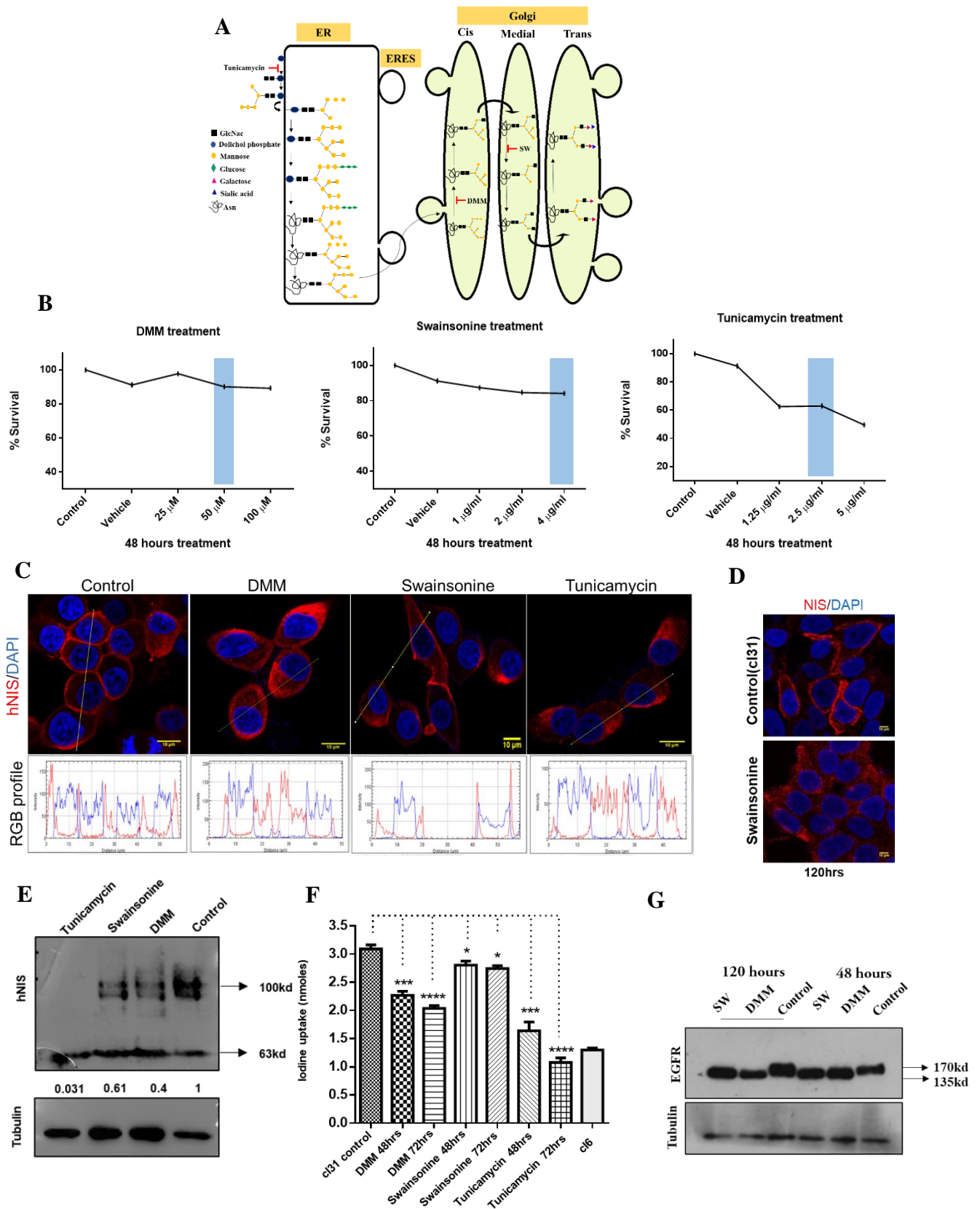


**Figure 4.3.7: N-linked glycosylation controls the localization of NIS to plasma membrane**

**4.3.7A: Diagrammatic representation of the process of N-linked glycosylation and the steps**

where the glycosylation inhibitors act in the subsequent process. **4.3.7B:** Graphs showing the effect of DMM, swainsonine and tunicamycin on the cell (MCF-7) viability. Blue region marked depicts the concentration selected for the study. **4.3.7C:** IF images showing the subcellular localization of NIS in cl31 cells post 48 hours of DMM, Swainsonine and tunicamycin treatment. RGB histogram plot shows membrane (sharp peaks of red intensities) and cytoplasmic (distributed pattern of red peaks) patterns of NIS (red). Nucleus is stained with DAPI (blue). **4.3.7D:** Immunofluorescence images showing the loss of membranous NIS (red) expression post 120 hours of swainsonine treatment. DAPI (blue) shows nucleus. **4.3.7E:** Western blot showing decrease in the 100kDa fraction of mature NIS post 48 hours of DMM, tunicamycin treatment. Tubulin was used as an endogenous loading control. **4.3.7F:** Graphs depicting the effect of N-linked glycosylation inhibitors on the function of NIS post 48 and 72 hours of drug treatment. **4.3.7G:** Western blot showing the effect of DMM and swainsonine on EGFR glycosylation status. Tubulin used as an endogenous loading control.

#### **4.3.8 Glycosylation gene expression profile of cells expressing NIS on membrane versus NIS in cytoplasm**

After validating the importance of N-linked glycosylation process for localization of NIS, we carried out a high throughput screen for a set of 84 key genes involved in the process of N-linked glycosylation. We found 32 genes up-regulated in membranous NIS expressing clones as compared to cytoplasmic clones and parental MCF-7 cells (data adapted from previous thesis of the lab : LIFE09200904014). Cluster analysis using ClustVis software, interestingly revealed that the membrane clones cluster separately from the cytoplasmic clones and MCF-7 cells with respect to their glycosylation gene expression status (**Figure 4.3.8A**). From the various class of enzymes involved in glycosylation process, we analysed the mannosidase class of genes and found a few candidates like MAN1A1, MAN1B1, MAN2A1, MAN2A2,

MAN1C1 to be up-regulated in membrane clones as compared to cytoplasmic clones and MCF-7 cells (**Figure 4.3.8B**).

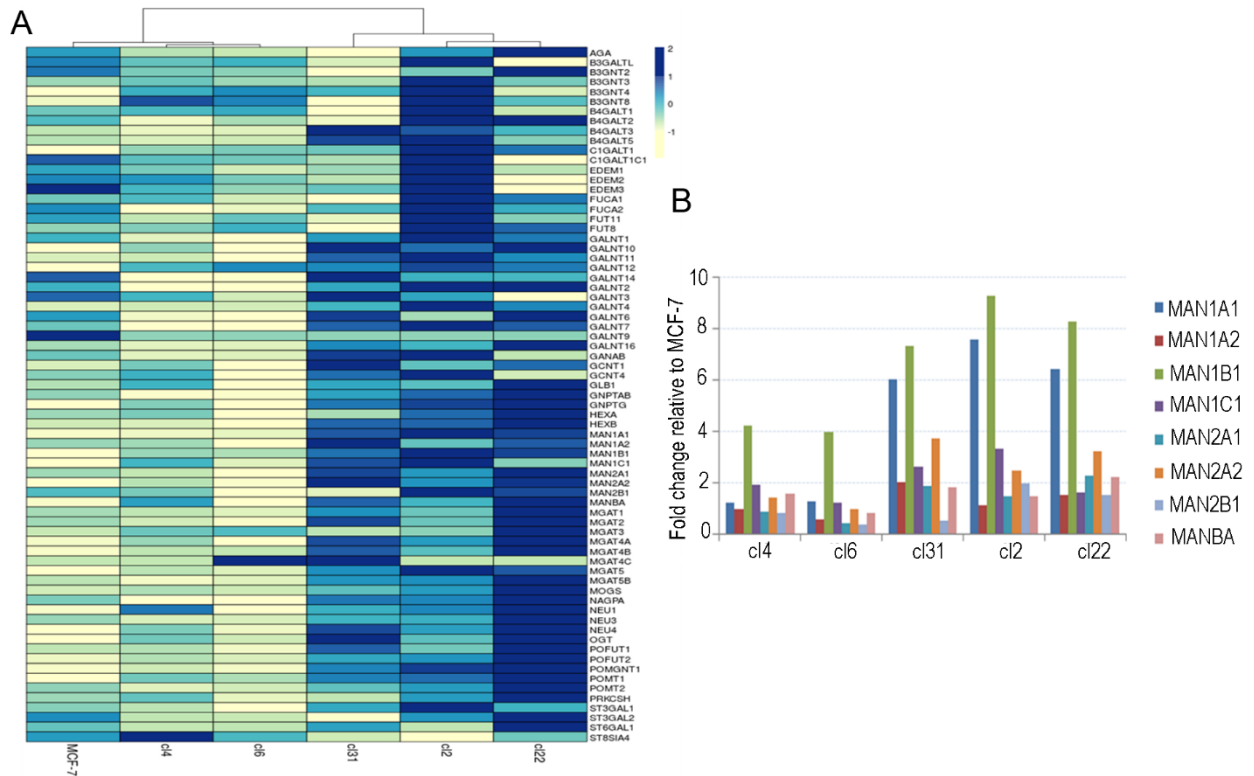


**Figure 4.3.8: Genes encoding enzymes for N-linked glycosylation, show a differential expression across membrane versus cytoplasmic cell clones (data adapted from previous thesis of the lab: LIFE09200904014). 4.3.8A:** Cluster analysis and heat map showing the differential expression profile for key genes encoding important enzymes for the process of N-linked glycosylation across MCF-7, cytoplasmic clones (cl4,cl6) and membrane clones (cl31,cl2 and cl22) respectively. **4.3.8B:** Graph showing the fold change in mannosidase group of genes in cl4, cl6, cl31, cl2 and cl22 with respect to parental MCF-7.

### **4.3.9 The role of mannosidase in modulating the localization of NIS in breast cancer cell clones**

Mannosidase group of enzymes, which are involved in the early steps of glycosylation process, were our primary interest, since we had observed a defect in the ER to Golgi transit in MCF-7 cells. We selected 3 such mannosidase genes that were up-regulated in the membrane clones as compared to cytoplasmic clones i.e. MAN1A1, MAN1B1 and MAN2A1. RNA interference (siRNA) mediated knockdown of these genes was verified by measuring the mRNA turnover of these mannosidase encoding genes in cl31 cells. **Figure 4.3.9A** shows a significant drop in the transcripts of MAN1A1, MAN1B1 and MAN2A1, after siRNA treatment. MAN1A1, MAN1B1 and MAN2A1 knockdown also led to a decrease in the function of NIS in cl31 cells, which was statistically significant (**Figure 4.3.9B**). Further, we also validated the impact of mannosidase knock down on the sub cellular localization of NIS. The lack of these mannosidase encoding genes also disrupts the membrane localization of NIS in cl31 cells (**Figure 4.3.9C**). RGB plot profile also shows that the membrane localized NIS (sharp peaks of red intensities) become more distributed like a cytoplasmic pattern after siMAN1A1, siMAN1B1 and siMAN2A1 treatments. The knockdown of these mannosidase alone and in combination lead to a decrease in the glycosylated form of NIS (100Kda), thus indicating the importance of these enzymes for the maturation of NIS (**Figure 4.3.9D**).

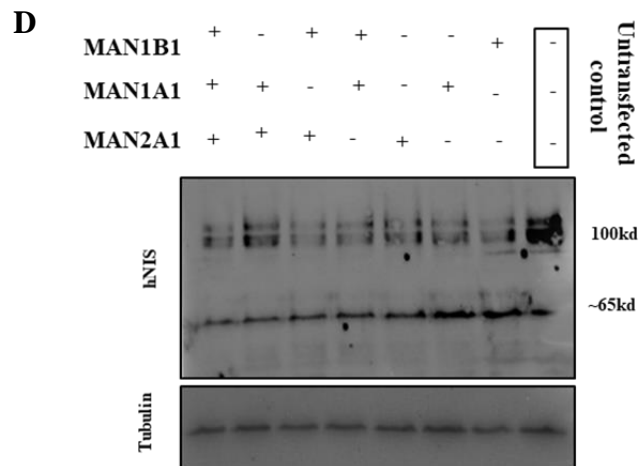
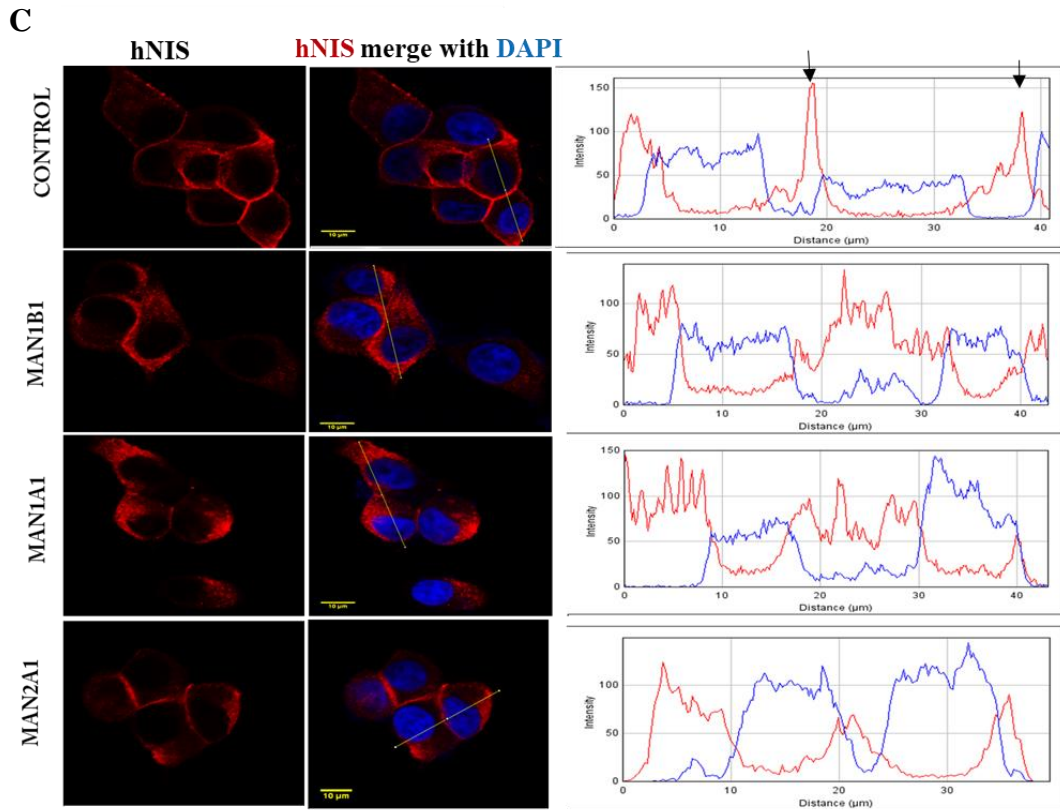
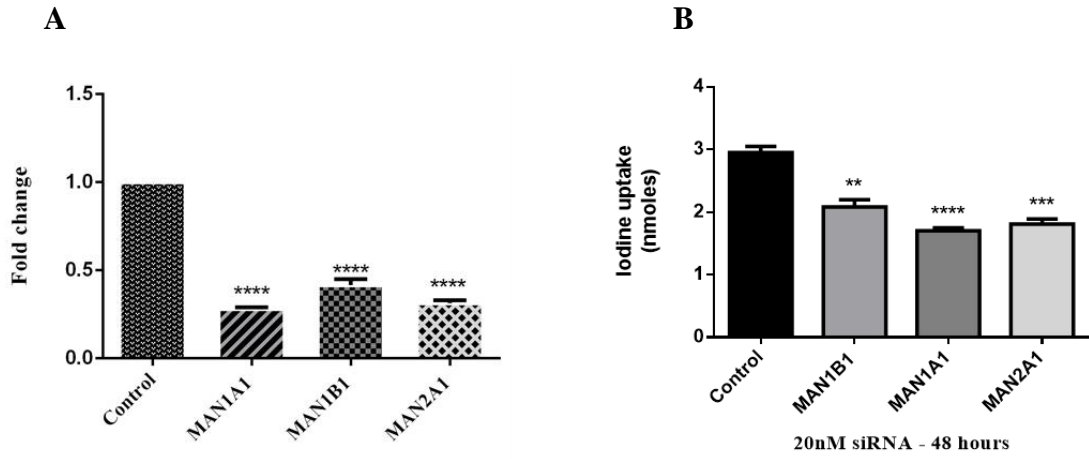


**Figure 4.3.9: Lack of mannosidase enzymes in BC cells leads to mis-localization of NIS**

**4.3.9A:** Graph indicating the relative mRNA expression of MAN1A1, MAN1B1 and MAN2A1

in cl31 cells after 48 hours of respective siRNA treatments. \*\*\*\* indicate  $p < 0.0001$ .

**4.3.9B:** Graph showing the effect of siMAN1A1, siMAN1B1 and siMAN2A1 on NIS function (Nano

moles of iodine uptake on y-axis) in cl31 cells.

**4.3.9C:** Immunofluorescence images and RGB

histogram plots showing the effect of mannosidase knockdown on NIS (red) localization in cl31

cells. Nucleus was stained with DAPI (blue). Scale bar represents  $10\mu\text{m}$

**4.3.9D:** Western blot depicting the change in the glycosylated NIS (100kd band) upon knockdown of MAN1B1,

MAN1A1 and MAN2A1 alone and in combination in cl31 cells. Tubulin used as an endogenous

loading control.

#### 4.3.10 The role of mannosidase in modulating the localization of HER3 in breast cancer cell clone

Since these mannosidase have a pan cellular effect on most glycoproteins in cells, the

localization of HER3 in response to these siRNA was also studied. MAN1A1, MAN1B1 and

siMAN2A1 were knocked down alone and in combination using siRNA in MCF-7 cells. It was

seen that siMAN1A1, siMAN1B1 and siMAN2A1 alone did not alter the sub cellular

localization of HER3. However, when we combined siMAN1A1, siMAN1B1 and siMAN2A1

together, a drastic decrease in the expression and membrane localization of HER3 is noted

(Figure 4.3.10A).

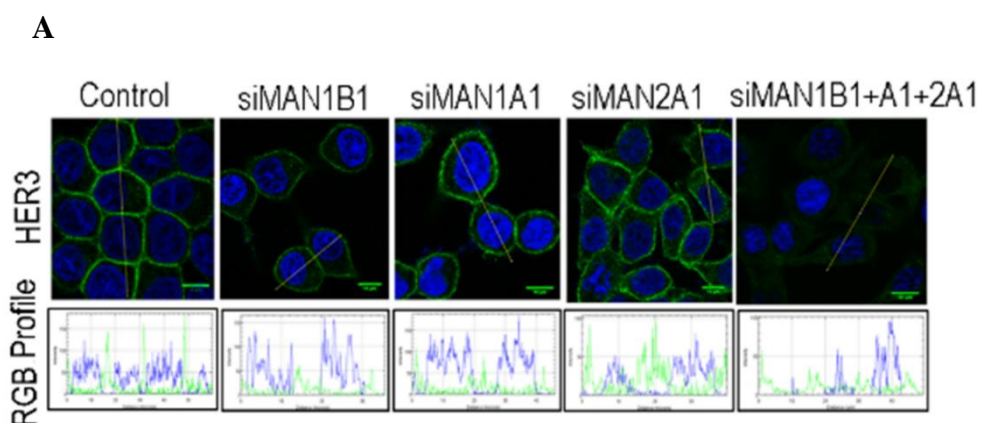


*Figure 4.3.10A MAN1A1, MAN1B1 and MAN2A1 together regulate the sub cellular localization of HER3 in MCF-7 cells 4.3.10A: IF images depicting the change in the localization pattern and expression of HER3 (green) post siMAN1B1, siMAN1A1, siMAN2A1 and triple combination in MCF-7 cells. RGB plot profile shows the distribution of HER3 in cells (green peaks). Blue marks the signal from nucleus.*

#### **4.3.11 NIS is directly associated with mannose modification in breast cancer cell models**

After establishing the fact that cellular mannosidase activity is essential for proper localization of NIS in breast cancer cells, we directly tested the presence of different forms of sugar moieties on NIS. For this purpose, NIS was purified from cl31, cl6 and MCF-7 cells by antibody based pull down i.e. immunoprecipitation (IP). Purified NIS appears at 100kDa (glycosylated part) and approximately 55kDa (non-glycosylated part) as seen previously from western blot results. The 100kDa fraction is enhanced in the IP lysates obtained from cl31 cells (**Figure 4.3.11A**). Lectin western blot done with two lectins i.e. L-PHA (which detects complex type glycoproteins by binding to the N-acetyl glucosamine residues) and conA (detects mannose rich type glycoproteins), show that mature NIS is not a complex type glycoprotein (L-PHA negative). However, mature NIS shows conA positivity, indicating that the end product of NIS belongs to mannose rich type of glycoproteins (**Figure 4.3.11B-C**). This conA positive NIS fraction was the highest from cl31 cells, verifying enhanced N-linked glycosylation in these cells.

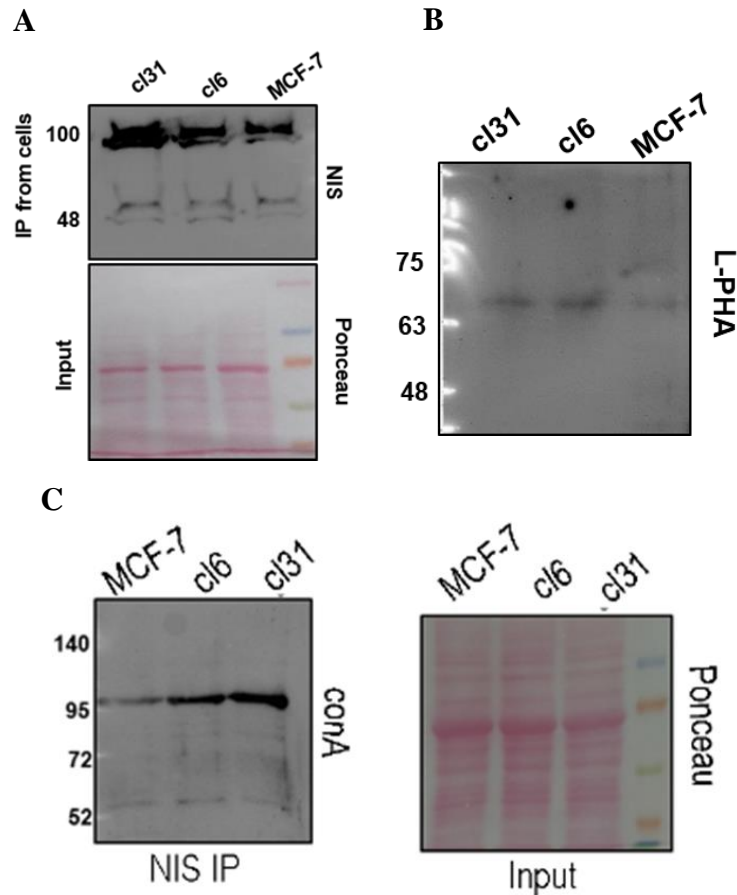


**Figure 4.3.11** NIS represents the mannose rich subtype of glycoproteins. **4.3.11A:** Western blot of purified NIS samples obtained by I.P from cl31, cl6 and MCF-7 cells respectively. Ponceau staining was used as a measure of loading. **4.3.11B-C:** Lectin western blot images of purified NIS samples obtained from MCF-7, cl6 and cl31 probed for L-PHA and conA lectins respectively. Ponceau staining was used as a measure of loading.

#### 4.4 Discussion

NIS is an attractive theranostic target in clinics due to its iodine uptake capability, however the clinical application of NIS mediated radio-ablation therapy for breast cancer faces a huge challenge due to the impeded localization of NIS to plasma membrane [125]. Various groups across the world have attempted to find the underlying cause and as a result N-linked glycosylation has been suggested as an important mediator of NIS localization in a cell [18,

[52](#)]. However, the key molecular mediators of glycosylation process and the exact reason behind the defective NIS localization in breast cancer remains elusive. Our study has addressed these questions pertaining the underlying cause for mis-localized NIS in BC, which had been a puzzling scenario till date.

We had developed a unique model system in breast cancer cells to study this phenomena. AttB-CAG NIS-IRES-F12.turbo construct when transfected in MCF-7 cells, gave rise to two distinct set of clones, i.e. one set expressing NIS at plasma membrane and another majority of clones expressing NIS at cytoplasm. This pattern resembled the scenario from BC patient samples, where a few patients showed membrane localization of NIS and majority others showed cytosolic expression of NIS with the same antibody tested [\[7\]](#). This differential localization of NIS gave us a strong platform to study the cellular and mechanistic basis for NIS localization in BC. This differential localization of NIS across clones could be explained based on clonal heterogeneity, where we analyzed the karyotype of the membrane clone (cl31), cytosolic clone (cl6) and parent MCF-7 cells. Karyotype analysis revealed differences across the 3 cell types tested, thus supporting the previous findings where reports have shown a similar aspect where clones from the same cell line display heterogenic nature [\[147\]](#). The difference in the localization of NIS also reflected at functional level where membranous NIS expressing clones showed a significantly enhanced iodine uptake, thus reassuring the true nature of these clones. Past studies have shown that tunicamycin which is an inhibitor of the first step of glycosylation, can cause impedance in the membrane localization of NIS [\[18\]](#) [\[148\]](#). Thus we tested the effect of various steps of N-linked glycosylation on NIS trafficking in BC, to gain insights into the importance of glycan processing for NIS localization. We used tunicamycin, Deoxymannojirimycin (DMM) and swainsonine. DMM is a known inhibitor of Golgi mannosidase 1 that processes the 8Mannose to 5Mannose form, which is an important event for further trafficking of glycans in Golgi complex [\[149\]](#). The treatment of DMM to cl31 cells,

lead to a loss of membrane localized NIS, which resembled the staining pattern of the cytosolic clones, within 48 hours of treatment. Whereas, Swainsonine which is a mannosidase II inhibitor that is involved in the processing of glycans in the later phases of glycosylation process in Golgi [150], showed a much deferred response i.e. it took 120 hours for swainsonine to cause a complete loss of membrane localization of NIS in cl31 cells. These results hinted towards the importance of the early glycan processing steps for determining the sub cellular localization of NIS. Further, we directly looked into the cellular path NIS takes in membrane versus cytoplasmic clones. Studying the localization of NIS in the key components of the secretory pathway i.e. Endoplasmic reticulum (ER), ER exit sites (ERES) and Golgi, revealed that NIS could pass from ER to Golgi in membrane clone (cl31) after the Golgi was completely reformed post BFA rescue. However, NIS from cytoplasmic clone (cl6) and MCF-7 cells, showed an accumulation in ER and ERES, whereas it's ER to Golgi transit was highly impeded, even when Golgi structure was reformed post BFA rescue. The proteins which are incapable of folding appropriately, must pass through the repetitive calnexin/calreticulin cycle in an attempt to gain trafficking and folding competency [151]. Thus looking into the association of NIS with calnexin would provide insights into its folding state, which is in turn co-related to proper glycan processing events. In order to capture the association of nascent NIS with calnexin, we picked up a 12 hour cyclohexamide (chx) treatment time point, where most of the glycosylated NIS was undetectable, followed by a short rescue. Our results showed significantly higher association of NIS with calnexin in MCF-7 and cl6 cells in contrast to cl31. The proteins which cannot fold properly after repeated cycles of calnexin/calreticulin, are transported to cytoplasm through the ER translocon channel, where they face proteosomal degradation process [152]. Thus, cytosolic NIS in cl6 and MCF-7 cells might be susceptible to proteasomes, which is not tested so far. Together, these data indicate an important aspect regarding the sub cellular localization of NIS i.e. NIS relies heavily on the early glycan processing events occurring at

the ER, which if gone wrong can lead to cytoplasmic accumulation of NIS, thus impairing its function.

Taking hints from the intracellular trafficking defect of NIS, in MCF-7, we thought of investigating the role of mannosidase that are required for the initial processing of N-glycan. We selected MAN1B1, MAN1A1 and MAN2A1 from the Glyco-RT profiler array for 84 key genes involved in the process of N-linked glycosylation. The results from the RT-profiler array revealed a sharp difference in terms of 32 gene up-regulation in membranous clones in contrast to MCF-7 and cytosolic clones. Clustering analysis, also clustered the membrane clones away from the MCF-7 and cytoplasmic clones based on the gene expression pattern. Mannosidase class of enzymes are important in the early events of glycan processing, and MAN1B1, MAN1A1 and MAN2A1 showed a distinct up-regulation in membrane clones.

MAN1B1 and MAN1A1 are class 1 alpha mannosidase that help in cleaving the terminal mannose moieties from the core glycan. MAN1B1 acts on the B branch of mannose. MAN1A1, MAN1B1 are localized in ER, while MAN2A1 is localized in the Golgi, which helps in the final maturation of glycoprotein. Knocking down the expression of these mannosidase by siRNA in membrane clone cells, caused a loss of NIS from the cell surface. Thus implying the importance of these mannosidase in regulating the translocation of NIS. These results confirm the fact that initial mannose modifications are important for the maturation of NIS. Thus our study identifies novel mediators of functional NIS expression and highlights the importance of the initial mannose cleavage in the trafficking of NIS to plasma membrane. Western blot results also bring out the fact that a combination of these mannosidase used could dramatically perturb the glycosylation of NIS. The triple combination knockdown of MAN1B1+MAN1A1+MAN2A1, had the maximum effect and it could almost completely abolish the glycosylated form of NIS. These mannosidase combination is not only important

for the sub cellular localization of NIS, but also HER3 which another important membrane glycoprotein for BC.

Supporting our observation highlighting the importance of adequate mannose processing events for correct localization of NIS in BC, we asked whether NIS is a mannose rich type glycoprotein. Lectin western blot results of purified NIS from cl31, cl6 and MCF-7 cells, showed that completely glycosylated form of NIS was Con A positive and L-PHA negative, thus demonstrating that NIS is not a complex type glycoprotein but belongs to mannose rich type of N-glycans.

In conclusion, we hypothesise that inadequate mannose processing in breast cancer cells is a key factor that abrogates NIS trafficking in BC cells. Thus, this finding paves way for exploring the use of N-linked glycosylation inducers like cAMP which can elevate the number of dolichol pyrophosphate oligosaccharides [\[137\]](#), for enhancing the expression of NIS at the cell surface in BC. Thereby making the application of NIS as a gene therapy candidate for breast cancer close to translation in clinics.

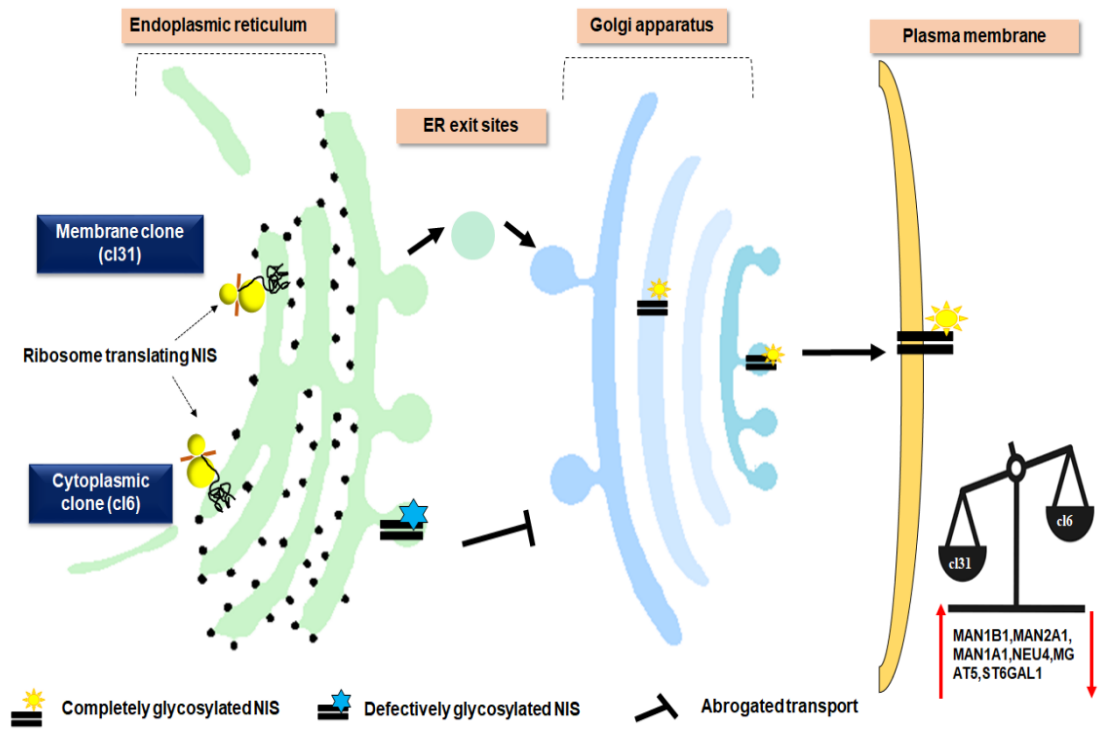


*Figure 4.4.1: Diagrammatic representation of differential NIS protein trafficking across cytoplasmic and membrane over-expressing cell population*